

**PART I: PALLADIUM-*PEPPSI-IPENT*^{Cl}; A USEFUL CATALYST FOR
CHALLENGING AMINATION REACTIONS**

**PART II: GENERATION OF BENZYNES IN FLOW REACTORS
FOLLOWED BY SUBSEQUENT DIELS-ALDER REACTIONS**

ABIR ALI KHADRA

A DISSERTATION SUBMITTED TO THE FACULTY OF GRADUATE
STUDIES IN PARTIAL FULFILLMENT OF THE REQUIREMENTS FOR THE
DEGREE OF DOCTOR OF PHILOSOPHY

GRADUATE PROGRAM IN CHEMISTRY
YORK UNIVERSITY
TORONTO, CANADA

MAY, 2018
© ABIR ALI KHADRA, 2018

ABSTRACT:

The first part of this research focuses on developing efficient methods to address challenging Buchwald –Hartwig amination reactions using Pd-NHC pre-catalysts. Specifically, we focused on: a) coupling of sterically hindered primary and secondary amines and b) coupling of 2-aminopyridine derivatives with aryl and heteroaryl halides.

Although several approaches have been developed and proven to be effective for coupling of sterically hindered amines, they have limited utility and substrate scope. *Pd-PEPPSI-IPent^{Cl}* (**P**yridine **E**nhanced **P**re-catalyst **P**reparation **S**tabilization and **I**nitiation) proved to be a very effective catalyst for coupling hindered primary and secondary amines under mild reaction conditions (i.e. Na-BHT (BHT = 2,6-Di-*tert*-butyl hydroxyl toluene), 80 °C, DME) tolerating base sensitive functional groups such as ester, keto, and nitrile groups.

While the synthesis of 2-aminopyridine derivatives is commonly carried out by metal-catalyzed coupling of 2-halopyridines with aniline derivatives, the use of 2-aminopyridine as a nucleophilic partner in Pd catalysis is very difficult as these substrates tend to bind irreversibly to the palladium center and shut down the catalytic cycle. However, *Pd-PEPPSI-IPent^{Cl}* has been found to resist the binding of 2-aminopyridines, making it a very active catalyst for these couplings. The steric bulk of the 3-pentyl substituents on the aryl rings of the NHC ligand that drives the cross-coupling by facilitating reductive elimination also mitigates the poisoning effect of the 2-aminopyridine functionality in the starting material/and or products. We also found that placing electron-donating or electron-withdrawing substituents at the 6-position of the 2-aminopyridine ring reduces the poisoning effect and facilitate the catalytic cycle with mild bases (i.e. Na-BHT).

The second part of this research investigated the formation of benzyne derivatives from *ortho*-trimethylsilyl triflates using tetra-*n*-butylammonium fluoride (TBAF) as the benzyne-forming trigger in the flow system. The numerous advantages of microfluidic devices enabled the formation of these species at room temperature which were immediately trapped in Diels-Alder reactions with five-membered heterocyclic dienes to generate bicyclic alkenes of biological interest. The yields of Diels-Alder reaction with benzyne follow the order: furans > pyrroles > thiophene.

Dedications

It is my genuine gratefulness and warmest regard that I dedicate this thesis to my friend Suzann Mansour, her kindness and devotion, her inspiration throughout the years of our friendship will not be forgotten. Suzann; you left incredible fingerprints of grace in my life, wish you were here.

I also dedicate my work to my daughter Celina, I am truly thankful to have you in my life.

ACKNOWLEDGMENTS

First, I would like to express my special thanks to my supervisor Prof. Michael G. Organ for providing me with a golden opportunity to be one of his graduate students. The free environment that he provides to his students to work independently, to be creative and to develop problem-solving skills allowed me to be a much more confident chemist that I would imagine. Also, I would like to extend my thanks to Prof. Arturo Orellana for his constructive criticism, sharing his valuable knowledge in organic chemistry during my research evaluations at the end of each year, and during the problem sessions. His support and encouragement were extremely valuable especially when I became a new mother. In addition, I would like to thank Prof. Pierre Potvin for agreeing to be my research committee, his fruitful suggestions and advice in the lab during my CHEM 4000 course enabled me to be well prepared for graduate school.

Next, I would like to thank Dr. Howard Hunter for his willingness to help and share his immense knowledge in NMR spectroscopy, his patience to answer my endless questions especially at the beginning of my studies, and his attempts to cheer me up whenever a reaction does not work.

I would like to express my gratitude to my colleagues that I have had the pleasure to work with, especially to my best friends Sepideh Sharif who stood by me and helped me through the difficult times, to Xia Chen and many discussions about food and calorie counting, to Kristina Somerville-Rucker with her rare sense of humor, lovely spirit that forces you to smile no matter what. To my wise and loyal friend Zahra Vaziri who was always there for me especially during my pregnancy; to Dr. Jennifer Farmer and her valuable advices to cope stress; to an amazing friend Dr. George Achonduh; to Dr. Niloufar Hadie and her incredible sense of humor and her passion to live life to the maximum; to Matthew Pompeo and his unique professionalism; to Andrei Nikolaev and his passion to organic chemistry and willingness to participate in discussion on reaction mechanisms

for hours and hours; to Nour Bizzari and her distinct personality, to Jee Kwak and the smile that never leaves his face, to Dr. John Day and Dr. Gregory Price and their willingness to help me in the lab, and to my childhood best friend and cousin, Rami Valari Spasov who always reminded me to take care of myself and respect my needs when I was totally ignoring them.

Finally, this work could not be completed without the support of my family, especially my father who taught me how to be determined, patient and to pursue my goals no matter what. To my precious mom who stayed with me for almost a year and took care of my daughter Celina, the love of my life; to my wise and forgiving brother Houssam, to my sophisticated, prestigious brother Hassan and to my youngest brother Ghaleb who taught me how to love myself and live life to the maximum, to the wise woman, my sister in law Kate Brooks-Khadra. Thank you for all your support, for enduring my unpredictable working hours and for being understandable for every time I was questioned about my graduating date.

TABLE OF CONTENTS

ABSTRACT.....	ii
DEDICATION.....	iv
ACKNOWLEDGEMENTS.....	v
TABLE OF CONTENTS.....	vii
LIST OF TABLES.....	x
LIST OF FIGURES.....	xi
LIST OF SCHEMES.....	xiii
LIST OF ABBREVIATIONS.....	xvii
PUBLICATIONS.....	xx

PART I: PALLADIUM-PEPPSI-IPENT^{Cl}; A USEFUL CATALYST FOR CHALLENGING AMINATION REACTIONS

CHAPTER 1-Introduction.....	1
1.1 Significance of Aniline Derivatives.....	1
1.2 Synthesis of Aniline Derivatives.....	3
1.2.1 Nucleophilic Aromatic Substitution.....	3
1.2.2 Aniline Derivatives from Nitrobenzene.....	4
1.2.3 Aniline from Nitrobenzene and Grignard Reagents.....	5
1.3 Metal-Catalyzed Amination Reactions.....	9
1.3.1 Copper-Catalyzed C-N Bond Formation.....	9
1.3.2 Palladium-Catalyzed C-N Bond Formation.....	12
1.3.2.1 Mechanism of Buchwald-Hartwig Amination.....	13
1.4 Ligand Development in Palladium-Catalyzed Buchwald-Hartwig Amination.....	16
1.4.1 Phosphine Ligands.....	17
1.4.1.1 Quantifying Electronic and Steric Properties of Phosphine Ligands.....	17
1.4.1.2 Phosphine Ligands in Palladium-Catalyzed Amination.....	18
1.4.1.3 Deficiencies of Phosphine Ligands.....	27

1.4.2 <i>N</i> -Heterocyclic Carbenes.....	28
1.4.2.1 Steric Characteristics of NHC.....	30
1.4.2.2 Electronic parameter of NHC Ligands.....	31
1.4.2.4 Pd-NHC Complexes in Buchwald Amination.....	33
1.5 Challenges in C-N Bond Formation.....	36
1.5.1 Synthesis of Sterically Hindered Aniline Derivatives.....	36
1.5.2 Synthesis of 2-Aminopyridine Derivatives.....	39
1.6 Plan of study.....	43
1.6.1. Synthesis of Sterically Hindered Arylamines.....	43
1.6.2 Synthesis of 2-Aminopyridine.....	44
CHAPTER 2-Synthesis of Hindered Anilines.....	45
2.1 Reaction Optimization.....	45
2.2 Substrate Scope with Primary Amines.....	47
2.3 Substrate Scope with Secondary Amines.....	48
2.4 Conclusion.....	52
CHAPTER 3-Reactions of 2-Aminopyridine in Cross-Coupling.....	53
3.1 Catalyst Screening.....	53
3.2 Coupling of Electron-Poor 2-Aminopyridines.....	56
3.3 Impact of the Size of the C6-Substituent on the Catalytic Cycle.....	57
3.4 Coupling of Cyano-Substituted-2-Aminopyridine.....	58
3.5 Poisoning Effect of the 2-Aminopyridine Coupled Product on Pd Catalyst.....	59
3.6 Substrate Scope.....	62
3.7 Conclusion.....	63
CHAPTER 4-Experimental Procedures.....	64
 PART II: GENERATION OF BENZYNES IN FLOW REACTORS FOLLOWED BY SUBSEQUENT DIELS-ALDER REACTIONS	
CHAPTER 5-Chemical Reactions in Flow.....	91
5.1 Introduction.....	91

5.1.1 Reaction Time in Batch versus Flow-Reactors.....	92
5.1.2 Mixing in Batch versus Flow-Reactors.....	95
5.1.3 Heat Transfer in Batch versus Flow-Reactors.....	99
5.1.4 In-Line Analysis in Flow Reactors.....	101
5.2 Benzyne.....	107
5.2.1 History and Background.....	107
5.2.2 Benzyne Isomers.....	108
5.2.3 Structure of <i>o</i> -Benzyne.....	109
5.2.4 Generation of Benzyne.....	111
5.2.5 Reactions of Benzyne.....	112
5.2.6 Plan of Study.....	114
CHAPTER 6-Results and Discussion.....	115
Conclusion.....	128
CHAPTER 7-Experimental Procedures.....	129
CHAPTER 8-References.....	143

LIST OF TABLES

PART I: PALLADIUM-PEPPSI-IPENT^{Cl}; A USEFUL CATALYST FOR CHALLENGING AMINATION REACTIONS

Table 1: Effect of bite angle on amination reaction between 36 and 37	21
Table 2: Catalyst and base optimization.....	46
Table 3: Coupling of primary amines.	48
Table 4: Coupling of secondary amines.....	49
Table 5: Coupling of <i>N</i> - <i>tert</i> -butylbenzylamine.	50
Table 6: Substrate scope with less hindered amines.	51
Table 7: Catalyst screening for coupling 2-aminopyridine.....	53
Table 8: Impact of the placement of methyl groups on 2-aminopyridine on the coupling with 110 using Pd- <i>PEPPSI-IPent</i> ^{Cl} precatalyst.....	55
Table 9: Impact of electron-poor groups on the coupling of 2-aminopyridines using Pd- <i>PEPPSI-IPent</i> ^{Cl} precatalyst.....	56
Table 10: Impact of the size of the C6-substituent of 2-aminopyridine derivatives.....	57
Table 11: Coupling 4-cyano-2-aminopyridine.....	58
Table 12: Investigating poisoning effect of 4-cyano-2-aminopyridine.....	59
Table 13: Impact of moving the primary amine from C2 to C3 on the pyridine nucleophile in the coupling of 106	61
Table 14: Substrate scope for coupling 2-aminopyridine derivatives to various aryl chlorides with the mild base using Pd- <i>PEPPSI-IPent</i> ^{Cl}	63

PART II: GENERATION OF BENZYNES IN FLOW REACTORS FOLLOWED BY SUBSEQUENT DIELS-ALDER REACTIONS

Table 1: Diffusion time versus size of the reactor.....	97
Table 2: Nitration of phenol in batch and flow conditions.....	101
Table 3: Effect of residence time, diene equivalents and the reaction temperature on the cycloaddition of benzyne and furan.....	117
Table 4: Reaction between benzyne precursor 52 and different dienes.....	118
Table 5: Reaction between benzyne precursor 68 and different dienes.....	120
Table 6: Reaction between benzyne precursor 69 and different dienes.....	121
Table 7: Ring opening of 56 with different organolithiums.....	124
Table 8: Optimization study for the synthesis of 93 directly from 52	126
Table 9: Optimization study for the synthesis of 94 directly from 52	127

LIST OF FIGURES

PART I: PALLADIUM -PEPPSI- IPENT^{Cl}; A USEFUL CATALYST FOR CHALLENGING AMINATION REACTIONS

Figure 1: Selected examples of biologically active aniline derivatives.....	1
Figure 2: Back-bonding in phosphine-metal-CO complexes.....	18
Figure 3: Tolman cone angle.....	18
Figure 4: Singlet state of NHC carbenes.....	28
Figure 5. Percent buried volume (% V _{Bur}) of selected NHC obtained from DFT-Optimized geometries of [(NHC)Ir(CO) ₂ Cl] complexes.....	31

Figure 6: Nolan and co-worker's correlation of average ν_{CO} for $[(L)Ir(CO)_2Cl]$ complexes with Tolman electronic parameter.....	33
Figure 7: NHC pre-catalysts for Buchwald-Hartwig amination.....	34
Figure 8: Pd-PEPPSI pre-catalysts developed by Organ.....	35
Figure 9: Example of sterically hindered anilines.....	36
Figure 10: Examples of 2-aminopyridine derivatives as therapeutic agents.....	40

PART II: GENERATION OF BENZYNES IN FLOW REACTORS FOLLOWED BY SUBSEQUENT DIELS-ALDER REACTIONS

Figure 1: Chemical reactions in flow setting.....	92
Figure 2: Reactant concentration versus time (flask reactor) or distance (flow reactor) for simple first-order reaction under well mixed homogeneous conditions.....	94
Figure 3: Flow reactor as infinite small separated flask reactors.....	95
Figure 4: Types of flow.....	96
Figure 5: Damkohel number and side-product formation.....	98
Figure 6: Temperature profiles in a batch (a) and a flow reactor (b) simulated for an exothermic model reaction between HCl and NaOH; y is the channel thickness and L is the channel length.....	99
Figure 7: Temperature distribution profile in batch and in microreactor (MR).....	100
Figure 8: Second-generation MACOS system with in-line analysis.....	102
Figure 9: Flow reactor set up for Diels-Alder reactions.....	116
Figure 10: Reactor design used for control experiments to examine benzyne lifetime.....	122
Figure 11: Design reactor used to synthesize 1,2-dihydronaphthols from benzyne precursors.....	125

LIST OF SCHEMES

PART I: PALLADIUM PEPPSI- IPENT^{Cl}; A USEFUL CATALYST FOR CHALLENGING AMINATION REACTIONS

Scheme 1: General retrosynthesis of aromatic amines.....	2
Scheme 2: Formation of arylamines through S _N Ar.....	3
Scheme 3: Formation of arylamines through benzyne intermediate.....	4
Scheme 4: Arylamines formation through nitration followed by reduction.....	4
Scheme 5: Chemoselective reduction of NO ₂ using Rh catalyst in the presence of other reducible groups.....	5
Scheme 6: Mechanism of aniline synthesis using Grignard reagents and nitrobenzene.....	6
Scheme 7: Substrate scope for preparation of polyfunctional diarylamines.....	7
Scheme 8: Metal-free amination using aryl(TMP)iodonium trifluoroacetate.....	8
Scheme 9: Substrate scope for metal-free amination using aryl(TMP)iodonium trifluoroacetate...8	
Scheme 10: Ullmann and Goldberg copper-mediated amination reactions.....	9
Scheme 11: Chan's protocol for coupling substrates containing nitrogen.....	10
Scheme 12: Substrate scope using B(OH) ₃ -promoted catalytic Chan-Lam reaction.....	11
Scheme 13: First Pd-Catalyzed C-N bond formation by Migita and co-workers.....	12
Scheme 14: Pd-catalyzed Buchwald-Hartwig amination.....	13
Scheme 15: Different methods for generating Pd catalyst in Buchwald-Hartwig amination.....	14
Scheme 16: Proposed catalytic cycle for Pd-catalyzed Buchwald-Hartwig amination.....	15
Scheme 17: Buchwald amination using first-generation phosphine ligand.....	19

Scheme 18: First-and second-generation phosphine ligands.....	20
Scheme 19: Amination of cyclic and acyclic secondary amines using PPF-OMe ligand.....	22
Scheme 20: Amination of secondary amines at rt using DavePhos.....	23
Scheme 21: Chemoselective amination of aniline using Xphos.....	24
Scheme 22: Selective amination of primary versus secondary amine using BrettPhos.....	25
Scheme 23: Third-generation phosphine ligands.....	25
Scheme 24: Fourth-generation phosphine ligand.....	26
Scheme 25: Liability of phosphine ligands in palladium catalysis.....	27
Scheme 26: Generation of NHC by deprotonation.....	28
Scheme 27: Mechanism of benzoin condensation proposed by Breslow.....	29
Scheme 28: Formation of first stable NHC.....	30
Scheme 29: First application of <i>N</i> -heterocyclic carbenes in Heck reaction.....	30
Scheme 30: Buchwald protocol for the synthesis of sterically hindered anilines derivatives.....	38
Scheme 31: Lalic's protocol for the synthesis of sterically hindered aniline derivatives.....	39
Scheme 32: Metal-free synthesis of 2-aminopyridines.....	41
Scheme 33: Knochel protocol for the synthesis of 2-aminopyridine derivatives using organozinc.....	42
Scheme 34: Metal-catalyzed amination to form 2-aminopyridine derivatives.....	43
Scheme 35: Determining the origin of the reduced product 109	47
Scheme 36: Likely mechanism of epimerization for compound 122 and 129	49

Scheme 37: Coupling *N-tert*-butylbenzylamine with a more electrophilic aryl chloride.....51

Scheme 38: Impact of *N*-phenyl-2-aminopyridine on amination reaction of **170** with **171**.....60

Scheme 39: Variation of the catalyst loading on coupling **106** with **150b**.....62

PART II: GENERATION OF BENZYNES IN FLOW REACTORS FOLLOWED BY SUBSEQUENT DIELS-ALDER REACTIONS

Scheme 1: Quenching of *o*-bromophenyllithium with different electrophiles.....94

Scheme 2: Scale-up the synthesis of benzyl azide in flow reactors.....103

Scheme 3: Multistep synthesis in flow.....103

Scheme 4: Multistep synthesis of (+)-dumetorine in flow.....104

Scheme 5: Three-component coupling reaction of benzyne.....105

Scheme 6: Synthesis of boscalid in flow.....106

Scheme 7: First indication for the existence of aryne.....107

Scheme 8: ¹⁴C-Labeled chlorobenzene with sodium amide.....108

Scheme 9: Benzyne isomers.....108

Scheme 10: *p*-Benzyne in Bergman cyclization reaction.....109

Scheme 11: Resonance structures of *o*-benzyne.....109

Scheme 12: Geometric strain in accommodating triple bond in six-membered ring.....110

Scheme 13: Energy of LUMO in unstrained alkyne versus benzyne.....110

Scheme 14: Different methods for generating *o*-benzynes.....111

Scheme 15: Different reactions of *o*-benzynes.....112

Scheme 16: Benzyne incorporation in natural products.....	113
Scheme 17: Benzyne precursors used in this study.....	115
Scheme 18: Synthesis of benzyne precursors 68 and 69	115
Scheme 19: Synthesis of 76 and 77	116
Scheme 20: Mechanism for the formation of compounds 81	119
Scheme 21: Control experiments conducted in a batch setting.....	123
Scheme 22: Side-reaction between <i>n</i> -BuLi and THF.....	124
Scheme 23: Syn and anti products formed in Table 7, entry 2.....	125
Scheme 24: Hoffman elimination reaction between organolithium and TBAF.....	127

LIST OF ABBREVIATIONS

Ac	acetyl
Ad	adamantyl
BHE	β -hydride elimination
BHT	2,6-di- <i>tert</i> -butyl hydroxyl toluene
BINAP	2,2'-bis(diphenylphosphino)-1,1'-biphenyl
Boc	<i>tert</i> -butyl carbamate
Brettphos	2-dicyclohexyl phosphino-3,6-dimethoxy-2',4',6' triisopropyl -1,1'- biphenyl
Bu	butyl
BuLi	<i>n</i> -butyl lithium
<i>t</i> BuLi	<i>tert</i> -butyl
°C	degree celsius
Cat.	catalyst
COSY	correlation Spectroscopy
CPME	cyclopentyl methyl ether
CyDMEDA	<i>trans</i> - <i>N,N'</i> -dimethyl-1,2-cyclohexanediamine
Db	dibenzylideneacetone
DCE	1,2-dichloroethene
DCM	dichloromethane
DPPF	bis(diphenylphosphino)ferrocene
DME	dimethoxyethane
Equiv.	molar equivalents
Et ₂ O	diethyl ether
EtOAc	ethyl acetate
GC/MS	gas chromatography/Mass spectrometry
HRMS	high-resolution mass spectroscopy
HFIP	hexafluoroisopropanol

Hz	hertz
IHept	1,3-Bis(2,6-di(4-heptyl)phenyl)imidazole-2-ylidene
IPent	1,3-Bis(2,6-di(3-pentyl)phenyl)imidazole-2-ylidene
IPent ^{Cl}	1,3-Bis(2,6-di(3-pentyl)phenyl)-4,5-dichloroimidazole-2-ylidene
IPr	1,3-Bis(2,6-diisopropylphenyl)imidazole-2-ylidene
IPr ^{Cl}	1,3-Bis(2,6-diisopropylphenyl)-4,5-dichloroimidazole-2-ylidene
JosiPhos	(R)-1-[(S _P)-2-(diphenylphosphino) ferrocenyl]ethyldicyclohexylphosphine
KO ^t Bu	potassium <i>tert</i> -butoxide
L	length
MI	migratory insertion
mp	melting point
NaO ^t Bu	sodium <i>tert</i> -butoxide
NHC	<i>N</i> -heterocyclic carbene
NMR	nuclear magnetic resonance
NOESY	nuclear overhauser effect spectroscopy
OA	oxidative addition
PEPPSI	pyridine-enhanced pre-catalyst preparation, stabilization, and Initiation
PPFA	(R)- <i>N,N</i> -Dimethyl-1-[(S)-2- (diphenylphosphino) ferrocenyl] ethyl amine
PPF-OMe	1-[2-(diphenylphosphino)-ferrocenyl]ethyl methyl ether
rt	room temperature
RE	reductive elimination
SAR	structure-activity relationship
SIMes	1,3-bis(2,4,6-trimethylphenyl)imidazolidine-2-ylidene
SIPr	1,3-bis(2,6-diisopropylphenyl)imidazolidine-2-ylidene
S _N Ar	nucleophilic aromatic substitution
TBAF	tetrabutylammonium fluoride
TEP	Tolman's electronic parameter

TFA	trifluoroacetate
THF	tetrahydrofuran
TLC	thin-layer chromatography
TMP	2,4,6-trimethoxyphenyl
TMPDA	<i>N,N,N',N'</i> -tetramethyl-1,3-propanediammine
TMS	trimethylsilyl
TOCSY	total correlated spectroscopy
TOF	Turn-over frequency
TON	Turn-over number
TsN ₃	Tosyl azide
XPhos	2-Dicyclohexylphosphino-2',4',6'-triisopropylbiphenyl

Publications:

Some portions of this work appears in the following publications:

1. Khadra, A.; Mayer, S.; Mitchell, D.; Rodrigues, M. J.; Organ, M. G. *Organometallics*, **2017**, 36, 3573-3577. A General Protocol for the Broad-Spectrum Cross-Coupling of Nonactivated Sterically Hindered 1° and 2° Amines.
2. Khadra, A.; Mayer, S.; Organ, M. G. *Chem. Eur. J.* **2017**, 23, 3206-3212. Pd-PEPPSI-IPent^{Cl}: A Useful Catalyst for the Coupling of 2-Aminopyridine Derivatives.
3. Khadra, A.; Organ, M. G. *J. Flow. Chem.* **2016**, 6, 293-296. *In situ* Generation and Diels-Alder Reaction of Benzyne Derivatives with 5-Membered Ring Heterocycles Using a Microcapillary Flow Reactor.

PART I: PALLADIUM PEPPSI- IPENT^{Cl}; A USEFUL CATALYST FOR CHALLENGING AMINATION REACTIONS

CHAPTER 1: INTRODUCTION

1.1 Significance of Aniline Derivatives.

Aniline derivatives are structural motifs that are frequently encountered in biologically active compounds, such as pharmaceuticals and pesticides, as well as in conductive materials, and ligands for transition metals.

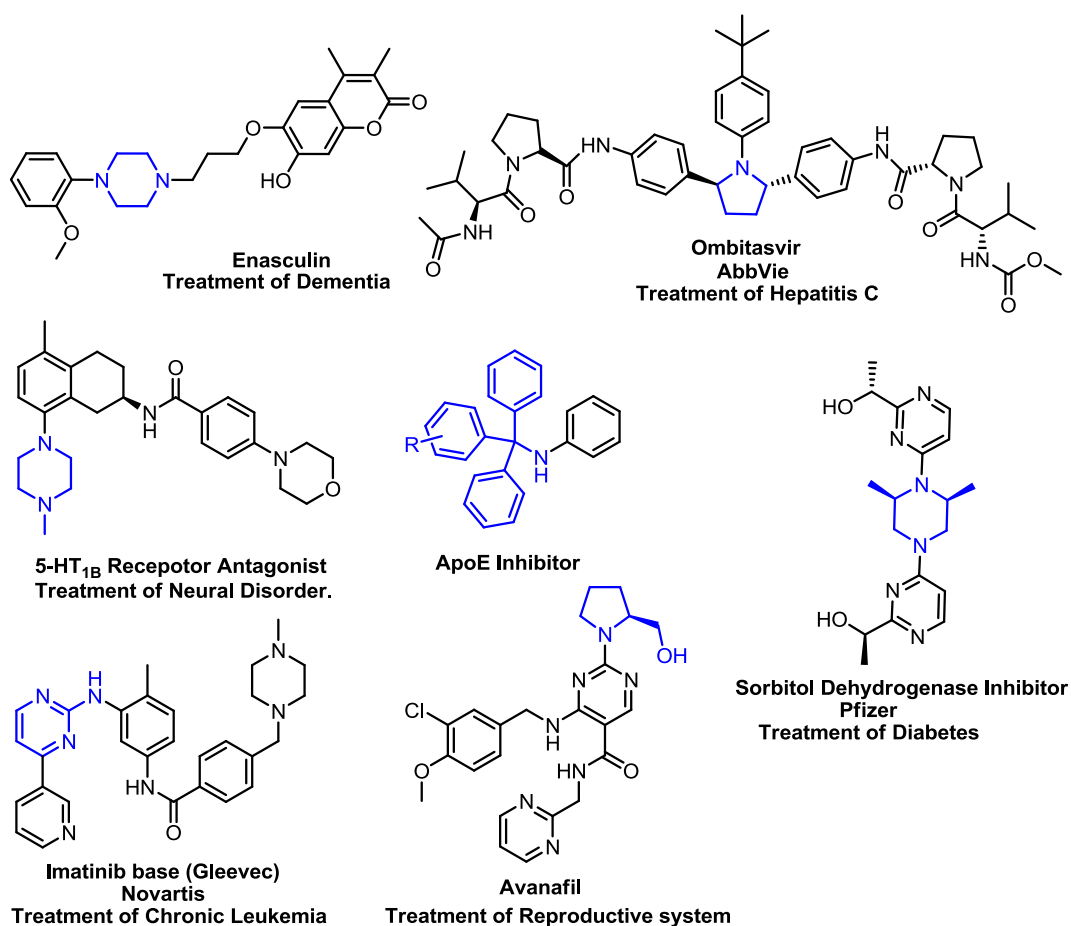
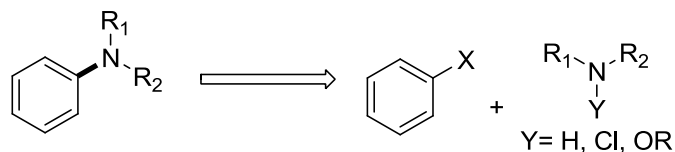


Figure 1: Selected examples of biologically active aniline derivatives.

. For instance, Enasculin is a coumarin with a phenyl piperazine moiety that has used for the treatment of dementia.¹ Serotonin, (5-hydroxytryptamine, or 5-HT)_{1B}, receptor antagonist was developed for the treatment of certain neural disorders.²

Triarylmethylamines have emerged as a new class of inhibitors to apolipoprotein E (apoE) production. ApoE is a cholesterol-and-lipid carrier protein that is associated with Alzheimer's disease, aging, atherosclerosis, and other lipid disorders.³ Imatinib, a 2-phenylamino-pyrimidine derivative that was developed by Novartis Pharma AG is used to treat patients with chronic myeloid leukemia (CML).⁴ Sorbitol Dehydrogenase Inhibitor (Figure 1) developed by Pfizer, is used for treating diabetic patients.⁵ Ombitasvir is an antiviral used for the treatment of Hepatitis C and this drug was developed by AbbVie in 2014.⁶ Avanafil has been identified as potent and highly selective phosphodiesterase-5 inhibitors for the treatment of erectile dysfunction.⁷

The next section will detail the synthetic methods typically used in the formation of anilines (Scheme 1), including those which are sterically hindered.



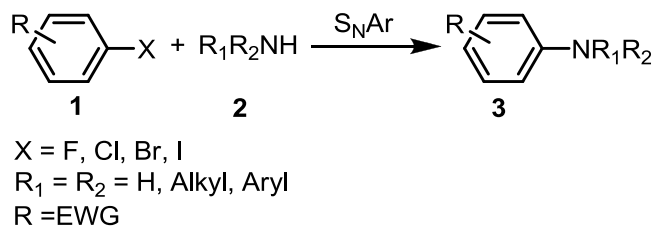
Scheme 1: General retrosynthesis of aromatic amines.

1.2 Synthesis of Aniline Derivatives.

The synthesis of aniline and aniline derivatives can be divided into two main categories: (a) classical and (b) metal-catalyzed methods. The section below will discuss each of these methods briefly.

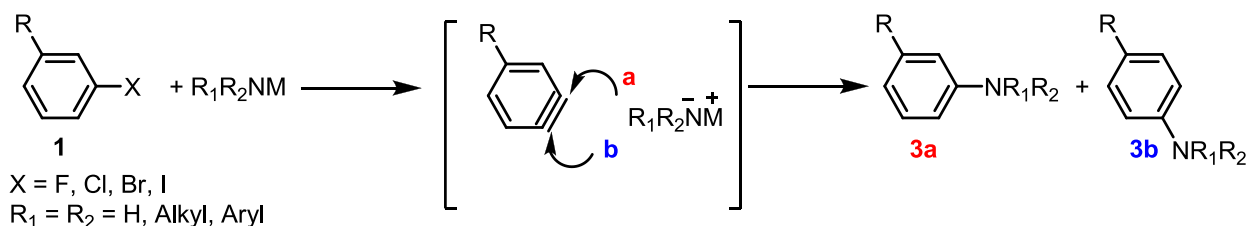
1.2.1 Nucleophilic Aromatic Substitution.

One of the oldest methods to prepare aniline derivatives is through nucleophilic aromatic substitution (S_NAr) of haloarenes **1** with amines **2** (Scheme 2). These reactions are usually conducted at high temperature and/or pressure to ensure full conversion.⁸ The presence of electron-withdrawing groups on the haloarenes facilitates substitution reactions and results in higher yields compared to the corresponding reaction conducted using unactivated or electron-rich haloarenes.⁸ This is due to the enhanced electrophilicity of the leaving group by electron-withdrawing substituents and heightened stability of the anionic intermediate which is known as a “Meisenheimer complex”. These reactions are usually carried out in the absence of base but the presence of weak bases such as carbonate or alkali bases has been shown to enhance conversions and improve yields.⁹



Scheme 2: Formation of arylamines through nucleophilic aromatic substitution.

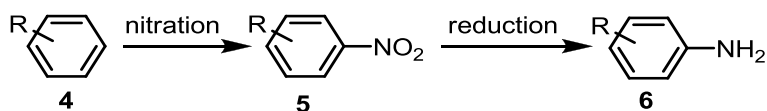
In most cases, the use of metal amides instead of neutral amines in S_NAr reactions changes the reaction mechanism and results in the formation of an aryne intermediate (Scheme 3). The formation of these highly reactive arynes has been confirmed by isotopic labeling,¹⁰ flash photolysis experiments, and mass spectrometry.¹¹ Additionally, benzyne has been trapped as a stable nickel complex.¹² For a given metal amide, the rate of aryne formation follows the order of $Br > Cl > F$ ¹³ and, for a given halogen, the elimination process follows a reactivity order of $Na > Li > MgBr$.¹⁴ Since there are two possible sites for nucleophilic attack (a or b, Scheme 3), this protocol typically results in the formation of regioisomers that are inseparable in many cases, which is a major drawback of this method. Additionally, the use of such strong bases limits the substrate scope and makes this procedure incompatible with base-sensitive functional groups.



Scheme 3: Formation of arylamines through benzyne intermediate.

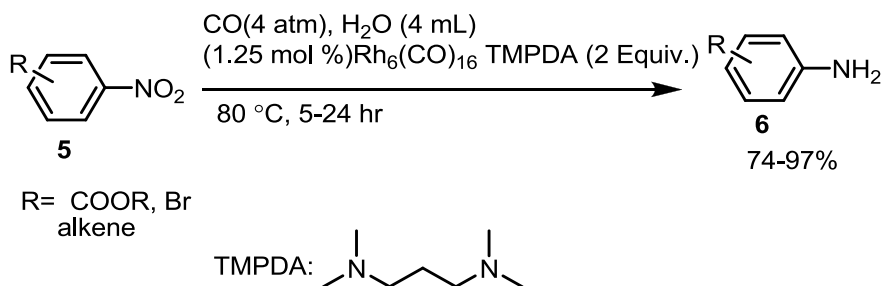
1.2.2 Aniline Derivatives from Nitrobenzenes.

Prior to metal-catalyzed sp^2C-N bond formation, aniline synthesis was carried out primarily by nitration of aromatic compounds, followed by reduction (Scheme 4).



Scheme 4: Arylamines formation through nitration followed by reduction.

Many aromatic compounds undergo nitration with a wide range of nitrating agents, with the most common conditions utilizing a mixture of concentrated nitric and sulfuric acids. Such harsh conditions are incompatible with a wide range of functionalities, which limits the use of this method. Subsequent reduction of the nitro compounds to the corresponding aniline may take place using a variety of methods such as catalytic hydrogenation or by using reducing agents. The most common reducing agents being Fe, Zn, or Sn in acid.¹⁵ The presence of other reducible functional groups such as ketones is problematic as a selective reduction of the nitro group can be quite challenging. This problem was addressed by Imanaka and co-workers, as they reported deoxygenation of nitro-aromatics with CO as reducing agent in the presence of water (Scheme 5). Upon screening different catalysts, Rh₆(CO)₁₆/TMPDA demonstrated high chemoselectivity in the presence of other reducible groups.¹⁶

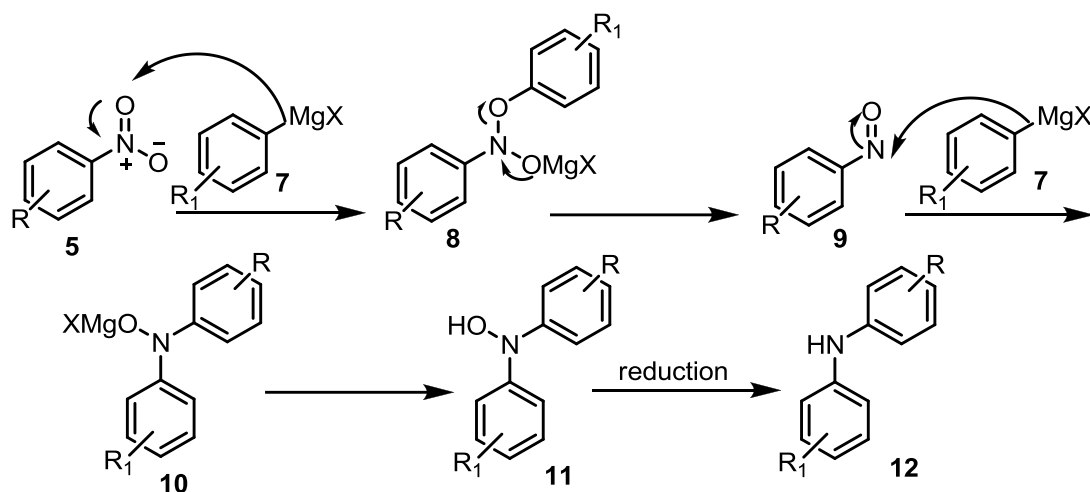


Scheme 5: Chemoselective reduction of NO₂ using Rh catalyst in the presence of other reducible groups.

1.2.3 Aniline from Nitrobenzene and Grignard reagents.

The synthesis of diarylamines using excess aryl Grignard and nitrobenzene has been known for several years. After multiple mechanistic investigations, it has been agreed that the reaction proceeds via nucleophilic attack by the aryl Grignard at the nitro group.¹⁷ This results in the formation of nitrosobenzene which then reacts with a second equivalent of Grignard reagent,

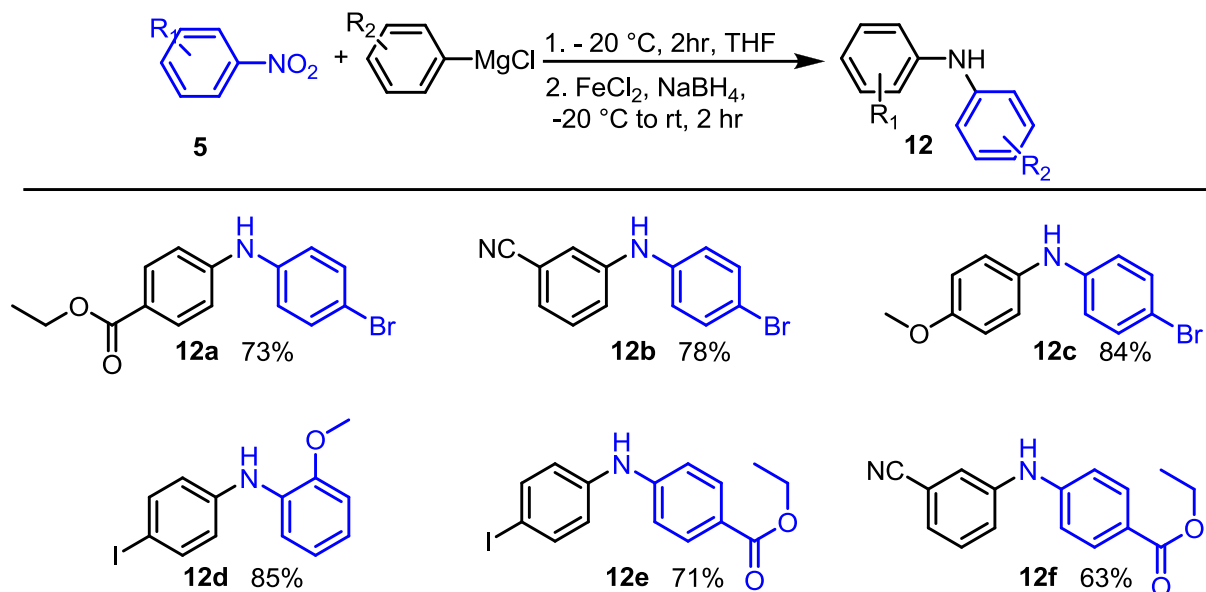
followed by reduction to deliver the desired diarylamine (Scheme 6). This reaction is limited to the use of aryl Grignard reagents, as alkyl derivatives are known to attack the aromatic ring instead of the nitro group.¹⁸



Scheme 6: Mechanism of aniline synthesis using Grignard reagents and nitrobenzene.

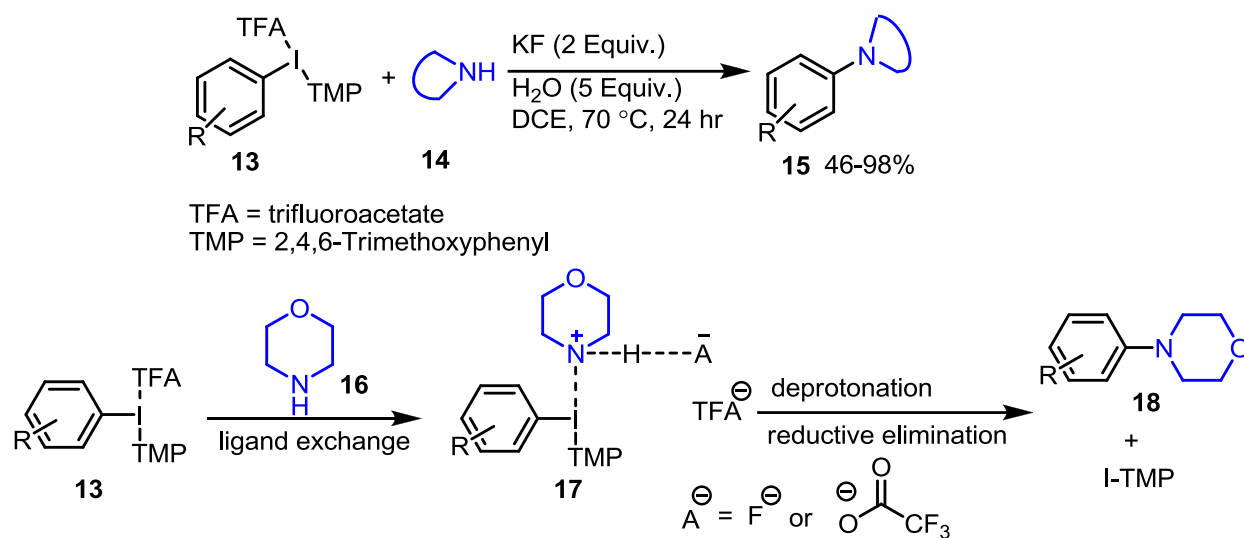
More recently, excellent work has been published by Sapountzis and Knochel for the preparation of polyfunctional diarylamines using Grignard reagents with excellent yields and wide substrate scope, including sensitive groups such as ester, nitrile and iodo substituents. In the latter cases, the addition at the nitro group is faster than the addition to the electron-poor groups like carbonyl and esters.

Moreover, the reaction is compatible with both electron-donating and electron-withdrawing substituents on the nitrobenzene. The only major drawback of this method is the necessity to use two equivalents of Grignard reagents.¹⁹

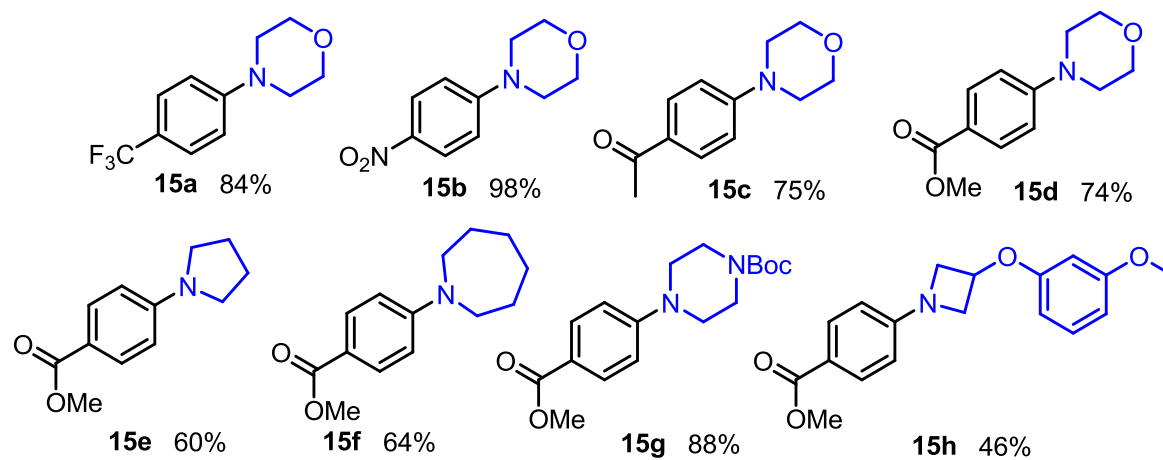


Scheme 7: Substrate scope for preparation of polyfunctional diarylamines.

Another metal-free, mild approach to $\text{sp}^2\text{C-N}$ bond formation has been reported by Stuart and co-workers, who utilized diaryliodonium salts and coupled them with unhindered secondary cyclic amines (Scheme 8).²⁰ The proposed mechanism for this transformation is demonstrated in Scheme 8. Ligand exchange of the trifluoroacetate for the coordinated amine group yields iodane intermediate **17**. This may be facilitated by mild nucleophilic activation through hydrogen-bonding of the amine to fluoride anion, trifluoroacetate or excess amine present in the reaction mixture. Finally, deprotonation and reductive elimination may occur subsequently or in a concerted fashion to deliver the aryl amine and TMP-I. This reaction accommodates a variety of substrates including those that currently pose a challenge to the classical metal-free C-N coupling reactions such as ester and keto groups. However, only cyclic amines have been employed as the nucleophilic partner suggesting that this process has a significant limitation.



Scheme 8: Metal-free amination using aryl(TMP)iodonium trifluoroacetate.

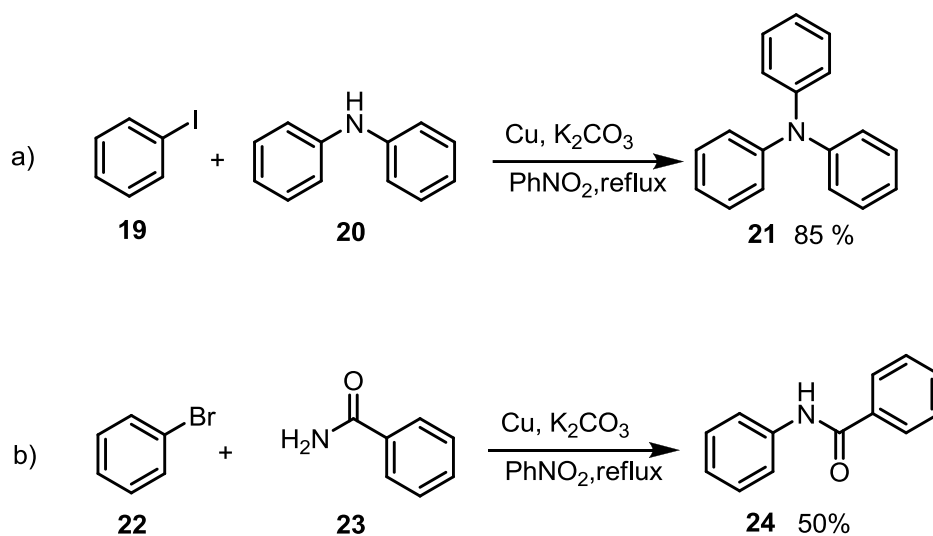


Scheme 9: Substrate scope for the metal-free amination using aryl(TMP)iodonium trifluoroacetate.

1.3 Metal-Catalyzed Amination Reactions.

1.3.1 Copper-Mediated C-N Bond formation.

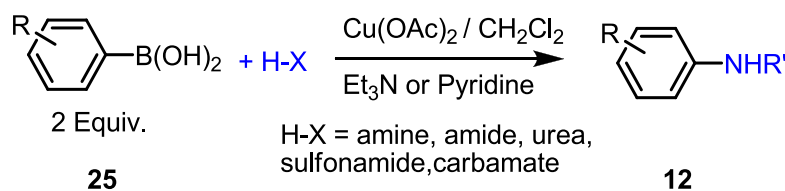
One of the earliest examples of metal-catalyzed C-N bond formation was reported by Ullmann in 1903 (Scheme 10 a),²¹ and this was followed by Goldberg's report of amide *N*-arylation reactions. (Scheme 10 b).²² In these reactions, an aryl halide is coupled with an amine or amide in the presence of a base and a copper salt or copper powder.



Scheme 10: Ullmann and Goldberg copper-mediated amination reactions.

The need for a high reaction temperature and stoichiometric amounts of copper, combined with the modest yields of products, constitute major drawbacks and limit the application of these methods. In spite of these limitations, Ullmann and Goldberg reactions represented the state-of-the-art in copper-mediated C-N coupling reactions for almost a century.²³

In 1998, Chan,²⁴ Evans,²⁵ and Lam²⁶ independently published a new method to conduct copper-mediated amination reactions.

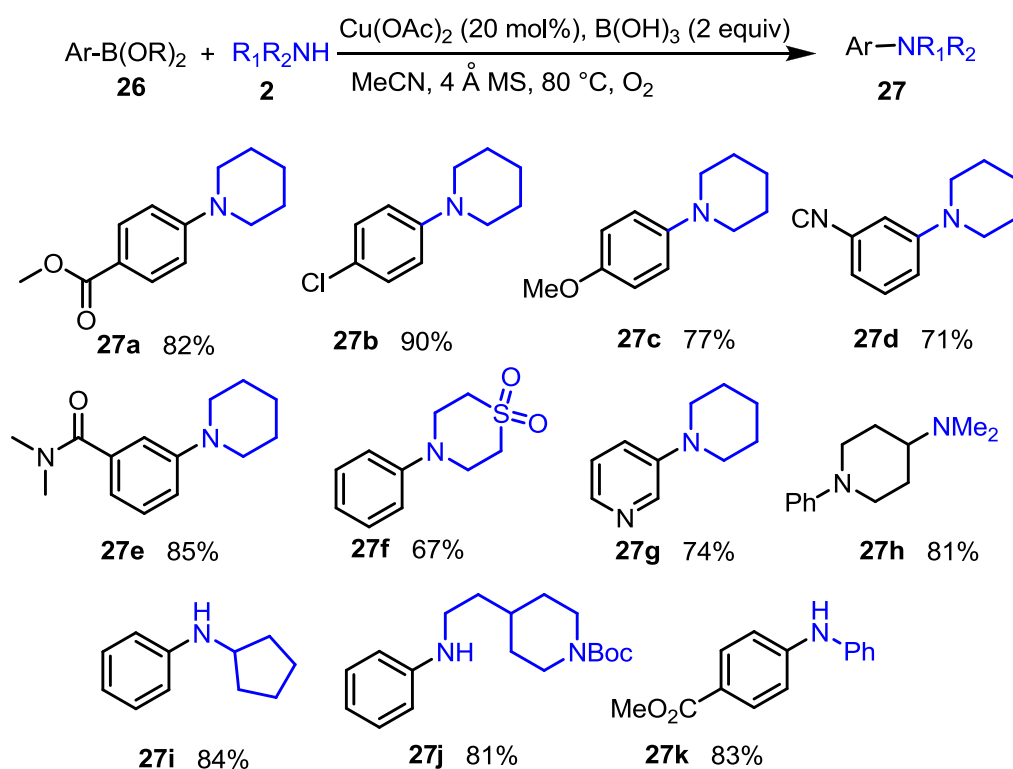


Scheme 11: Chan's protocol for coupling substrates containing nitrogen.

Chan and co-workers reported a variety of C-N bond forming reactions using arylboronic acids (2 equivalents) in the presence of copper diacetate and a base such as triethylamine or pyridine. A variety of nitrogen-containing compounds such as amines, anilines, carbamates, sulfonamides, and urea(s) undergo a coupling reaction to deliver the desired product in moderate to excellent yields (Scheme 11). Further optimization by Collman and co-workers revealed that catalytic amounts of copper could affect the transformation.²⁷ The ability to conduct these reactions under mild conditions, coupled with the wide commercial availability of arylboronic acids made this method popular for synthetic applications. However, the Chan-Evans-Lam amination does have notable limitations, such as the significant formation of side-products (i.e reduced product, diaryl ether, and phenols) and the lack of general reactivity of arylboronic acid pinacol (BPin) esters, especially with arylamines.²⁸ Aryl BPin are readily accessible by transition-metal catalysis, they are generally more stable than arylboronic acids, and therefore improving their reactivity is quite desirable. To address these issues, a more thorough understanding of the exact mechanism was needed.

Stahl's report on the related etherification provided a solid foundation for understanding these copper-based oxidative couplings.²⁹ In 2017, Watson and co-workers extended Stahl's work and reported a detailed investigation of the Chan-Lam reaction mechanism.³⁰

A combination of spectroscopic techniques, computational modeling, and crystallography enabled a complete mechanistic description of the process including off-cycle resting states, the origin of oxidation/protodeboronation side reactions and the source of amine and organoboron reactivity issues. The identification of key mechanistic events has allowed the development of a simple solution to these problems. By controlling the oxidation of Cu(I) to Cu(II), and manipulating three synergistic roles of boronic acid diminished the formation of side-products and made this process more general, thus overcoming the limitations associated with this valuable transformation. Despite these advances and the broad substrate scope, the coupling of sterically hindered amines remained unreported and low yield was obtained with ortho-substituted arylboronic esters (Scheme 12).

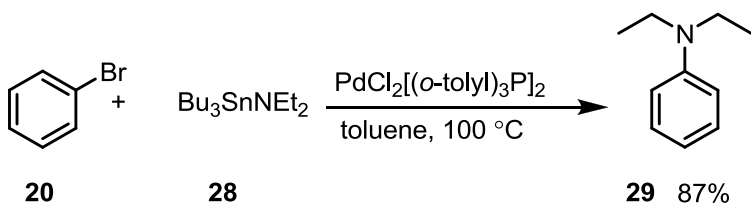


Scheme 12: Substrate scope using B(OH)₃-Promoted Catalytic Chan-Lam reaction

1.3.2 Palladium-Catalyzed C-N Bond Formation.

In 2010 a noble price was awarded to Richard Heck, Ei-ichi Negishi and Akira Suzuki for developing the most practical methods to form C-C bonds. Their tremendous achievement had laid the foundations of the field of palladium-catalyzed cross-coupling reactions, which now have become the most versatile and widely used methods in organic synthesis. This discovery revolutionized the way chemists construct molecules while at the same time provide methods to improve and overcome the challenges associated with C-C bond forming processes. Coupling reactions was not only limited to C-C bond formation but was extended to include C- heteroatom (C-O, C-S and C-N) bonds.

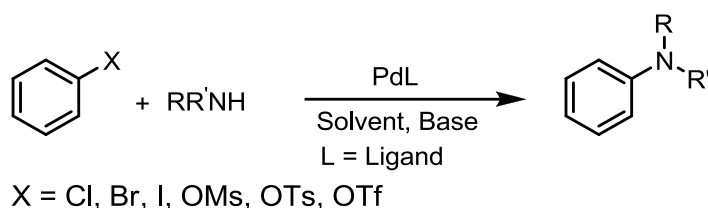
Since the seminal report by Migita et al. demonstrated the Pd-catalyzed C-N bond formation using aryl bromides and *N, N* dimethylamino butyl tin (Scheme 13),³¹ a tremendous progress has been made in the field of Pd-catalyzed amination reactions. In 1985, Yagupol'skii and co-workers reported the first free amine in Pd-catalyzed aryl amination.³²



Scheme 13: First Pd-Catalyzed C-N bond formation by Migita and co-workers.

Later, the contributions from the Buchwald and Hartwig research groups have established the powerful nature of this method by reacting different aryl halides and aryl triflates with anilines in the presence of a suitable base and ligand. The reaction's synthetic utility stems primarily from overcoming the problems associated with methods described above (e.g. $\text{S}_{\text{N}}\text{Ar}$,

Nitration/Reduction of arenes etc.). With most classical methods suffering from limited substrate scope and functional group tolerance, the Buchwald-Hartwig amination reactions allow for the facile synthesis of arylamines under relatively mild conditions while significantly expanding the repertoire of the possible C-N bond formations. As a result, Buchwald-Hartwig amination has become an indispensable tool for medicinal and organic chemists (Scheme 14).



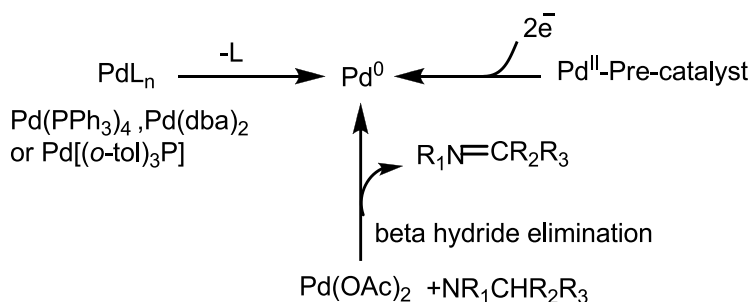
Scheme 14: Palladium-catalyzed Buchwald-Hartwig amination.

1.3.2.1 Mechanism of Buchwald-Hartwig Amination.

1.3.2.1a Catalyst Activation

The accepted mechanism for Buchwald-Hartwig amination includes four elementary steps (Scheme 16). The first step is catalyst activation. There are several approaches to generate the active catalyst in amination reactions and using a Pd^0 source is the simplest approach. Examples of Pd^0 species include $\text{Pd}(\text{PPh}_3)_4$, $\text{Pd}(\text{dba})_2$, and $\text{Pd}[(o\text{-tol})_3\text{P}]_2$. While these catalysts provide Pd^0 required for the reaction to commence, the electronic and steric properties of palladium in these species do not meet the threshold for good catalyst performance with most substrates to deliver the desired product. Therefore, changing the ancillary ligands is crucial to improving the catalyst performance.³³ Pend and co-workers demonstrated that mixing $\text{Pd}(\text{dba})_2$ with bulky phosphine ligands is effective for the generation of active catalysts used in amination and sulfonation reactions.³⁴ Another method for catalyst activation is using $\text{Pd}(\text{II})$ sources with an added ligand. The most commonly used $\text{Pd}(\text{II})$ reagent is $\text{Pd}(\text{OAc})_2$. Alkylamines that contain β hydrogens may

activate the catalyst through β -hydride-elimination.³⁵ However, aniline and ammonia do not have β hydrogens and so cannot activate the catalyst through this path. Although the activation mechanisms are still not clear, reactions with anilines and ammonia require $> 80^\circ\text{C}$ if $\text{Pd}(\text{OAc})_2$ is used. In the case of ammonia, an incomplete conversion to products was observed when using $\text{Pd}(\text{OAc})_2$, but the full conversion was achieved upon using $\text{Pd}(0)$ complex.³⁶ A general strategy for catalyst design is the use of $\text{Pd}(\text{II})$ pre-catalyst that is coordinated to an ancillary ligand responsible for tuning the steric and electronic properties of the metal that help to enhance catalytic performance. The pre-catalyst may also contain other stabilizing ligands that are displaced during the reaction or reductively eliminated to generate an active catalyst (Scheme 15). Amines or bases utilized in the reaction are in most cases responsible for generating $\text{Pd}(0)$. However, if the reduction is not facile, reducing agents such as LiO^iPr or organometallic reagents such as Grignard is used.³⁷

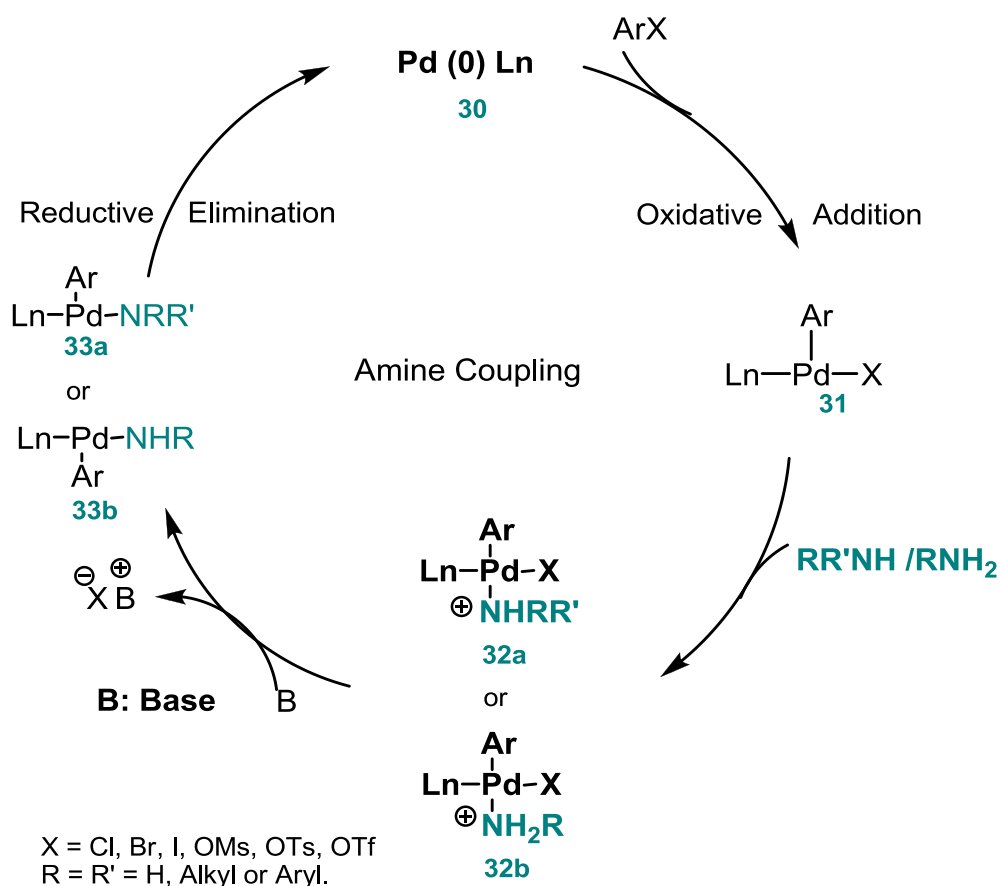


Scheme 15: Different methods for generation of $\text{Pd}(0)$ catalyst in Buchwald-Hartwig amination.

1.3.2.1b Catalytic cycle

Once the active catalyst is generated, oxidative addition of $\text{Pd}(0)$ into the C-X bond generates intermediate **31** (Scheme 16). Although the rate of oxidative addition primarily depends on the catalyst, the steric and the electronic properties of the substrate also affect the reaction rates. Electron-poor aryl halides or aryl pseudohalide are electrophilic and undergo oxidative addition

easily, hence they are often referred to as “activated substrates”. Electron-rich and sterically congested aryl halides are more challenging substrates for oxidative addition, thus they are “deactivated” substrates. After oxidative addition, amine coordination takes place followed by deprotonation of the resulting Pd-ammonium complex (**32a** or **32b**) by the external base to furnish a Pd-amido complex (**33a** or **33b**).³³



Scheme 16: Proposed catalytic cycle for Pd-catalyzed Buchwald-Hartwig amination.

The rate of amine binding depends on both the catalyst and the amine’s steric and electronic properties. Electron-rich and sterically unhindered amines bind more readily to the metal species compared to less basic or more sterically hindered substrates. Bulky amines exhibit weaker coordination with the catalytic species resulting in a slower overall rate and, typically, low reaction

yields.³⁸ The subsequent deprotonation of the resulting Pd-ammonium complex depends on the propensity of the ammonium species to undergo deprotonation i.e, the more acidic the ammonium species, the more readily the deprotonation step occurs. Alkylamines ($pK_a \sim 35$ in DMSO) coordinate to the Pd(II) center readily, but deprotonation of the resulting metal-ammonium complex ($pK_a \sim 8\sim 10$) step is quite challenging with mild bases, such as carbonate (pK_a of $HCO_3^- \sim 10.5$). Conversely, anilines ($pK_a \sim 30$ in water, 25 in DMSO) have a lower binding affinity to the Pd(II) center but this is compensated by a faster deprotonation, due to the higher acidity of the anilinium complex ($pK_a \sim 5$) (all pK_a values in DMSO).³⁸

The last step in the catalytic cycle is the reductive elimination of the amido complex (**33a**, or **33b**) to deliver the desired product. Electron-rich complexes have a lower tendency to reductively eliminate than do electron-poor ones while increasing the steric bulk around the metal center enhances the rate of reductive elimination.³⁹

1.4 Ligand Development in Palladium-Catalyzed Buchwald-Hartwig Amination

In palladium-catalyzed cross-coupling reactions, ancillary ligands have a profound effect on the catalytic capacity of the metal, and as a consequence ligand design has become extensively studied. By implementing different functional groups on the ligand architectures such as electron-donating groups or electron-withdrawing groups, chemists are now able to improve the catalytic performance and increase the reaction efficacy and substrate scope of the Buchwald-Hartwig amination, as well as other cross-coupling reactions.

Catalytic performance can be evaluated based on two quantitative parameters: *Turn-Over Number (TON)* and *Turn Over Frequency (TOF)*. *TON* is defined by the number of catalytic cycles performed by a catalyst for a given reaction before its decomposition or deactivation. On the other

hand, *turn over Frequency (TOF)* is a number of catalytic cycles occurring at the metal center per unit time. The ultimate goal of ligand engineering is to increase the *TON*, therefore, increasing the catalyst stability and to increase *TOF*, thus reducing the overall reaction time and increase the overall catalytic productivity.

1.4.1. Phosphine Ligands

1.4.1.1 Quantifying Electronic and Steric Properties of Phosphine Ligands.

Tertiary phosphine ligands have been used extensively in cross-coupling reactions due to their electron-rich nature and significant steric shielding of the metal's coordination sphere. The electronic and the steric properties of these ligands can be tuned by varying the substituents attached to the phosphorous atom. Quantitative parameters to measure a ligand's electron donating strength and its steric bulk around the metal center were developed by Tolman in 1970.⁴⁰ The overall donor strength of a ligand to the metal can be determined by measuring the carbonyl stretching frequencies of their corresponding $\text{Ni(CO)}_3\text{L}$ species, otherwise known as its Tolman Electronic Parameter (TEP). In these complexes, a reduction in the carbonyl stretching frequency-wavenumber (ν) correlates to a metal center being more electron-rich due to the ligand's electron donation (Figure 3). Given the toxicity of Ni(CO)_4 , it is more common to determine ligand donicity experimentally from the carbonyl stretching frequencies of the corresponding $\text{Ir(CO)}_2\text{CIL}$ complexes which Crabtree has correlated directly to TEP values.⁴¹

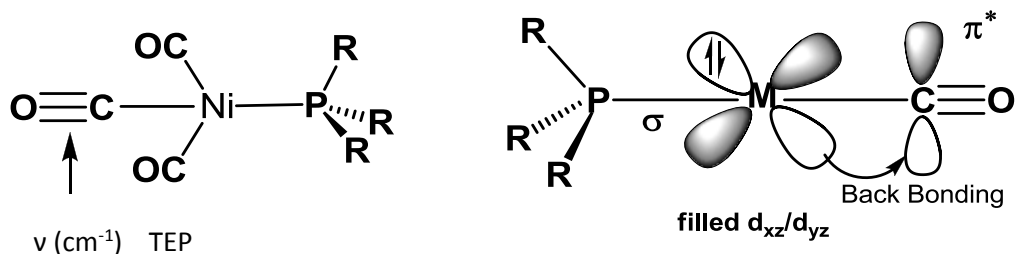


Figure 2: Backbonding in phosphine-metal-CO complexes.

The steric bulk of phosphine ligands may be quantified by measuring the ligand cone angle known as the Tolman Cone Angle, which is defined by the angle formed between the metal center and the outer edge of the ligand's outermost atoms (Figure 2). The Tolman Cone Angle is based on the standard distance of Ni-P (2.28 Å) and this calculation does not take ligand flexibility into consideration.⁴²

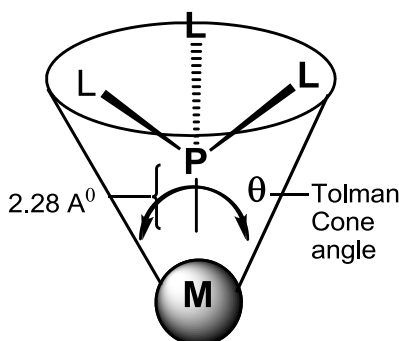
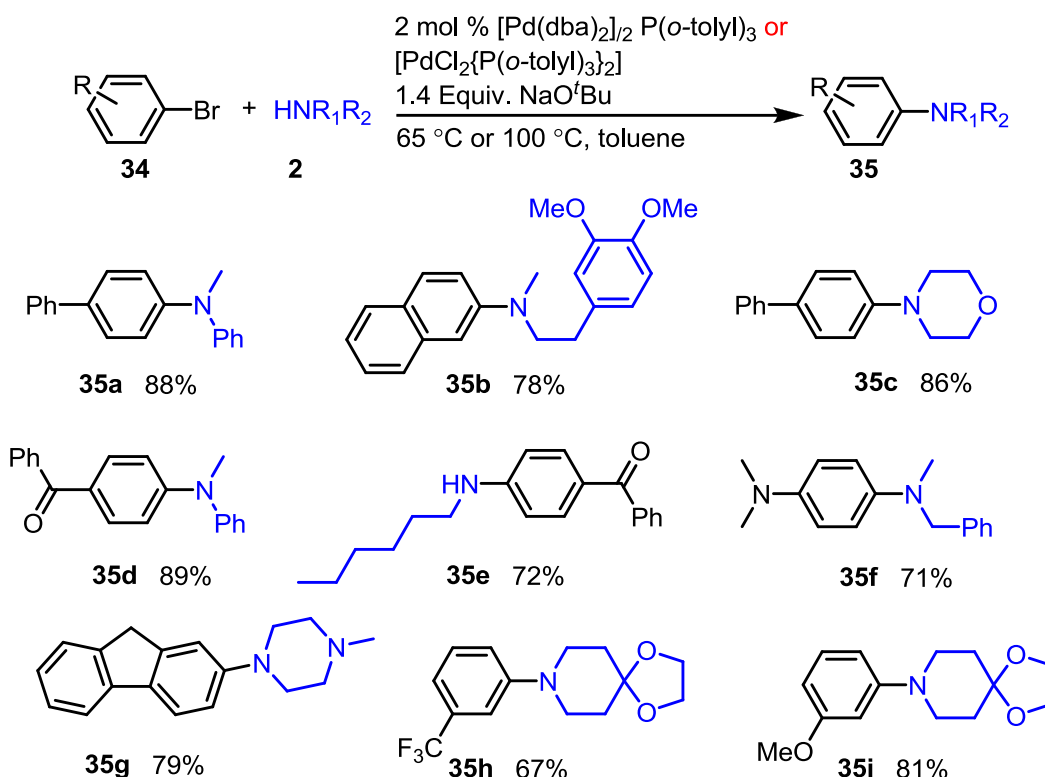


Figure 3: Tolman cone angle.

1.4.1.2 Phosphine Ligands in Palladium-Catalyzed Amination.

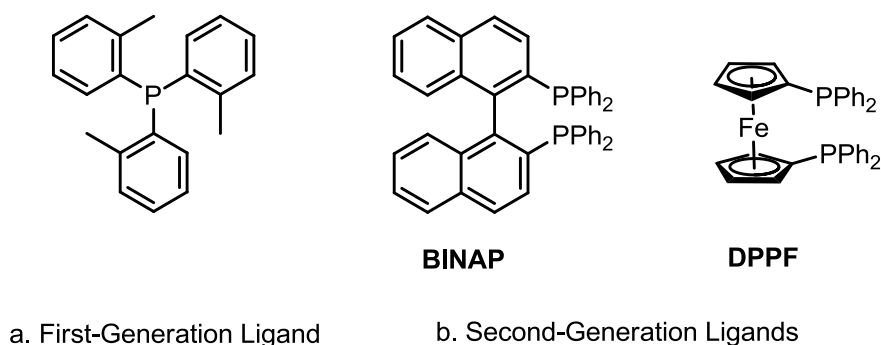
The use of triphenylphosphine as a ligand in Pd-catalyzed cross-coupling reactions is commonplace due to its commercial availability, ease of handling and low cost. However, the lack of broad applicability to the synthesis of more challenging and interesting products with this ligand

led to the development of tri-*o*-tolylphosphine which was used in Migita's amination protocol³¹ and in the approach to couple simple amines by Buchwald⁴³ and Hartwig⁴⁴. The original reports by Buchwald and Hartwig used PdCl₂ or Pd (dba)₂ with P(*o*-tolyl)₃ as a ligand, and a reasonable range of electron-rich and electron-poor aryl bromides were coupled with a limited number of secondary amines (Scheme 17).



Scheme 17: Buchwald amination using first-generation phosphine ligand.

Despite the reasonable utility of this method, it had limitations. First, only secondary, non-bulky amines were good candidates. Primary amines could only be coupled with a limited class of activated aryl bromides. Second, these methods were incompatible with both aryl chlorides and aryl iodides as electrophilic coupling partners.



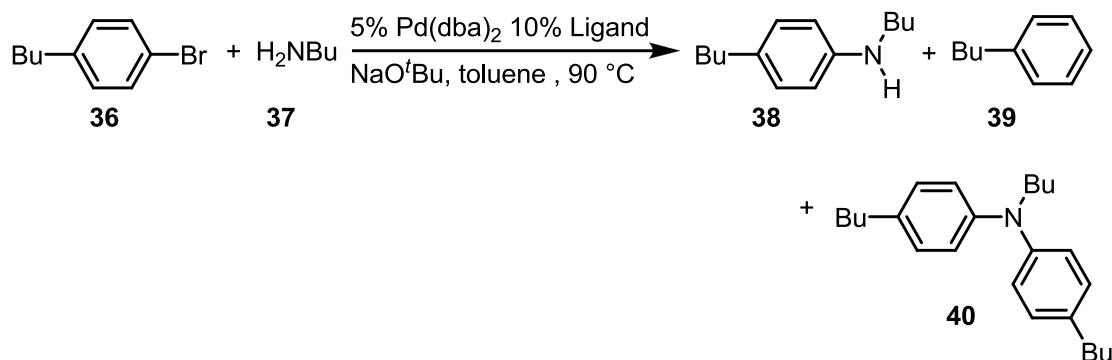
Scheme 18: First and second-generation phosphine ligands.

The second-generation ligand systems developed were aryl-substituted bisphosphine ligands. The Buchwald group focused on BINAP³³ while Hartwig and co-workers turned their attention towards the use of DPPF.⁴⁵ Buchwald's interest in bidentate ligands for C-N cross-coupling stemmed from the fact that previous transition metal complexes bearing bidentate ligands were shown to slow β -hydride elimination reactions while promoting both oxidative addition and reductive elimination. During the course of these studies, it was demonstrated that using BINAP with Pd_2dba_3 promoted the cross-coupling of primary amines and improved the yields of more challenging substrates.³³

Hartwig reported that using DPPF not only enabled the coupling of primary amines and aryl halides that were not possible with $\text{P}(o\text{-tolyl})_3$, but he also demonstrated that sterically hindered phosphine ligands are not necessary to promote the cross-coupling of primary amines. In 1998, Hartwig described the effects of varying the steric and electronic properties and the bite angle of various bidentate phosphine ligands on product ratios in the amination of aryl bromides, and the results obtained showed that catalysts containing electron-rich, modestly hindered phosphine ligands with small bite angles ($\sim 90^\circ$) gave the best selectivity for the desired product versus the

reduced products, and ligands with small bite angles gave higher monoarylation –to- diarylation ratios (Table 1).⁴⁶

Table 1: Effect of bite angle on amination reaction between **36** and **37**.



Entry	Ligand	Bite angle	% Yield of 39	% Yield of 38	% Yield of 40
1	DPPN	82°	1.4 ± 1.0	78 ± 3.8	5.7 ± 0.7
2	BINAP	92.7 °	0.9 ± 0.2	91 ± 2.0	3.0 ± 0.3
3	DPPF	99.0 °	4.4 ± 0.2	52 ± 2.5	22 ± 1.0
4	DPPR	101 °	36 ± 2.0	12 ± 1.0	5.2 ± 3.4
5	DPPDPE	101	40 ± 2.5	11 ± 1.0	3.6 ± 0.9
6	DPPX	109	24 ± 1.8	47 ± 3.0	7.0 ± 1.4

DPPN

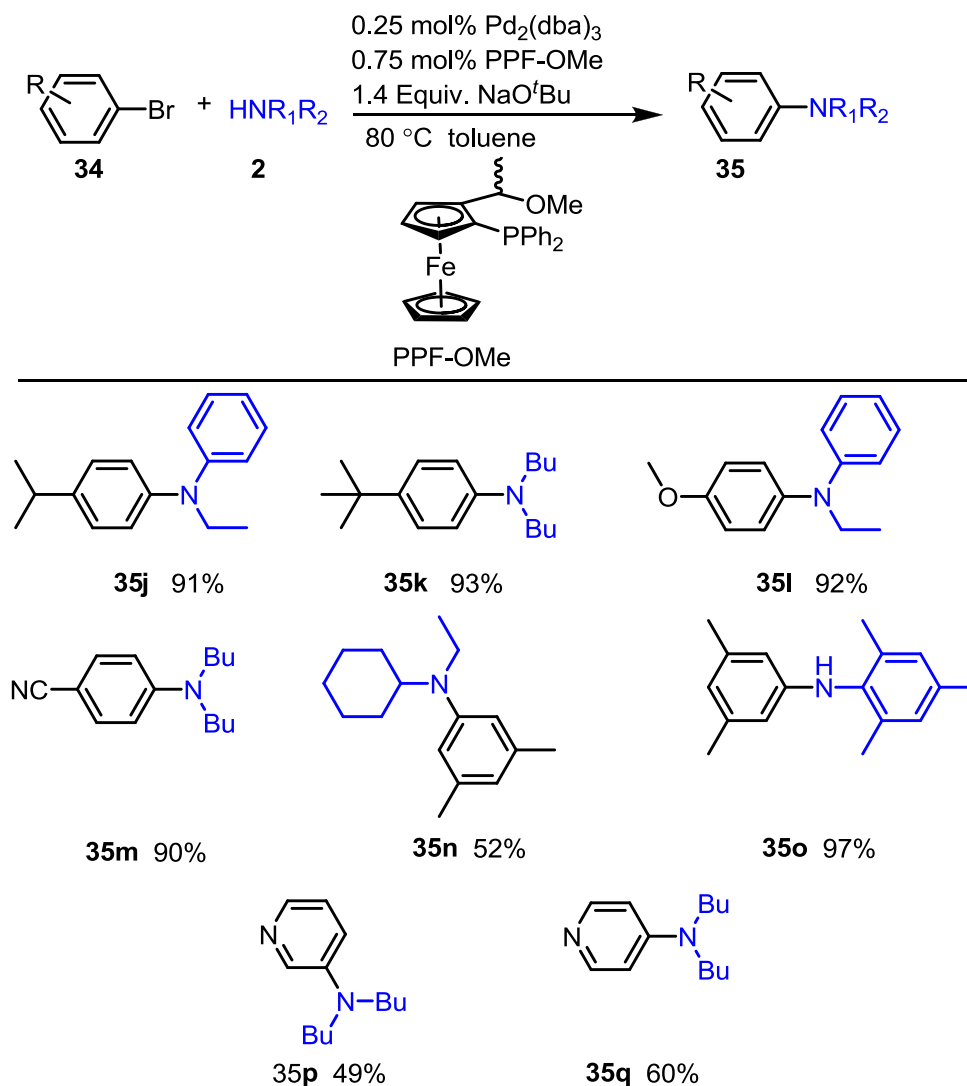
DPPR

Ar = o-tolyl DPPDPE

XantPhos

Despite these advances, the cross-coupling of several substrates types remained challenging, such as acyclic secondary amines,⁴⁷ leading to further exploration of alternative ligands. Buchwald

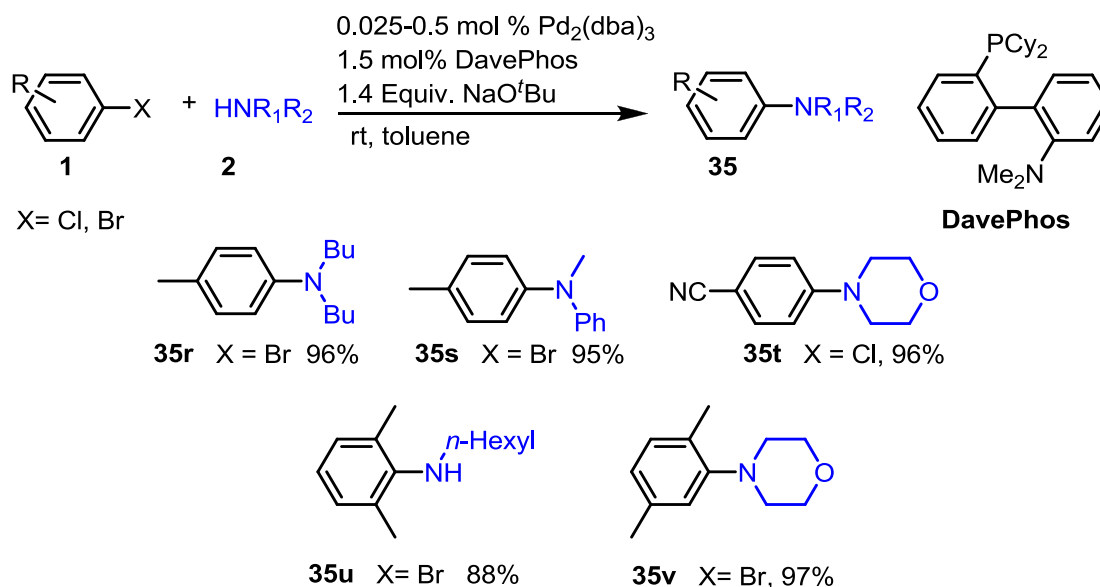
started investigating Kumada's ferrocenyl ligands to promote cross-coupling of secondary acyclic amines.³⁸ Upon screening different ligands, the PPF-OMe (Scheme 19) ligand was found to be effective in the cross-coupling of unactivated aryl bromides with cyclic and acyclic secondary amines in generally good yields but was ineffective for coupling unhindered primary anilines.⁴⁷



Scheme 19: Amination of cyclic and acyclic secondary amines using PPF-OMe ligand.

Despite these developments, cross-coupling of aryl chlorides remained quite challenging. In 1998, Buchwald published ^1H -NMR studies of amination reactions of aryl bromides using $\text{BINAP}/\text{Pd}(\text{OAc})_2$ and concluded that oxidative addition was the rate-limiting step.^{48,49} Therefore,

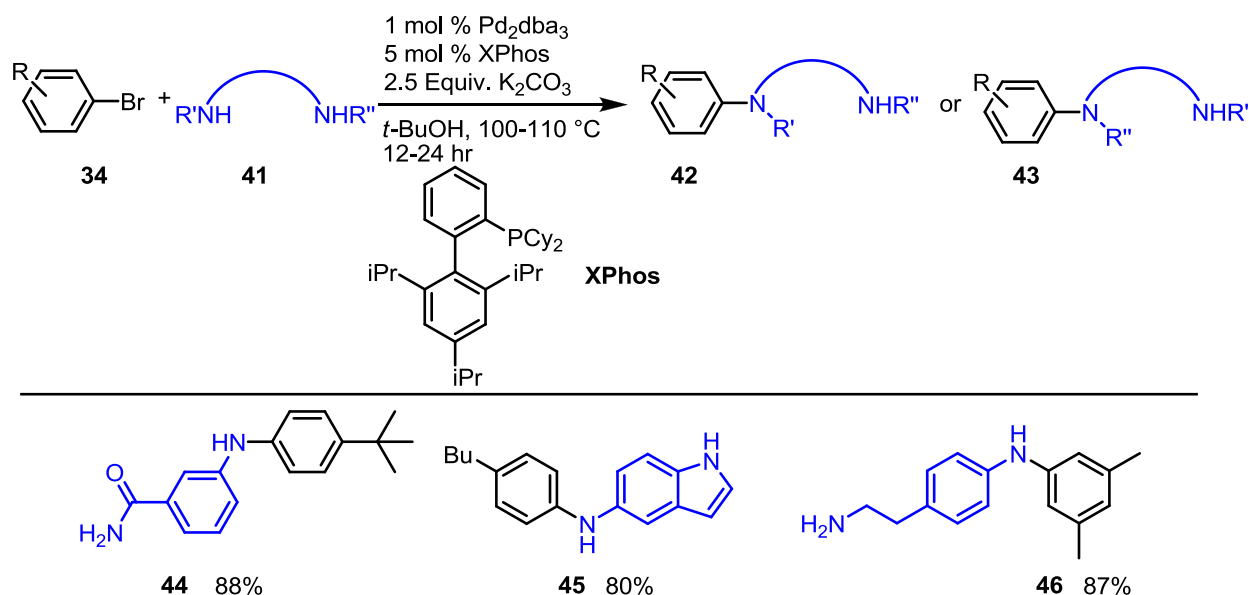
it was anticipated that the oxidative addition for aryl chlorides will be even more sluggish. To facilitate this slow step, they focused on preparing electron-rich bidentate phosphine ligands. First, they prepared the 2,2'-bis(dicyclohexylphosphino)-1,1'-binaphthyl ligand, which was effective in coupling pyrrolidine with 4-chlorotoluene. This important result, along with their experience with the bidentate monophosphine PPF-OMe, promoted the synthesis of the aminophosphine known as DavePhos⁴⁹ (Scheme 20). This ligand demonstrated a high reactivity and coupled with a wide range of aryl bromides and chlorides employing low catalyst loading and some reactions could be conducted at room temperature.



Scheme 20: Amination of secondary amines at rt using DavePhos.

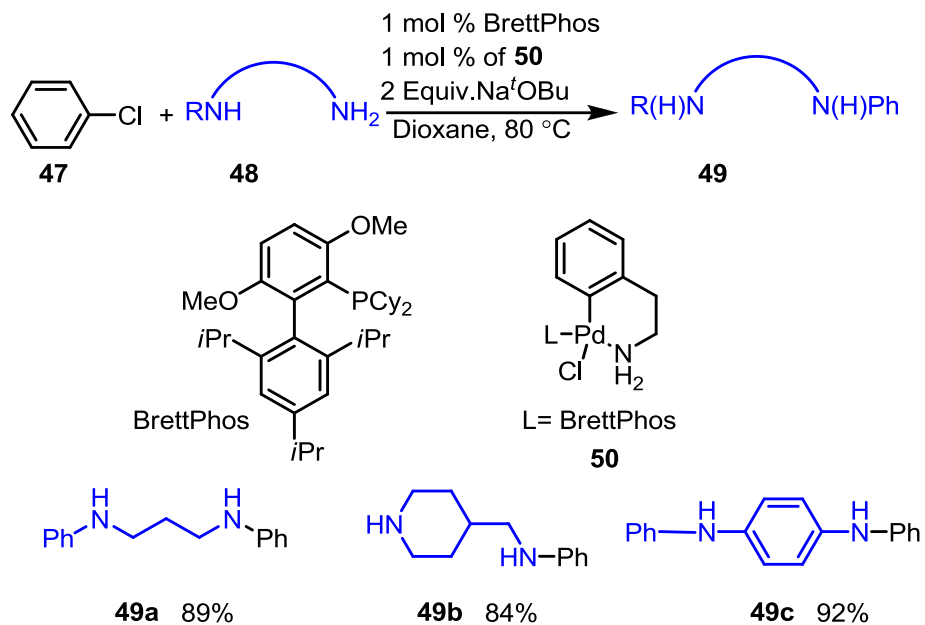
Although the presence of an amino or methoxy group was part of the design of these ligands, further studies showed that the nitrogen substituent could inhibit some reactions, thus their desamino analogs dialkylphosphino-2-biphenyl ligands were prepared and the results confirmed that these changes led to catalysts that showed wider generality.⁵⁰

Several biarylphosphine ligands have been reported including XPhos, SPhos, RuPhos, and BrettPhos, and these ligands demonstrated remarkable activity. XPhos allows chemoselective amination, where anilines undergo preferential arylation in the presence of another N-H group such as indolyl, alkylamino or amides (Scheme 21).⁵¹

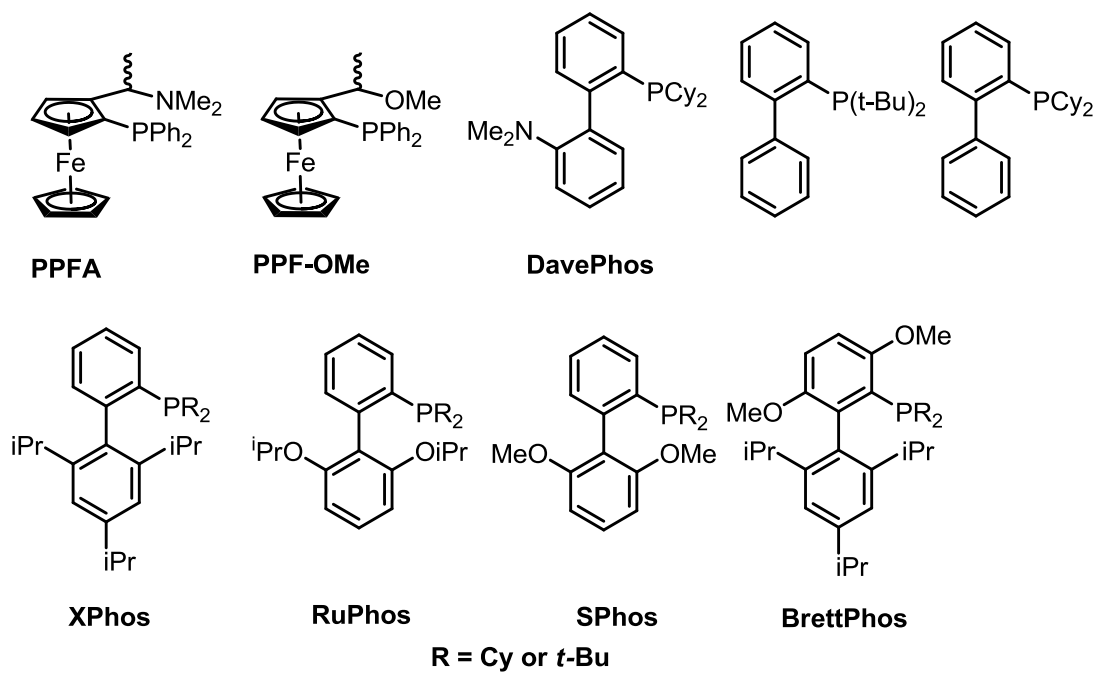


Scheme 21: Chemoselective amination of aniline using Xphos.

The use of BrettPhos promoted the amination of aryl mesylates⁵² and the monoarylation of primary amines with aryl chlorides. It is noteworthy that this catalytic system enabled monoarylation of some traditionally challenging diamine substrates containing two reactive amine sites, for example, primary and secondary amine (Scheme 22).



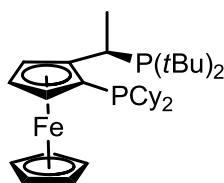
Scheme 22: Selective amination of primary versus secondary amines using BrettPhos.



Scheme 23: Third-generation phosphine ligands.

Although third-generation ligands (biaryl monodentate phosphines) have clearly demonstrated their utility in Buchwald-Hartwig amination, the need to further expand the reaction scope and develop milder reaction conditions is a continuing goal. Second-generation bidentate phosphine ligands proved to be better at stabilizing late transition metals such as palladium. The increased steric bulk around the metal center and the presence of two binding sites on the ligand can be extremely beneficial for the coupling of primary amines which have a high potential for diarylation. Additionally, bidentate phosphine ligands are less prone to be displaced by nucleophilic amine substrates. This nucleophilic attack on the metal center can limit the catalyst lifetime through the formation of inactive species, and this has been reported to occur with pyridine and ammonia.⁵³

These deficiencies led to the development of a fourth-generation ligand, “JosiPhos”, that is bidentate, rigid, electron-rich and sterically hindered. The nature of the ligand backbone of JosiPhos enhances chelation with the metal, thereby making the complex less susceptible to catalyst decomposition via ligand displacement by the electron-rich amines or heteroaromatic substrates. This increases the efficiency of coupling with ammonia, halopyridines, and other challenging substrates.

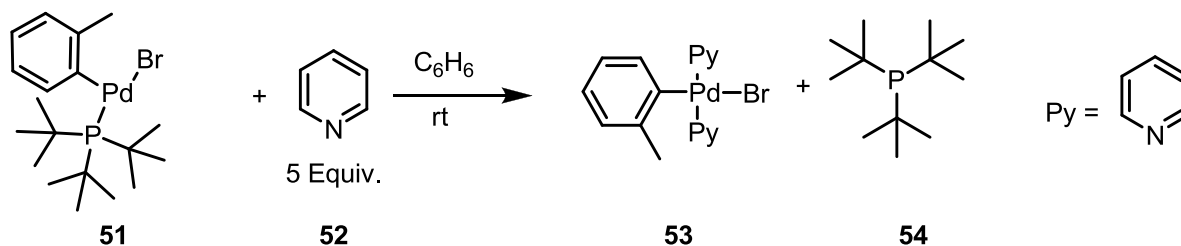


JosiPhos

Scheme 24: Fourth-generation phosphine ligand.

1.4.1.3. Deficiencies of Phosphine Ligands.

Although phosphine ligands are the most common ligands used in palladium catalysis, they suffer from several disadvantages. First, even the most strongly donating ligands, such as P^tBu_3 , are relatively labile and can dissociate readily from the metal, which disrupts the catalytic cycle significantly. This was demonstrated by Hartwig's report that the treating Pd(II) intermediate $[(\text{P}^t\text{Bu}_3)\text{Pd}(\text{o-tol})\text{Br}]$ with an excess amount of pyridine resulted in the complete substitution of the phosphine ligand by pyridine (Scheme 25).⁵⁴ Second, electron-rich phosphine ligands have a high propensity to oxidize in air, thus special handling in an inert atmosphere is often required. Finally, the high cost associated with bulky tertiary phosphine ligands has encouraged researchers to explore alternative catalytic systems.



Scheme 25: Liability of phosphine ligands in palladium catalysis.

As an alternative to phosphine ligands, *N*-heterocyclic carbenes (NHCs) have been used increasingly as ligands in Pd-catalyzed cross-coupling due to the high reactivity of Pd-NHC complexes. In comparison to phosphine ligands, NHCs are stronger σ -donors, rendering oxidative addition of the aryl halide to palladium more facile.⁵⁵ In addition, the significant steric bulk brought by NHC substituents facilitates the reductive elimination step of most catalytic cycles. Finally, the strong interaction between the carbenic carbon of the imidazole moiety and the metal increases the

stability of the complex under oxidative conditions and higher temperatures, thereby minimizing the need for the excess ligand.⁵⁶

1.4.2. N-Heterocyclic carbene (NHC) ligands.

NHCs are cyclic neutral compounds containing a divalent carbon atom with six valence electrons bound to at least one nitrogen atom within the heterocycle. This divalent carbene-type carbon exists in a singlet state, where both electrons occupy sp^2 orbital (Figure 4).

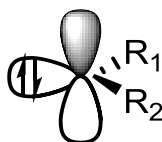
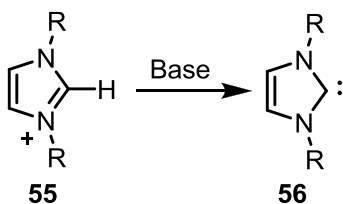


Figure 4: Singlet state of NHC carbenes.

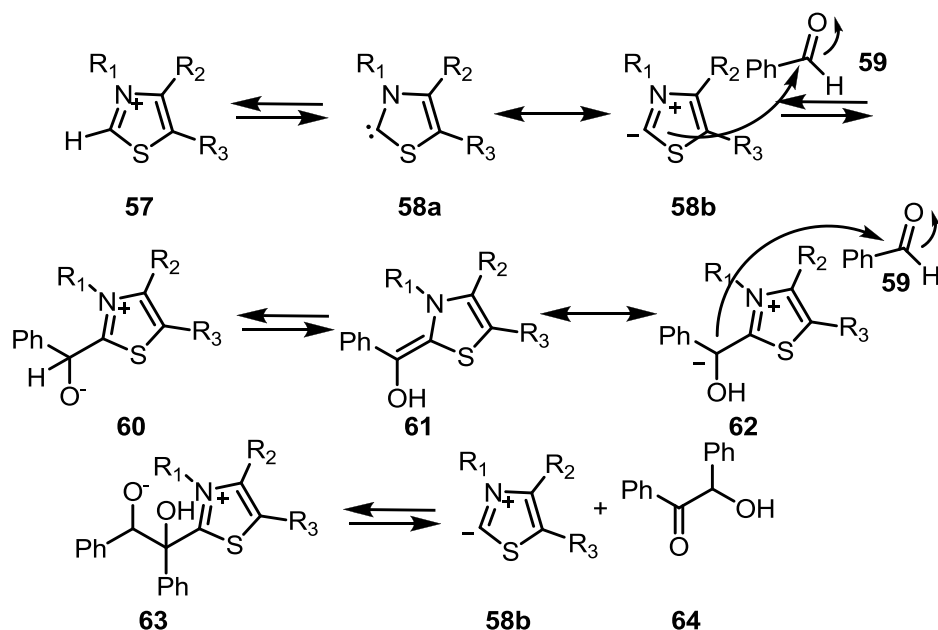
The induction and resonance effects of the nitrogen atom(s) stabilize the carbene's singlet state.⁵⁷ This is known as the “push-pull” effect. The nitrogen atom(s) is (are) inductively electron withdrawing yet contribute electron density by resonance. NHC(s) are formed by deprotonation of their corresponding salts whose pK_a values range between 20 and 25 (Scheme 26).



Scheme 26: Generation of NHC by deprotonation.

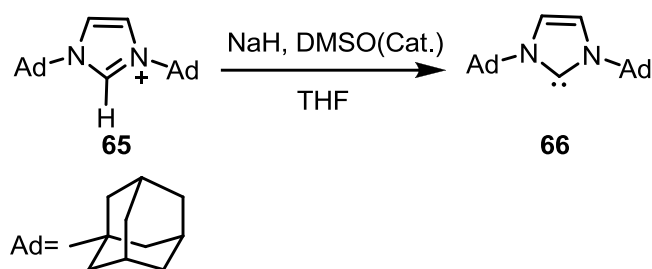
A variation of the size of the carbene ring, the presence of additional heteroatoms within the heterocycle or the substituents bonded to the nitrogen atom(s) lead to an array of different NHCs with different electronic and steric properties.

In 1943, Ugai and co-workers reported the first reaction using NHC, where they demonstrated that thiazolium salt can catalyze the self-condensation of benzaldehyde to produce benzoin.⁵⁸ Based on this report, Breslow *et al.* proposed a mechanism for this transformation in which the active catalytic species is a nucleophilic carbene derived from the thiazolium salt (Scheme 27).⁵⁹



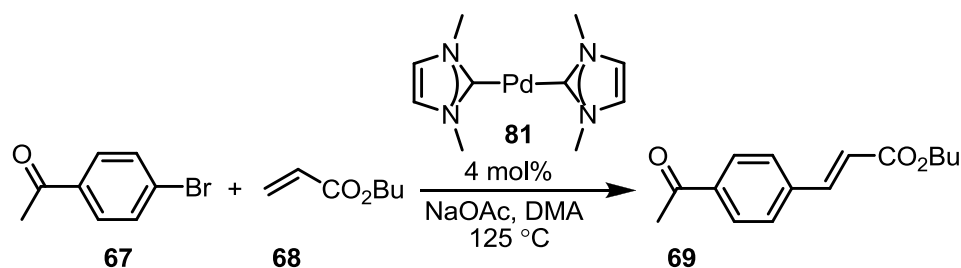
Scheme 27: Mechanism of benzoin condensation proposed by Breslow.

In 1962 Wanzlick synthesized the dimerized form of 1,3-diphenylimidazolidin-2-ylidene carbene.⁶⁰ Two decades later, Arduengo *et al.* reported the isolation of the first stable free carbene and this discovery is considered a landmark in organic synthesis (Scheme 28).⁶¹



Scheme 28: Formation of first stable NHC.

In 1995, Herrmann reported the first transformation promoted by a metal-NHC complex. In this initial report it was demonstrated that palladium NHC complexes are excellent catalysts for a number of Heck reactions (Scheme 29).⁶² As the number of available NHCs increased, a great interest for their use in catalysis began to develop, and they have been employed in a broad range of fields including organocatalysis for example in Suzuki-Miyaura couplings. More recently, tremendous efforts have been devoted to understanding the key structural features of the NHC and how this impacts the catalytic performance of M-NHC complexes.



Scheme 29: Application of *N*-heterocyclic carbenes in Heck reaction.

1.4.2.2. Steric Characteristics of NHC ligands.

The steric bulk of metal-NHC ligands is projected towards the metal center, therefore Tolman's cone angle analysis is unsuitable for quantifying the steric bulk of these complexes. To address

this issue, Nolan and Cavallo developed a steric parameter known as the “percent buried volume ($\%V_{\text{Bur}}$)”. The $\%V_{\text{Bur}}$ is defined as the fraction of the volume of the sphere occupied by the given ligand (Figure 5).⁶³ This value can be determined either from the X-ray crystal structure of the complex or computed using density functional theory. The standard NHC metal complex initially used to compute this parameter was $\text{Ni}(\text{CO})_3\text{L}$, the same metal complex that is used to calculate the Tolman cone angle of phosphine ligands. However, due to the difficulties in preparing bulkier NHC complexes, $[(\text{NHC})\text{Ir}(\text{CO})_2\text{Cl}]$ complexes were found to be a better alternative for determining NHC $\%V_{\text{Bur}}$, as they accommodate a square planar geometry.

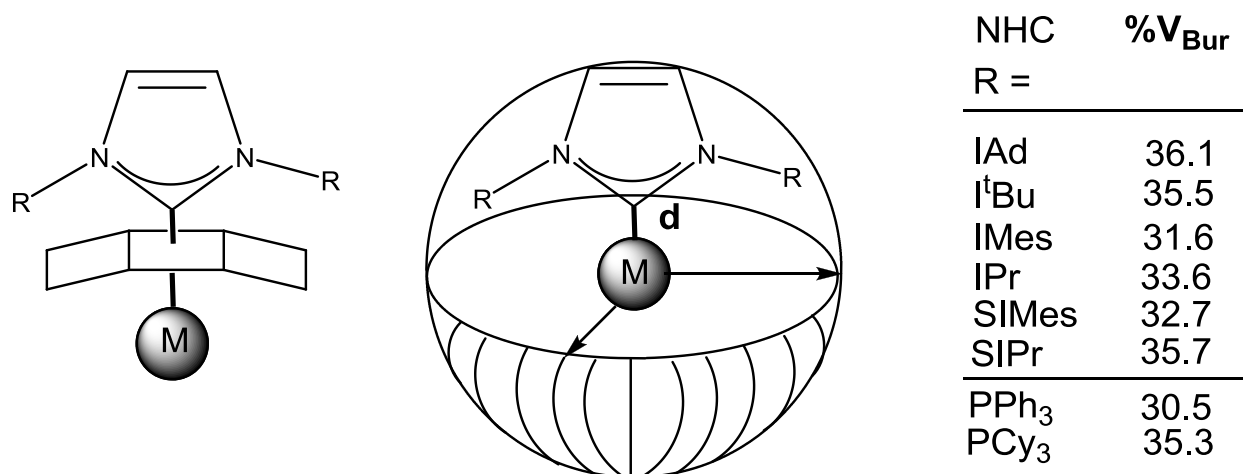


Figure 5. Percent buried volume ($\%V_{\text{Bur}}$) of selected NHC obtained from DFT-Optimized geometries of $[(\text{NHC})\text{Ir}(\text{CO})_2\text{Cl}]$ complexes, $d = 2.10 \text{ \AA}$ and the radius = 3.5 \AA .

1.4.2.3 Electronic Parameter of NHC ligands.

Since Tolman’s development of TEP in 1970, the standard method used for probing the electronic properties of a given metal in complexes is based on the use of IR spectroscopy with a coordinated *trans*-ligated carbonyl (CO) group. After the discovery of NHC ligands, a number of researchers have attempted to expand the application of TEP for these ligands. In 2003, Chianese *et al.* reported

the use of $[(L)Ir(CO)_2Cl]$ complexes to compare the electron-donating ability of a series of phosphine and NHCs ligands.⁶⁴ A linear relationship was obtained by correlating the IR stretching frequency of the Ir system in $[(L)Ir(CO)_2Cl]$ with TEP in $Ni(CO)_3L$ complexes. This discovery allowed a direct estimation of TEP value without the need for synthesizing the $LNi(CO)_3$ complex from its toxic precursor $Ni(CO)_4$.

Another milestone made in this field was achieved by Nolan and co-workers, who published a report that expands the correlation between the TEP and the average CO stretching frequencies of $[(NHC)Ir(CO)_2Cl]$ complexes of a large library of NHC ligands.⁶⁵ Based on these results, Nolan and Crabtree concluded that typical imidazole-2-ylidene NHCs are more electron-donating than even the most electron-rich phosphine ligands, therefore the metal in these complexes will be more electron-rich relative to their phosphine counterparts. It was also confirmed that for *N*-aryl NHC ligands, the nature of the *ortho*-alkyl substituents on the phenyl ring had little effect on their electron-donating ability. For example, the TEP of NHC (IMes) and NHC (IPr) were only different by 0.8 cm^{-1} . On the other hand, changing the nature of the substituent on the backbone of the NHC has a profound effect on ligand donicity as shown in the Nolan TEP studies. For example, the presence of electron-withdrawing chlorine atoms on the NHC backbone rendered the resultant ligand (i.e. IPr^{Cl}) significantly less donating than their unmodified counterparts. Surprisingly, for *N*-aryl NHCs, the electron-donating ability can be tuned by changing the substituent at the para position on the aryl ring.⁶⁶ This is unexpected considering that there is no conjugation between the orthogonal *N*-aryl and imidazole rings.

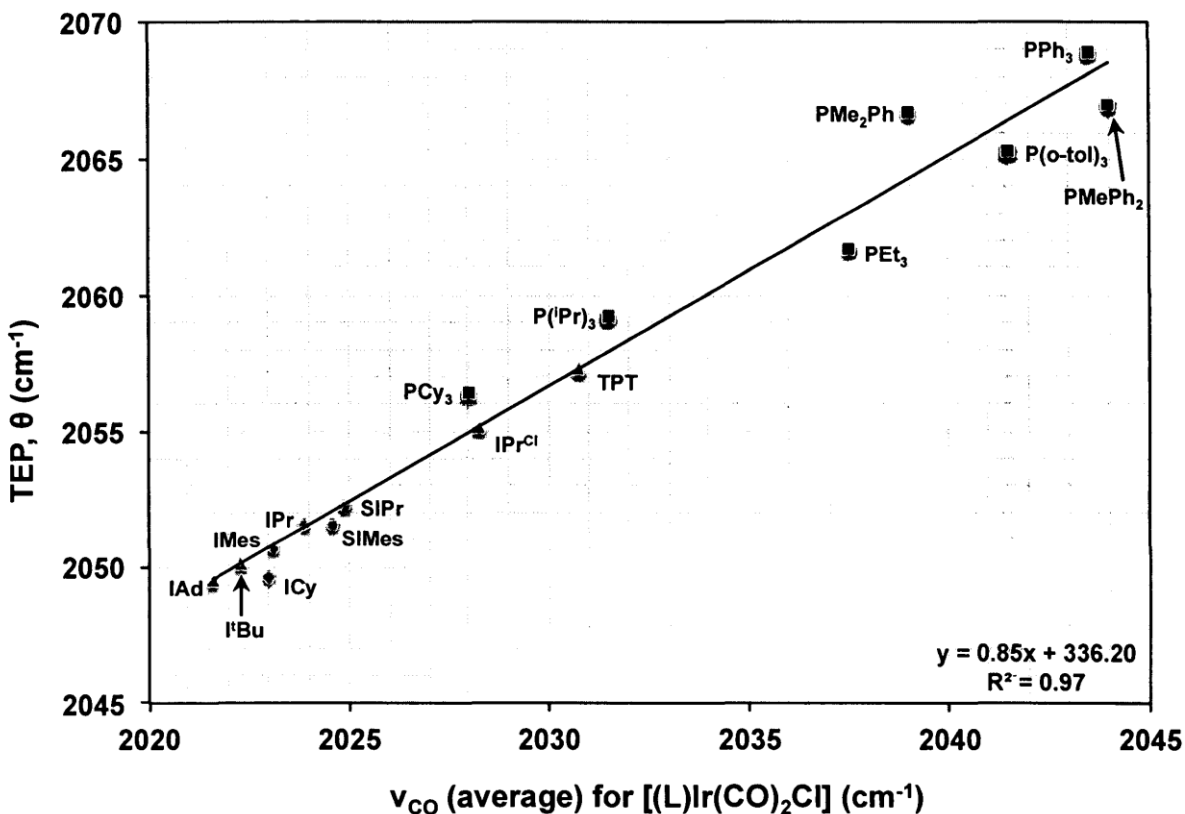


Figure 6: Nolan and co-worker's correlation of average ν_{CO} for $[(\text{L})\text{Ir}(\text{CO})_2\text{Cl}]$ complexes with Tolman electronic parameter.⁶⁴

1.4.2.3 Pd-NHC Complexes in Buchwald Amination.

Several NHC ligands have been reported in the literature for Pd-catalyzed C-N bond formation and a selection of important NHC ligands is summarized in Figure 7. Caddick and co-workers have designed a variant of (NHC)Pd(R-allyl)Cl catalysts for amine arylation. For example, ligand **70** forms an air-stable, highly active Pd complex that couples a wide range of aryl halides with primary and secondary alkyl amines at moderate (70 °C) or room temperature.⁶⁷ Nolan and co-workers reported the use of IPr ligand (**71**) in the Pd-catalyzed amination of aryl bromides with secondary cyclic and acyclic amines providing the desired products in high yields at room

temperature.⁶⁸ More sterically hindered NHC ligands have been developed more recently by Glorius (**72a** and **72b**), Dorta (**73a** and **73b**), Markó (**74**), and Organ (**75**).

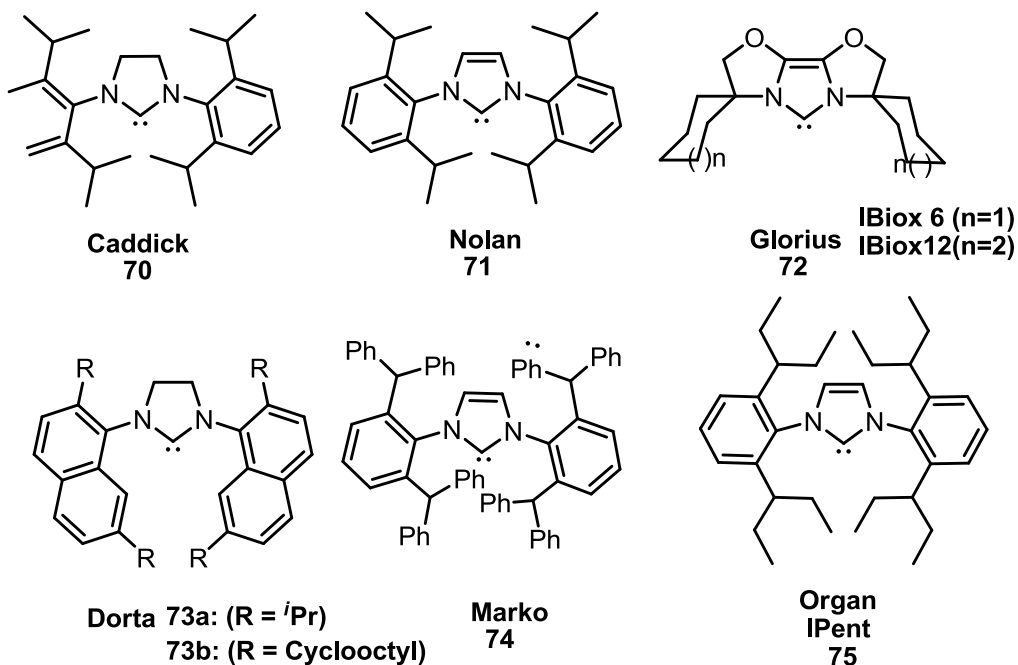


Figure 7: NHC pre-catalysts for Buchwald-Hartwig amination.

The pre-catalysts developed by the Organ group are becoming popular NHC-based Pd catalysts. These NHC-Pd(II) complexes with a *trans*-ligated 3-chloropyridine, known as *PEPPSI* complexes (Pyridine-Enhanced Pre-Catalyst Preparation, Stabilization and Initiation) have made a significant impact in many cross-coupling reactions including Suzuki,⁶⁹ Negishi⁷⁰ and especially amination reactions.⁷¹

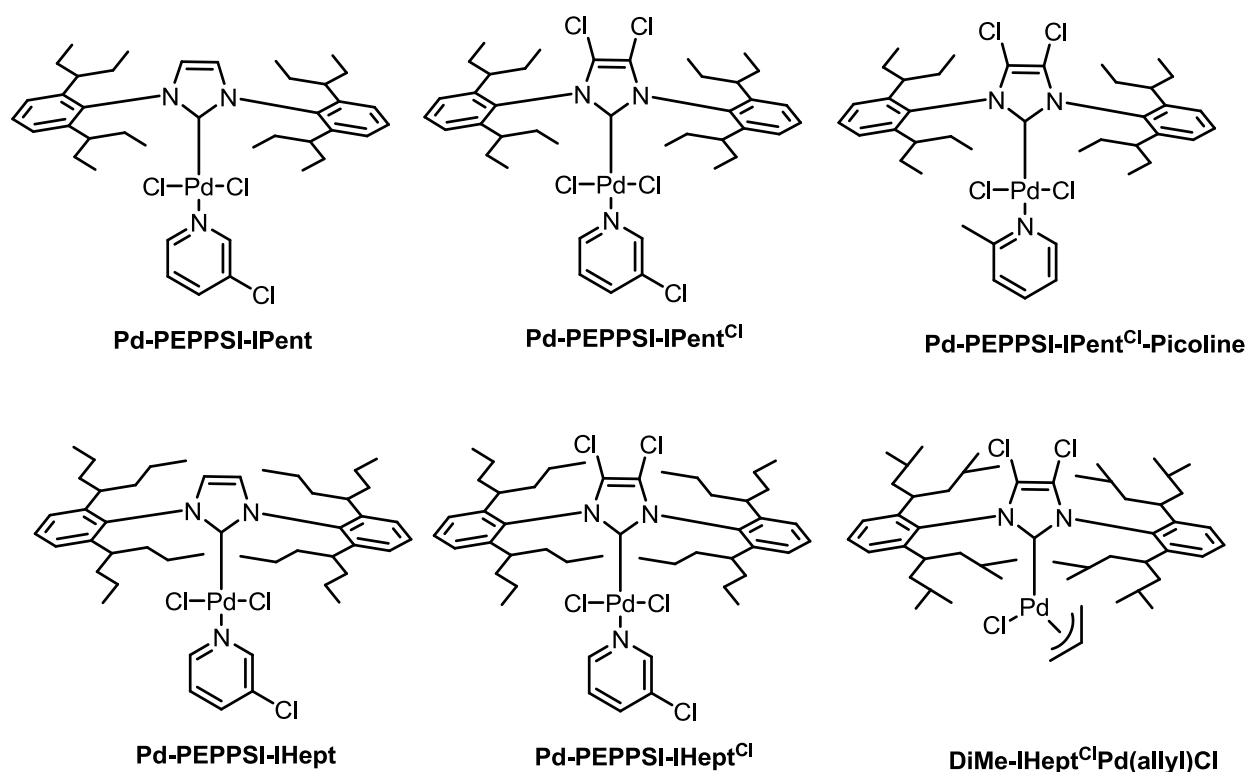


Figure 8: Pd-PEPPSI pre-catalysts developed by Organ.

The monoarylation of primary amines was achieved with excellent selectivity using Pd-PEPPSI-IPent^{Cl} precatalyst (1 mol% catalyst loading) and Na-BHT as a base.^{71c} A great substrate scope was reported, including base-sensitive functional groups (ketone, cyano, ester, and acids). Deactivated anilines were successfully coupled with aryl halides using Pd-PEPPSI-IPent^{Cl}-o-Picoline precatalyst using carbonate bases at room temperature.³⁷ More recently, the new rationally designed (DiMeIHept^{Cl}) pre-catalyst with highly branched alkyl chains on the aryl rings has been shown to be effective in selective ammonia arylations across a range of challenging substrates including heterocycles and those containing base-sensitive functionality. The less bulky congener Pd-PEPPSI IPent^{Cl} was effective in coupling *ortho*-substituted aryl halides providing the desired monoarylated product in high yield and selectivity.^{70a} It is also worth mentioning that due to the wide application of the Pd-PEPPSI-IPent catalyst in various cross-coupling reactions, including

Suzuki-Miyaura, Negishi, Stille-Migita and Buchwald amination, this catalyst was granted the “EROS Best Reagent Award” in 2017.⁷²

1.4 Challenges in C-N Bond Formation.

1.5.1 Synthesis of Sterically Hindered Anilines.

Recently, some medicinal chemistry efforts have focused primarily on developing aniline derivatives possessing highly branched alkyl content such as *tert*-butyl and adamantyl groups.⁷³ This stems from the fact that introducing such groups in the molecule enhances the lipophilicity and metabolic stability by protecting the reactive sites from enzymatic degradation. This is well demonstrated by comparing ferrostatin inhibitor 1 with its analog (Figure 9). Ferrostatin inhibitor-1 is an alkyl aryl amine with antioxidant properties that are believed to prevent oxidative damage to lipids in cell membranes.⁷⁴ Replacing the cyclohexyl and methyl ester substituents in ferrostatin inhibitor-1 with an adamantyl group and *tert*-butyl ester, respectively, significantly increases the drug's stability in the plasma ($t_{1/2} \geq 1.9$ min versus 120 min).

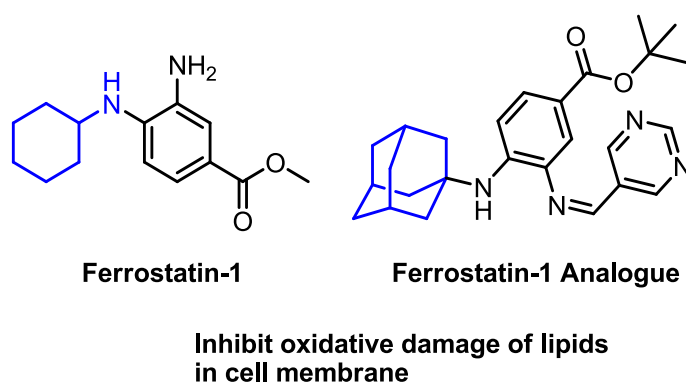
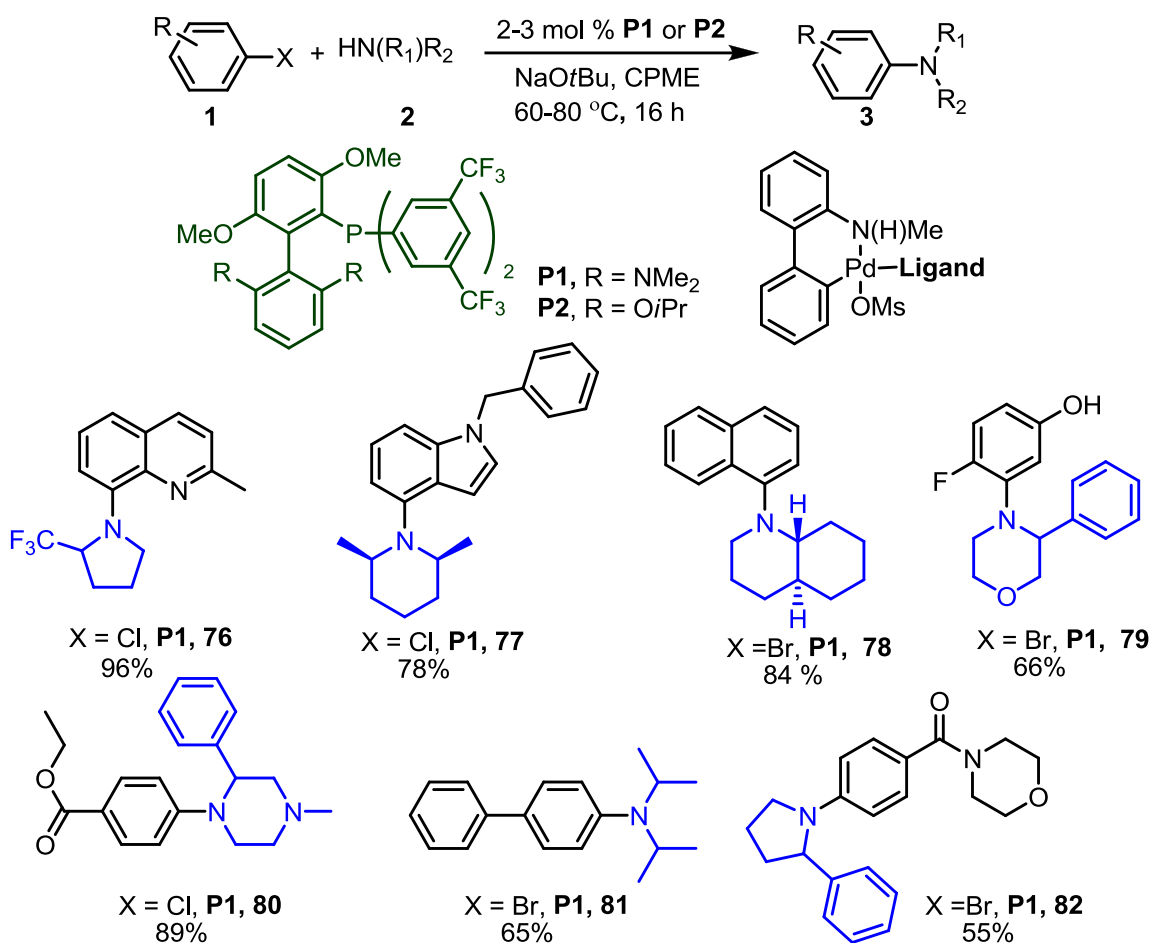


Figure 9: Examples of sterically hindered anilines.

However, from a synthetic point of view, incorporation of sterically hindered substituents remains quite challenging. The most commonly used methods to generate sterically hindered amines rely on *N*-aryl bond formation using amine derivatives (*vide supra*). Since these methods suffer from major drawbacks and limitations, therefore the development of alternative routes is highly demanded.

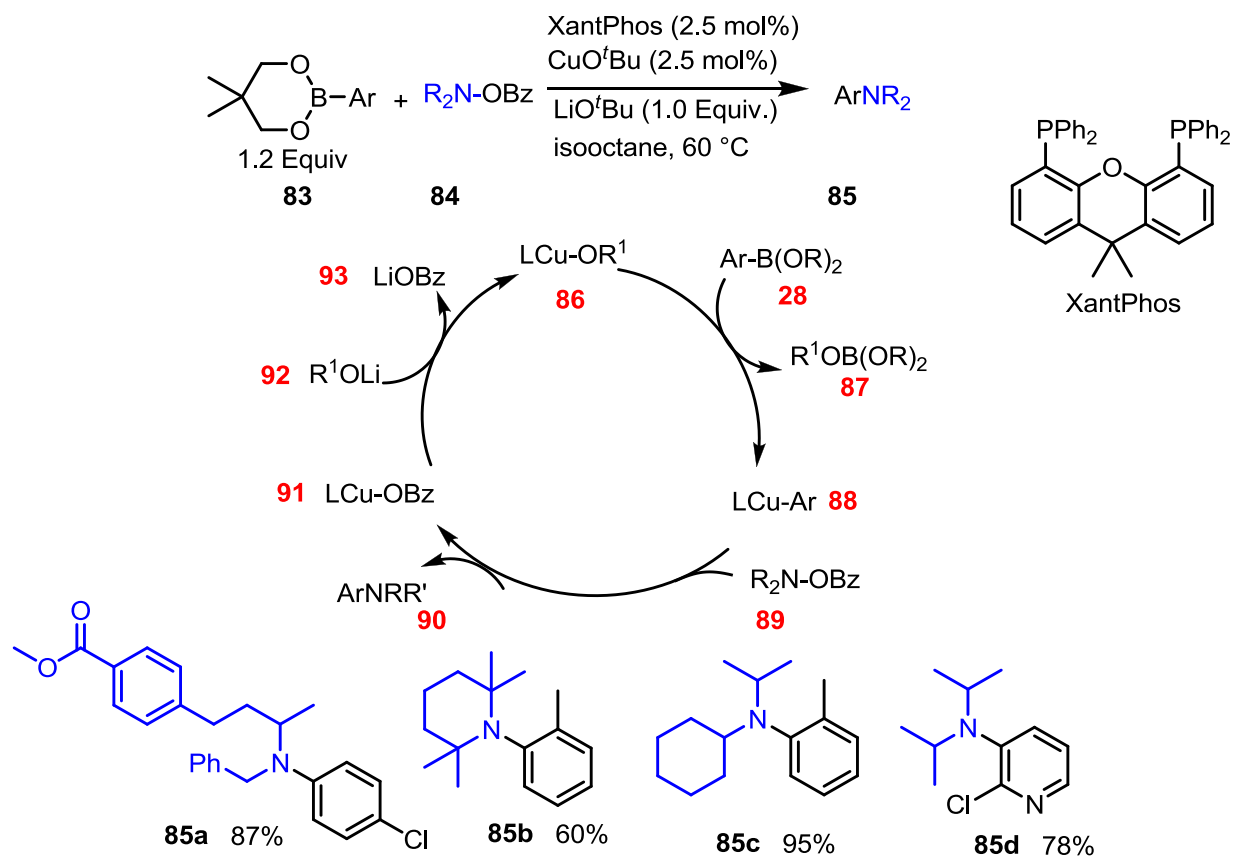
In 2015, Buchwald and co-workers developed two ligands **P1** and **P2**, for the Pd-catalyzed arylation of sterically demanding α -branched secondary amines (Scheme 30). These ligands are relatively less electron-rich than XPhos or BrettPhos which have been used for promoting Pd-catalyzed C-N bond formation. A less electron-rich ligand is expected to increase both the rate of reductive elimination and the rate of transmetalation by rendering the Pd(II) intermediates more electrophilic. It is important to mention that the use of NaOtBu as a base in this protocol might be problematic in tolerating base-sensitive functionality.⁷⁵



Scheme 30: Buchwald protocol for the synthesis of sterically hindered anilines derivatives.

Lalic and co-workers published an alternative approach for coupling sterically hindered amines using a copper-catalyzed amination reaction. Their protocol involves electrophilic amination of aryl boronic esters using 2.5-5 mol % catalyst derived from copper *tert*-butoxide with Xantphos ligand (Scheme 31). The transformation was conducted under mild conditions and a wide range of functional groups was tolerable. This report was unique in synthesizing some of the most hindered anilines made to date.⁷⁶ The proposed mechanism for this transformation is shown in Scheme 3. The reaction involves transmetalation from boron **28** to copper **86** to generate intermediate **88**.

Subsequent electrophilic amination of aryl copper intermediate generates the desired product along with intermediate **91**. Finally, the reactive copper is regenerated with lithium alkoxide.



Scheme 31: Lalic's protocol for the synthesis of sterically hindered aniline derivatives.

1.5.2 Synthesis of 2-aminopyridine derivatives.

2-Aminopyridine derivatives are important compounds that have been used as ligands in organometallic chemistry,⁷⁷ as fluorescent dyes⁷⁸ and as therapeutic agents, for example, compound **94** as an anti-HIV and compound **95** for the treatment of diabetes (Figure 10).⁷⁹

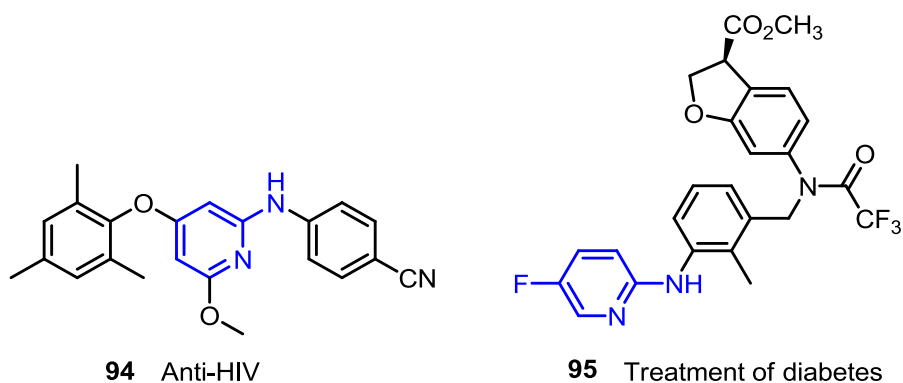
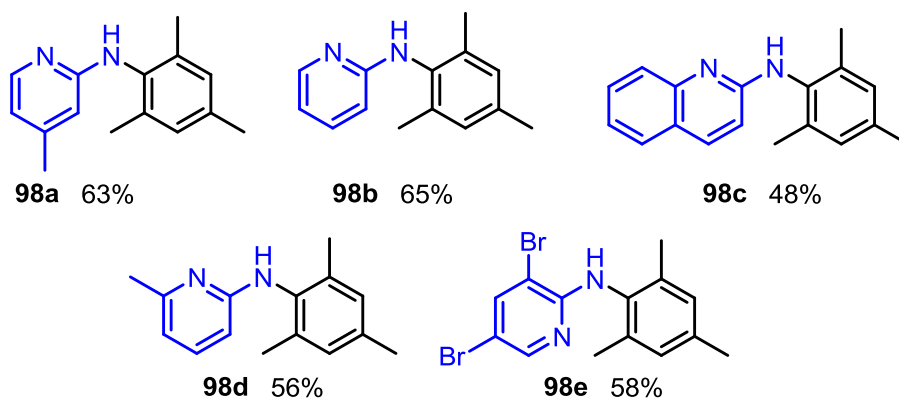
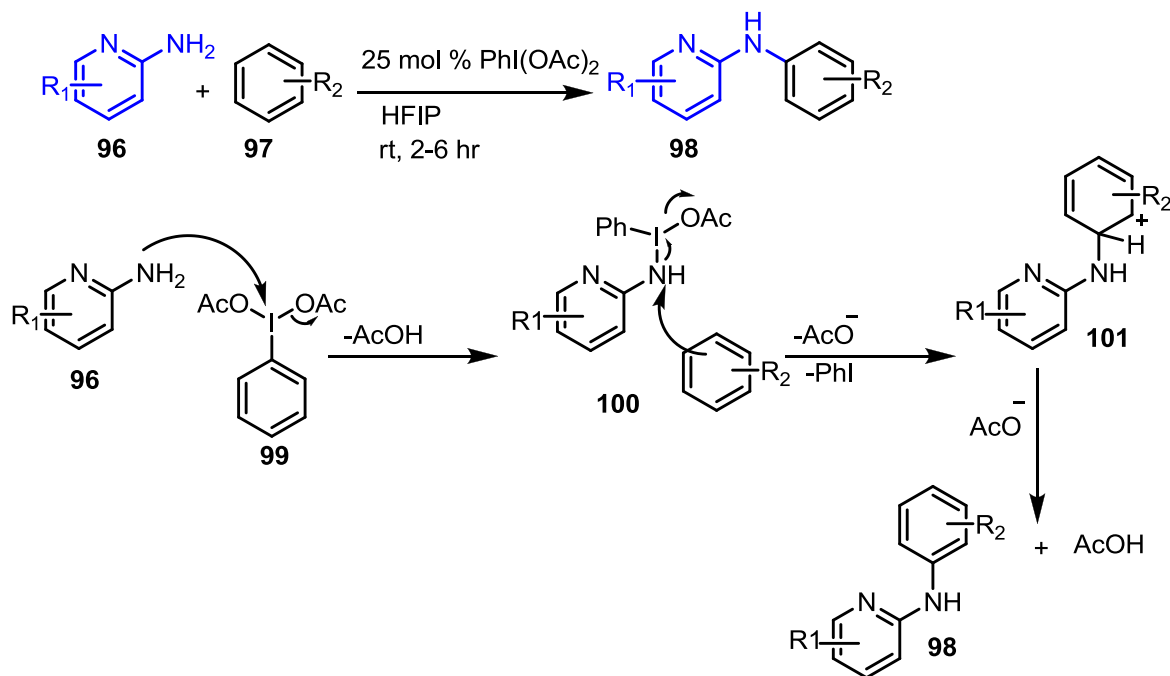


Figure 10: Examples of 2-aminopyridine derivatives as therapeutic agents.

The development of synthetic methods to access these compounds is important. Strategies for selective synthesis of aminopyridine derivatives include S_NAr of halopyridine substrates, but these methods produce an only modest yield of the desired product, require harsh conditions and only a limited class of substrates can undergo this transformation (*vide supra*).⁸⁰ Further, the modification of commercially available aminopyridines and *de novo* construction of the pyridine nucleus incorporating properly disposed amino groups similarly have notable limitations.⁸¹

Another metal-free approach for synthesizing 2-aminopyridine derivatives was reported by Chupakhin and co-workers in 2015 who utilized a hypervalent iodine reagent as an oxidant. This approach allows the coupling of arenes with electron-deficient amine derivatives providing a rapid access to scaffolds of bioactive compounds (Scheme 33). A major drawback of this method is its incompatibility with highly electron-rich arenes, this is due to the side oxidation reaction of the electron-rich arene by the idosobenzene diacetate.⁸² A plausible mechanism for this transformation is shown below; a nucleophilic attack of the amine to the hypervalent iodine reagent **99** results in the formation of intermediate **100**. A second nucleophilic attack of the arene results in the

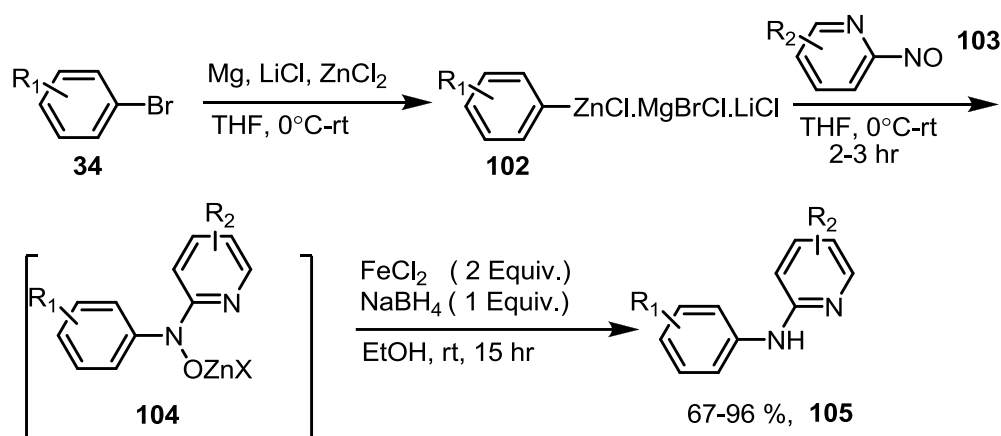
formation of sigma complex **101**. Finally, deprotonation and regaining aromaticity deliver the desired product.



Scheme 32: Metal-free synthesis of 2-aminopyridines.

Later on, Knochel and co-workers reported a protocol to synthesize functionalized secondary amines by the addition of functionalized organozinc reagents to nitrosoarenes (Scheme 33).⁸³ The

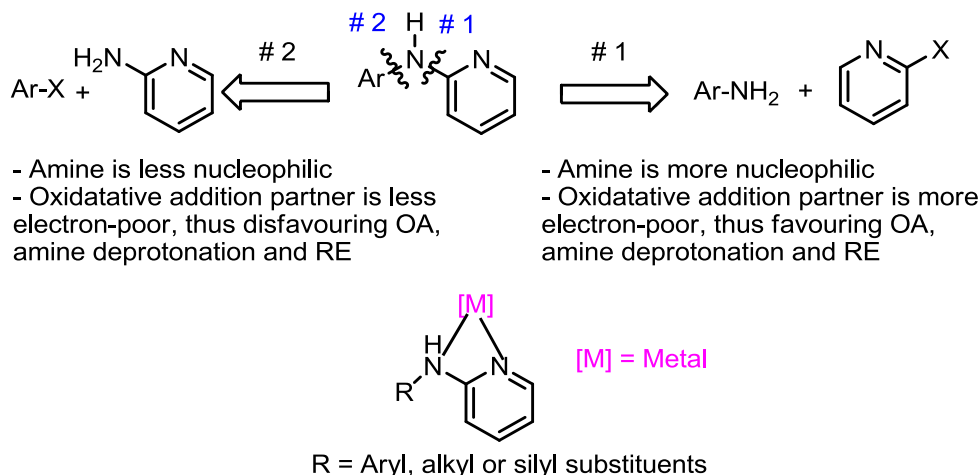
nitrosoarenes were prepared by oxidation of the corresponding arylamine using H₂O₂ and catalytic amounts of PhSeSePh. A potential problem that detracts from the utility of this synthetic method is in preparing nitrosoarenes. The oxidizing conditions required can result in a decomposition of the starting arylamine, especially in electron-rich systems.



Scheme 33: Knochel protocol for the synthesis of 2-aminopyridine derivatives using organozinc.

Palladium-catalyzed C-N bond formation provides an alternative for the formation of aminopyridine derivatives (Scheme 34). The first disconnection is more facile since the halopyridine partner is quite electron-deficient, thus facilitating all three steps of the catalytic cycle (O.A., deprotonation, and R.E). On the other hand, the second disconnection is more challenging, as the aminopyridine group is less nucleophilic. Additionally, 2-aminopyridines have been used extensively as ligands to stabilize early transition metal and lanthanide ions (Scheme 34).⁸⁴ The aminopyridine ligands used exhibited a relatively low steric demand, especially in the plane perpendicular to the pyridine moiety, this results in the formation of relatively stable metal-complexes.⁸⁵ Such property restricts the chemistry of these metal-complexes in catalysis. For these reasons disconnection number 2 is less commonly used in the literature.

However, it will be beneficial if this problem is addressed as it can greatly expand the substrate scope and give access to these scaffolds more readily.



Scheme 34: Metal-catalyzed amination to form 2-aminopyridine derivatives.

1.6 Plan of Study

1.6.1 Plan of study for the synthesis of sterically hindered aryl amines.

Despite the powerful and well-developed approaches for the synthesis of sterically hindered amines reported by Buchwald and Lalic, there are major drawbacks in each protocol. The use of aggressive base NaO^tBu in the Buchwald's method limits the substrate scope. On the other hand, the conversion of the amine into its corresponding *o*-benzoyl-*N,N*-dialkyl hydroxyamine derivative and the preparation of boronic acid in Lalic's method add at least two steps to the process. These activation steps introduce limitations in the scope of the starting materials involved. In order to address these deficiencies, we set out to develop a general and more practical strategy for the synthesis of sterically hindered primary and secondary amines employing a single catalyst under relatively mild reaction conditions. We were drawn to the use of Na-BHT as a mild base in

Pd-catalyzed C-N bond formation using a Pd-*PEPPSI* pre-catalyst. Below, we detail the development of conditions for the coupling of non-activated hindered primary and secondary amines with aryl chlorides bearing different functional groups.

1.6.2 Plan of study (II) synthesis of 2-aminopyridine derivatives.

Due to difficulties associated with the second disconnection mentioned above (i.e. the less nucleophilic amine and the ligation of 2-aminopyridine to the palladium center to form a relatively stale complex (Scheme 34), fewer efforts have been devoted in the literature to explore this route. We envision that, if these challenges were addressed, then we can expand the substrate scope of 2-aminopyridine derivatives and provide an easier means to access these valuable scaffolds. In the discussion section, we detail the progress made in coupling 2-aminopyridines with a variety of aryl(heteroaryl) chlorides bearing different functional groups using a single catalyst with different bases.

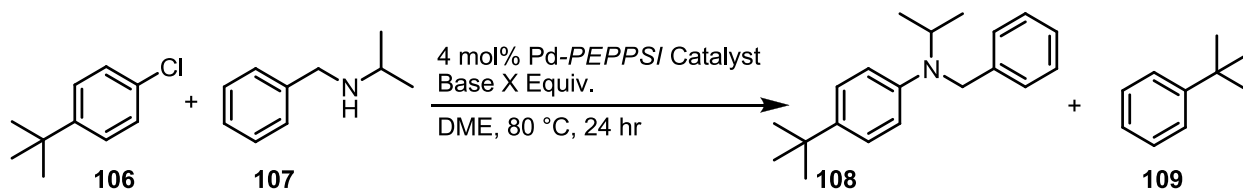
CHAPTER 2: SYNTHESIS OF HINDERED ANILINES

2.1 Reaction optimization:

We initiated our investigation by screening different catalysts and bases to couple *N*-isopropyl benzylamine with *tert*-butyl-4-chlorobenzene using conditions developed in Organ's lab (i.e. DME as a solvent at 80 °C Table 2). Using cesium carbonate, the mildest base in this study, Pd-PEPPSI *IPr* exhibited no reactivity and the crude NMR spectrum showed only starting materials (Table 2, entry 1). We have demonstrated earlier that increasing the steric bulk around the metal center greatly increases catalytic activity, so the same reaction was conducted using Pd-PEPPSI *IPent* (Table 2, entry 3) but the conversion remained unsatisfactory (<10 %). It was also established that chlorinating the backbone of the NHC ligand has a positive effect on catalyst activity, but the outcomes of running the same reaction with the chlorinated version of *IPr* and *IPent* were unsuccessful (Table 2, entries 2, 4). Based on these results, we decided to try a different base that is still mild but more soluble. Sodium 2,6-di-*tert*-butyl-4-methylphenolate (NaBHT) ^{71c} was an excellent candidate for the amination reaction. With a pK_a of ~11, this base is strong enough to deprotonate the metal alkyl ammonium complexes which are formed in the catalytic cycle, yet mild enough to tolerate base-sensitive functional groups. Conducting the reaction with both Pd-PEPPSI-*IPr* and Pd-PEPPSI-*IPr*^{Cl}, resulted only in aryl chloride reduction (i.e., the formation of **109** Table 2, entries 5, 6). While the major product with Pd-PEPPSI-*IPent* (Table 2, entry 7) was again the reduced product *tert*-butylbenzene, Pd-PEPPSI-*IPent*^{Cl} provided primarily the desired product (Table 2, entry 8). It is noteworthy that the formation of the *tert*-butylbenzene upon using Na-BHT base does not originate from the β-hydride elimination of the amine since the control experiment in Scheme 35 resulted in 67 % conversion of the starting material to **109**. Mechanistic

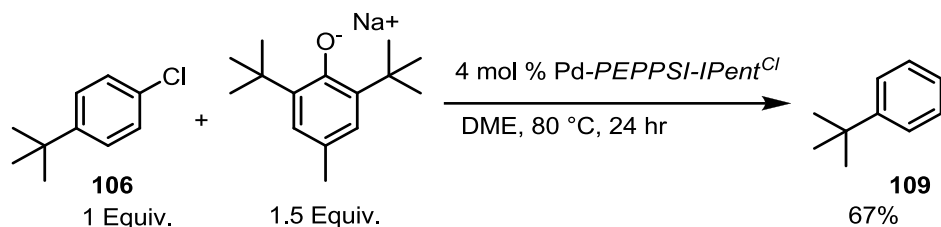
investigation of this side reaction is ongoing in the Organ lab, and so far, preliminary results have excluded the solvent as the hydride source.

Table 2: Catalyst and base optimization study.



Entry	PEPPSI	Base (Equiv.)	Percent Conversion of 106 to 108 ^a	Percent conversion of 106 to 109 ^a
1	<i>IPr</i>	Cs ₂ CO ₃ (3)	0	0
2	<i>IPr</i> ^{Cl}	Cs ₂ CO ₃ (3)	0	0
3	<i>IPent</i>	Cs ₂ CO ₃ (3)	<10	0
4	<i>IPent</i> ^{Cl}	Cs ₂ CO ₃ (3)	<10	0
5	<i>IPr</i>	NaBHT (1.5)	0 ^b	– ^d
6	<i>IPr</i> ^{Cl}	NaBHT (1.5)	10 ^c	– ^d
7	<i>IPent</i>	NaBHT (1.5)	25 ^c	– ^d
8	<i>IPent</i> ^{Cl}	NaBHT (1.5)	80 ^{e,c}	19

^aPercent conversion was determined by ¹H NMR spectroscopy of the crude reaction mixture. ^bThe only product in the crude reaction mixture was the reduction product (**109**) of oxidative addition partner **106**. ^cReduced product **109** along with starting material accounted for the remainder of the crude reaction mixture. ^dDetermining the percent of conversion of **106** to **109** was difficult due to peaks overlapping. ^eThe yield of the product following silica gel chromatography was 80%.



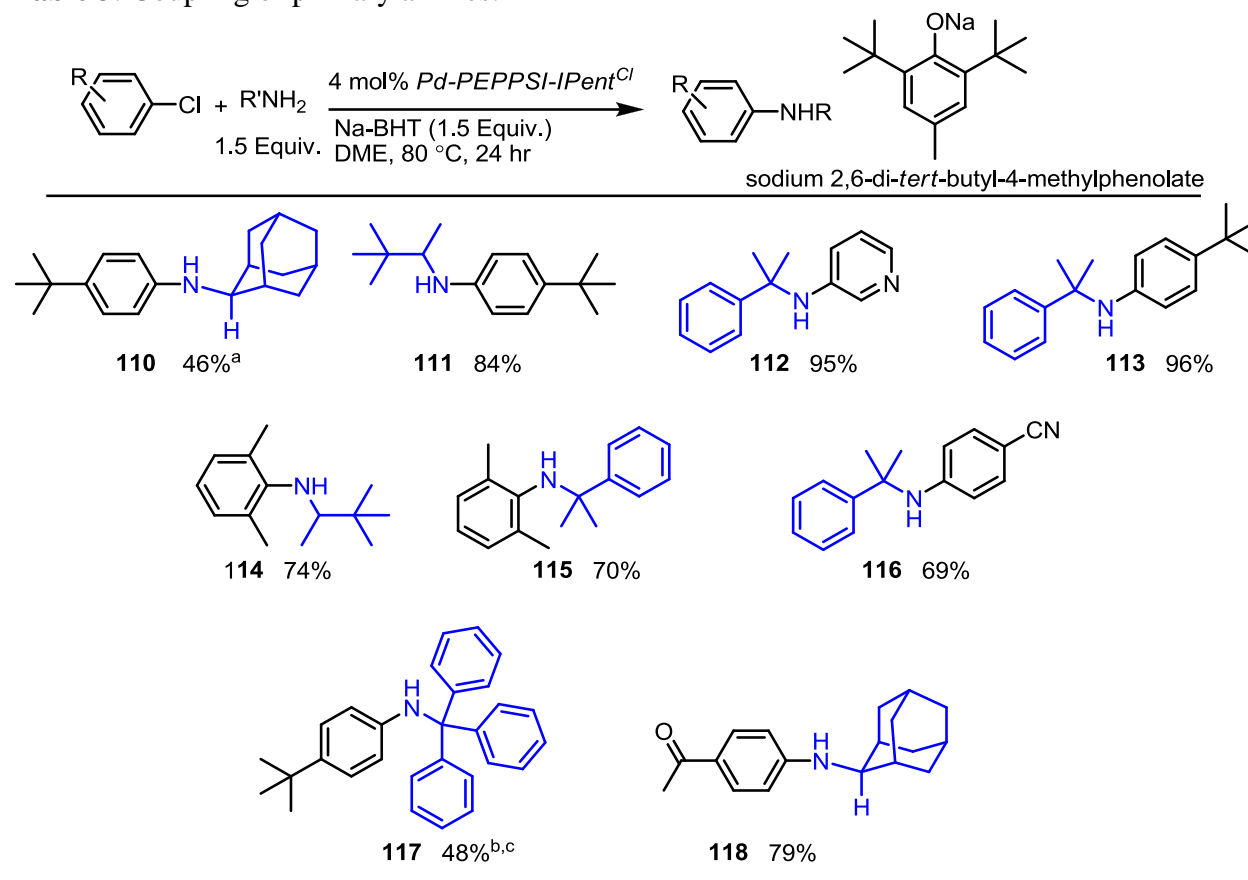
Scheme 35: Determining the origin of the reduced product **109**.

2.2 Substrate Scope with primary amines:

With the optimized conditions in hand, we next examined the substrate scope of the coupling with hindered primary amines (Table 3). The coupling of adamantyl amine proceeded well, providing products **110** and **118**. Coupling of heteroaryl chloride delivered the desired product in excellent yield (e.g. **112**). Amines containing α -quaternary carbon were also coupled providing products, **112**, **113**, **115** and **117**. Similarly, a steric hindrance at both *ortho* positions on the oxidative addition partner posed no problems leading to products **114** and **115**.

Notably, the mild nature of NaBHT means that sensitive groups that often lead to poor results in such couplings using bases such as *tert*-butoxide could now be tolerated (e.g., **116** and **118**). When we used *tert*-butoxide in the coupling to provide **117**, even though it did not contain a sensitive functional group, the yield was lower than anticipated due to competing formation of the *tert*-butyl phenyl ether, further illustrating the value of NaBHT as a base for amine coupling.

Table 3: Coupling of primary amines.

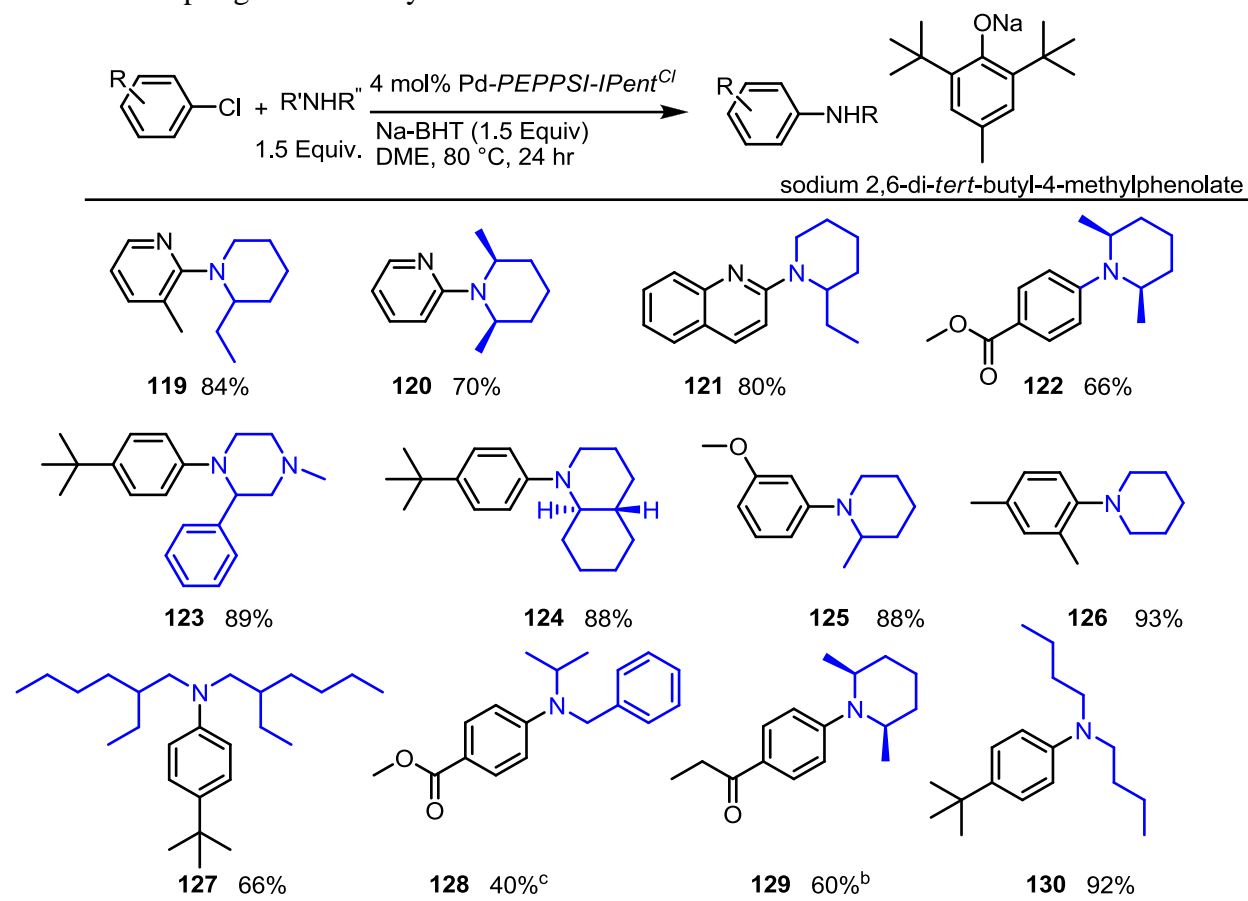


^a When the reaction was performed at 100 °C, the yield increased to 78%. ^b When the reaction was performed at 100 °C, the yield increased to 60%. ^c When the reaction was performed using 1.2 Equiv. NaO^tBu, conversion to **117** decreased due to the formation of the *tert*-butyl phenyl ether in 29% isolated yield.

2.2 Substrate Scope with secondary amines:

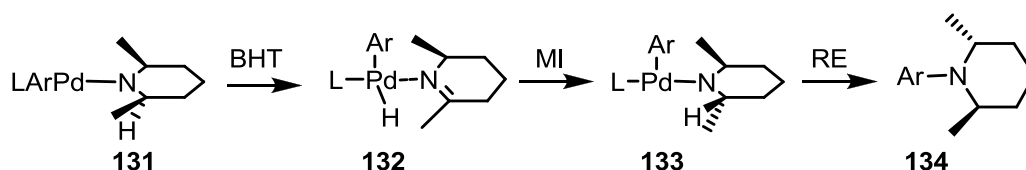
Next, we broadened our investigations to include hindered secondary amines (Table 4). The transformation demonstrated excellent generality across a wide variety of substrates including those bearing a base-sensitive functional group (e.g. **122**, **128**, and **129**). It is worth mentioning that the attempt to prepare tertiary amine **128** using *tert*-butoxide as a base reduced the yield from 40% (upon using Na-BHT) to 7%.

Table 4: Coupling of secondary amines.



^a Experiments were performed in duplicate and yields are following chromatography on silica gel. ^b A minor amount of epimerization was observed, the *trans* isomer was identified in the pure product. ^c Upon using *tert*-butoxide as a base the yield dropped to 7%. The relative configuration for the stereogenic centers in **127** is unknown.

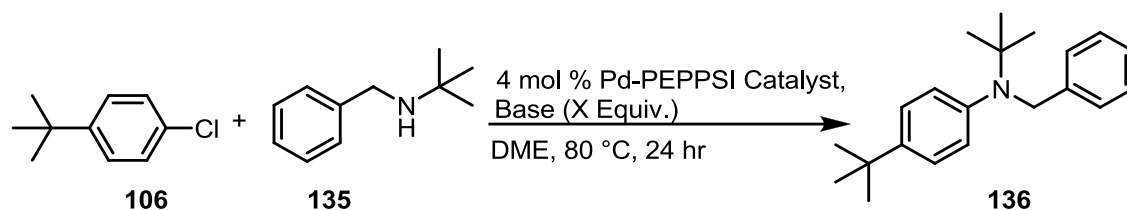
For compound **122** and **129** a small amount of epimerization was observed (14:1). The epimerization presumably takes place through β -hydride elimination followed by migratory insertion before reductive elimination to deliver the other isomer (Scheme 36).



Scheme 36: Likely mechanism of epimerization for compound **122** and **129**.

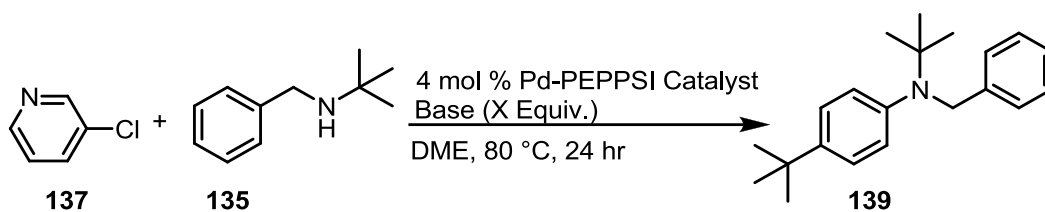
Attempts to couple *N-tert* butyl benzylamine failed completely (Table 5), even with the more electrophilic aryl chloride and the strongest base in this study KO^tBu (Scheme 37). In each case, recovery of the starting materials was observed.

Table 5: Coupling of *N-tert*-butylbenzylamine.



Entry	PEPPSI	Base (Equiv.)	Temperature in °C	Solvent	Percent Conversion of 106 to 136 ^a
1	<i>IPent</i>	Cs ₂ CO ₃ (3)	80	DME	0
2	<i>IPent</i> ^{Cl}	Cs ₂ CO ₃ (3)	80	DME	0
3	<i>IPent</i>	Cs ₂ CO ₃ (3)	100	DME	0
4	<i>IPent</i> ^{Cl}	Cs ₂ CO ₃ (3)	100	DME	0
5	<i>IPent</i> ^{Cl}	Cs ₂ CO ₃ (3)	100	Dioxane	0
6	<i>IPent</i>	LiO ⁱ Pr (1.2)	80	DME	0
7	<i>IPent</i> ^{Cl}	LiO ⁱ Pr (1.2)	80	DME	0
8	<i>IPent</i> ^{Cl}	KO ^t Bu (1.2)	80	DME	0
9	<i>IPent</i> ^{Cl}	NaBHT (1.5)	80	DME	0

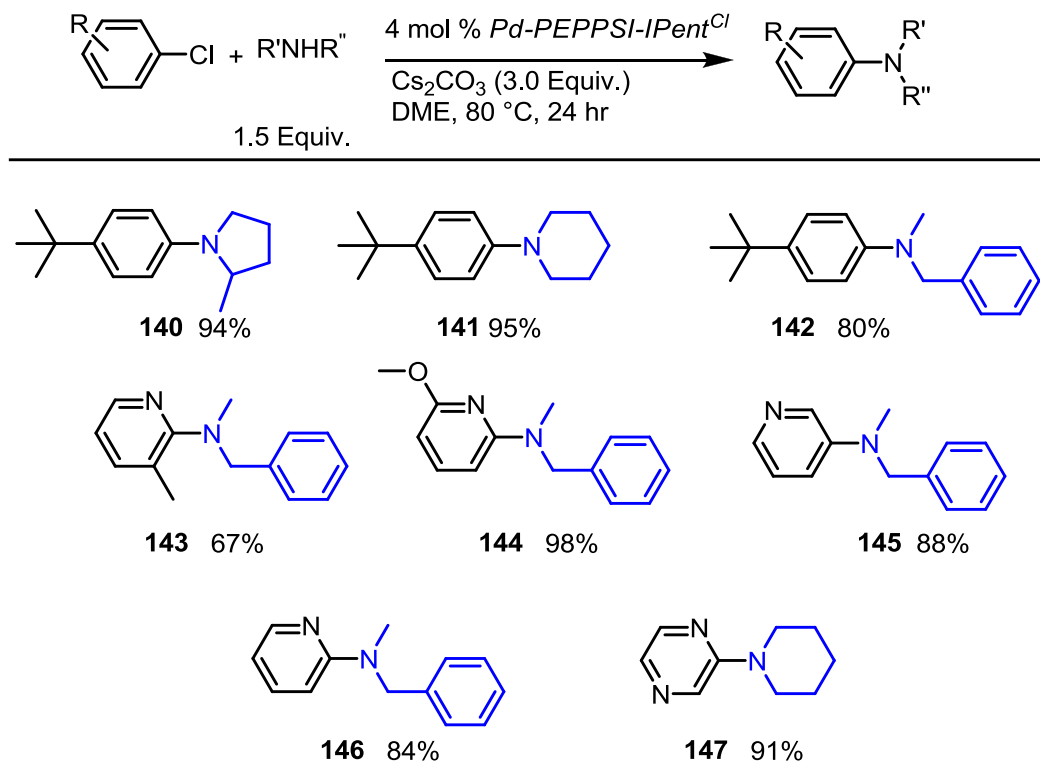
^aPercent conversion was determined by ¹H NMR spectroscopy of the crude reaction mixture



Scheme 37: Coupling *N*-*tert*-butylbenzylamine with a more electrophilic aryl chloride.

When significantly less hindered secondary amines were employed, excellent yields were obtained with the mildest base, cesium carbonate (Table 6) demonstrating the exceptional reactivity of Pd-PEPPSI *IPent*^{Cl} pre-catalyst

Table 6: Substrate scope with less hindered amines.



Experiments were performed in duplicate and yields are following chromatography on silica gel

2.4 Conclusion.

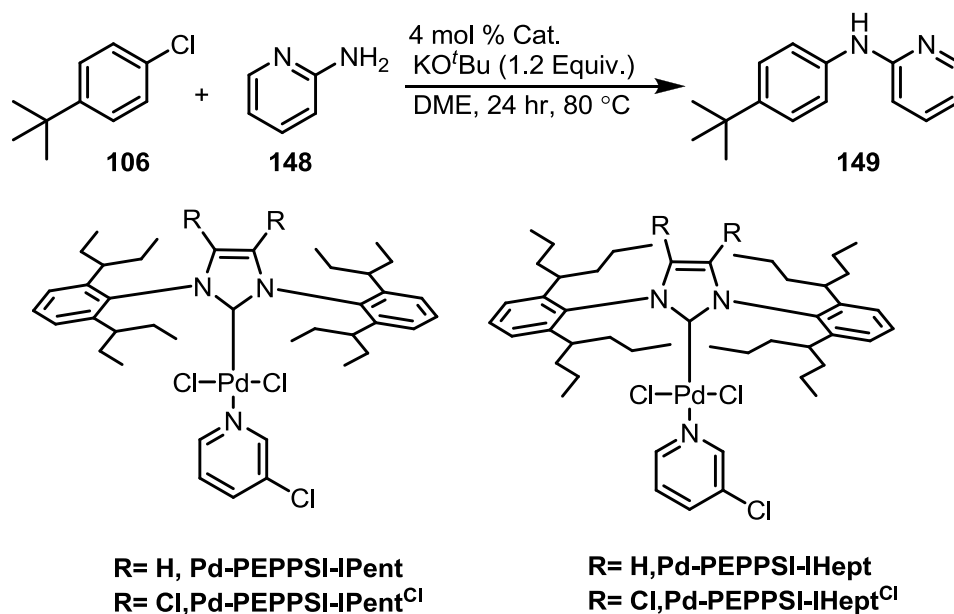
In summary, a protocol has been developed for the cross-coupling of hindered primary and secondary amines with a wide variety of aryl and heteroaryl chlorides including those bearing base-sensitive functional groups such as enolizable ketones, nitriles, and esters. This new method utilizes one catalyst: Pd-*PEPPSI IPent*^{Cl}, and a very mild and homogenous base (NaBHT) to facilitate the transformation at a moderate temperature (80°C). However, coupling more sterically hindered amines such as *N-tert*-butylbenzylamine, or tetramethylpiperidine was unsuccessful.

CHAPTER 3: REACTIONS OF 2-AMINOPYRIDINES IN CROSS-COUPLING

3.1 Catalyst Screening:

We started our investigation by using aryl chloride **106** and 2-aminopyridine **148**, and potassium *tert*-butoxide as a base. We wanted to evaluate the impact made by changing the bulk around the Pd center of the catalyst. Increasing the size of the group at the *ortho* positions on the *N*-aryl moiety of the NHC (Table 7, entry 1 vs. 2) was less effective than installing chlorine groups on the NHC backbone (Table 7, entry 1 vs. 3 and entry 2 vs. 4).

Table 7: Catalyst screening for coupling 2-aminopyridine.



Entry	Catalyst	% Yield of 149
1	Pd-PEPPSI-IPent	26
2	Pd-PEPPSI-IHept	22
3	Pd-PEPPSI-IPent ^{Cl}	55

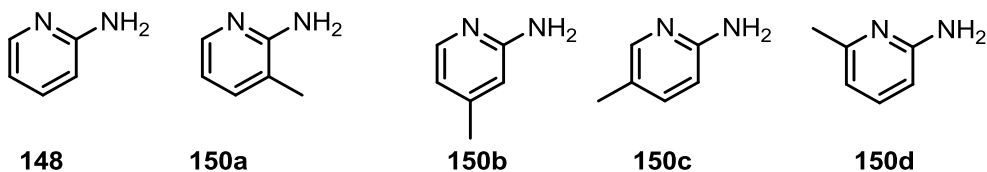
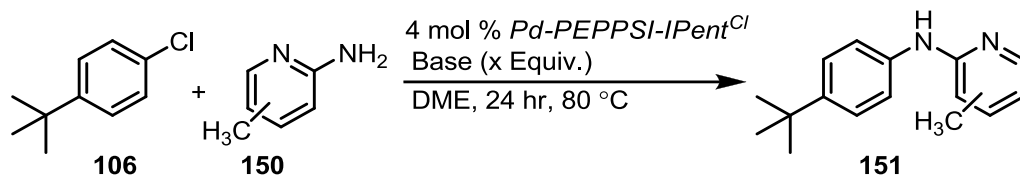
4	Pd-PEPPSI-IHept ^{Cl}	41
5	Pd-PEPPSI-IHept ^{Cl} -Picoline	41

Experiments were performed in duplicate and yields are following chromatography on silica gel.

These results are not surprising, since many cross-coupling reactions that have been done with chlorinated NHC cores led to remarkably higher reactivity than their hydrogen-substituted counterparts.⁵⁶ It is known that 2-aminopyridines have been used as ligands for Pd,⁸⁵ therefore the product formed can potentially poison the catalyst, but our results suggest otherwise. It is most likely that the chlorine atoms on the NHC core push the substituents on the *N*-aryl rings into the coordination sphere of the metal, thereby restricting the ability of the Pd to coordinate to the product.⁸⁶

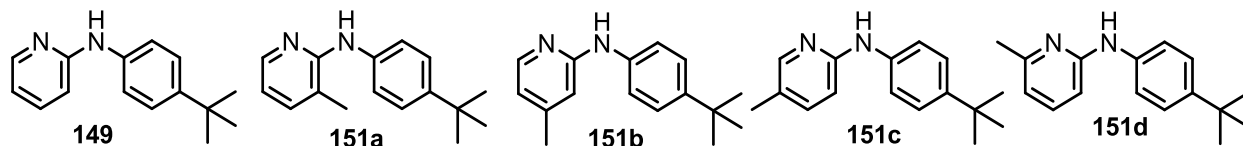
To test this hypothesis, we investigated the cross-coupling of methylated 2-aminopyridine with 4-*tert*-butyl-4-chlorobenzene (**106**). We envisioned that placing the methyl group at the 6-position would retard product coordination to Pd, whereas having the methyl group at the 3-position would slow coupling, but does not interrupt product coordination to the Pd center, and the results obtained agree with this hypothesis (Table 8). Upon using cesium carbonate, no coupling was observed with simple unsubstituted 2-aminopyridine (Table 8, entry 1) and no (or poor) conversion was obtained in all methylated derivatives except for 6-methyl-2-aminopyridine. As mentioned before, the presence of the methyl group at the 6-position prevents the metal from binding to the starting material and/or the product, thus avoiding a deleterious resting state which deactivate the catalyst. As we move progressively to stronger bases, coupling improves and the best yields were obtained when KO^tBu was used. There is a very clear trend in reactivity as we methylate from the 3-position to the 6-position. The C-4 and the C-6 methyl are the best comparisons in terms of their relationship to the amino group and any potential steric impact on the coupling.

Table 8: Impact of the placement of methyl groups on 2-aminopyridine on the coupling with **106** using Pd-PEPPSI-IPent^{Cl} precatalyst.^a



Entry	1	2	3	4	5
Cs₂CO₃ (3 Equiv.)	0	0	18	Traces	33
NaBHT (1.5 Equiv.)	28	26	43	59	54
K^oBu (1.2 Equiv.)	56	28	45	67	76

Product



^a Isolated yields and experiments were performed in duplicate and yields are following chromatography on silica gel

3.2 Coupling of electron-poor 2-aminopyridines:

Electron-poor fluorinated 2-aminopyridine displayed a similar trend, whereby stronger bases were required to achieve best results, and positioning of the group at the C-6 position led to best reactivity (Table 9, entry 4) and placing the substituents at the C-3 position results in no coupling and recovery of the starting materials.

Table 9: Impact of electron-poor groups on the coupling of 2-aminopyridines using Pd-*PEPPSI-IPent^{Cl}* precatalyst.^a

	152	153	154	155
Entry	1	2	3	4
Cs₂CO₃ (3 Equiv.)	0	0	0	18
NaBHT (1.5 Equiv.)	0	8	45	43
KO^tBu (1.2 Equiv.)	0	42	59	72
Product				
	156	157	158	159

^a Isolated yields and experiments were performed in duplicate and yields are following chromatography on silica gel.

3.3 Impact of the size of the C6-substituent on the catalytic cycle:

As the size of the group at the C6-position increases the reactivity improves (methyl, ethyl, and methoxy), even with milder bases (Table 10, entry 3). This provides further evidence for the proposal that it is catalyst poisoning that leads to poor results in these couplings. One might expect larger groups placed in proximity to the reacting amine site would slow reactivity and lead to poorer results. While it would be reasonable to propose that these larger groups do in fact slow the desired coupling, clearly their role in preventing catalyst poisoning is much more impactful on the success of this coupling.

Table10: Impact of the size of the C6-substituent of 2-aminopyridine derivatives.^a

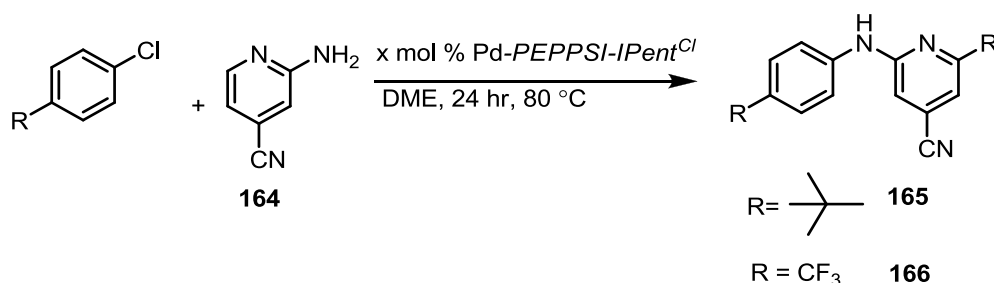
	 150d	 160	 161
Entry	1	2	3
Cs₂CO₃ (3 Equiv.)	33	25	63
NaBHT (1.5 Equiv.)	54	62	94
KO^tBu (1.2 Equiv.)	76	70	-
Product	 151d	 162	 163

^a Isolated yields and experiments were performed in duplicate and yields are following chromatography on silica gel.

3.4 Coupling of cyano-substituted 2-aminopyridine

Surprisingly, the coupling of 4-cyano-2-aminopyridine completely failed even with the strongest base KO^tBu (Table 11). Doubling the catalyst loading (4 mol% to 8 mol%) with Na-BHT resulted in the recovery of the starting materials with no sign of product formation (Table 8, entry 5). Even upon using a more activated aryl chloride (1-chloro-4-(trifluoromethyl) benzene) a low yield was obtained (Table 11, entry 6).

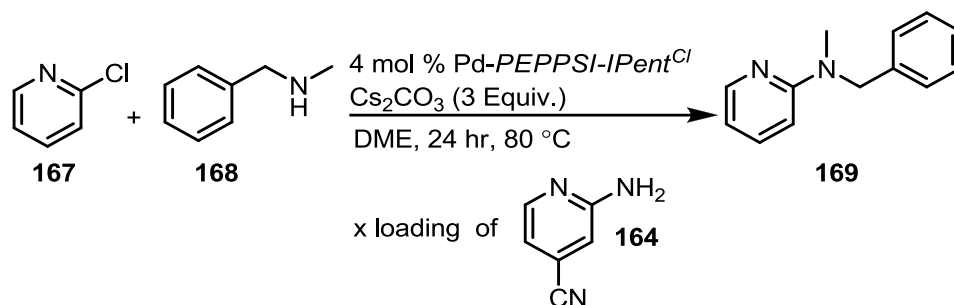
Table 11: Coupling 4-cyano-2-aminopyridine.



Entry	Base (Equiv.)	Catalyst loading	Aryl chloride	% Yield
1	Cs ₂ CO ₃ (3)	4 mol %	R= <i>tert</i> -butyl	0
2	Na-BHT (1.5)	4 mol %	R= <i>tert</i> -butyl	0
3	KO ^t Bu (1.2)	4 mol %	R= <i>tert</i> -butyl	0
4	Na-OPh (1.5)	4 mol %	R= <i>tert</i> -butyl	0
5	Na-BHT (1.5)	8 mol %	R= <i>tert</i> -butyl	0
6	KO ^t Bu (1.2)	4 mol %	R= CF ₃	15%

Based on the results above, we suspect that 4-cyano-2-aminopyridine has stronger poisoning effect (however, it is not clear how) than the rest of 2-aminopyridines used in this study. In order to confirm this, we conducted a control experiment shown in Table 12.

Table 12: Investigating poisoning effect of 4-cyano-2-aminopyridine.

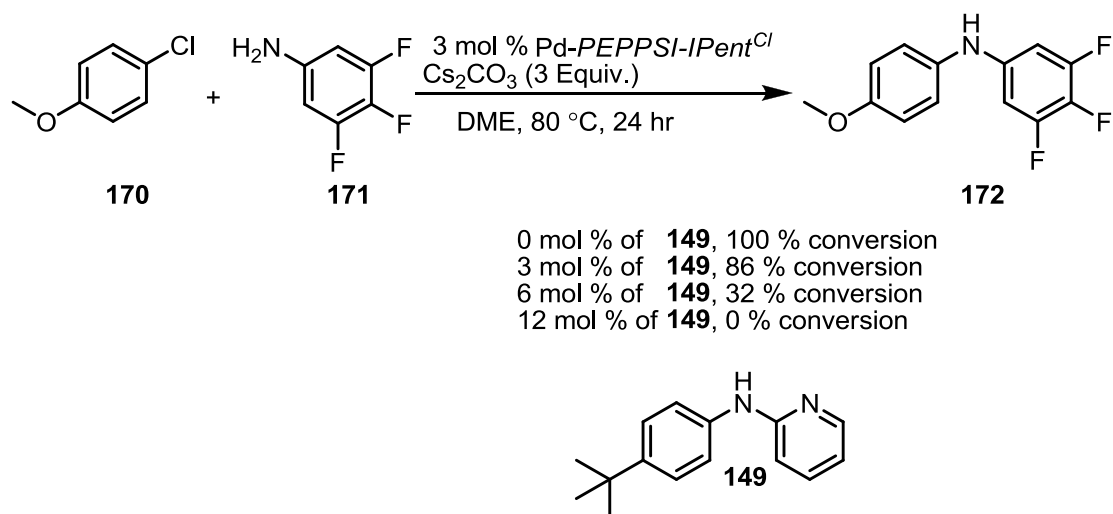


Entry	Loading of 164	Yield of 169
1	0 mol %	83%
2	4 mol %	53%

In the absence of poisoning reagent **164**, the amination reaction delivered the expected product in excellent yield (Table 12 entry 1), but when just 4 mol % of **164** (equal to catalyst loading) was added to the reaction mixture, the yield of the reaction dropped drastically (Table 9, entry 2). This indicates that 4-cyano-2-aminopyridine has a strong negative effect on the catalytic cycle.

3.5 Poisoning effect of the 2-aminopyridine coupled-product on Pd catalyst:

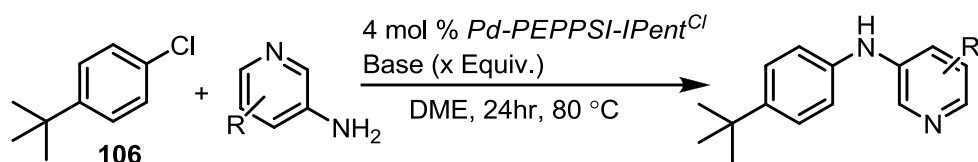
As mentioned before, 2-aminopyridine derivatives are commonly used as a ligand for Pd catalyst, and to support that, we ran three control experiments where substoichiometric amounts of **149** were added to a different amination reaction that is known to work very well with Pd-PEPPSI IPent^{Cl} (Scheme 38). The ratio of **149** to the pre-catalyst was increased gradually from 1:1 to 4:1, and the effect was clear. With 0 % of **149**, the reaction went to 100 % conversion, whereas the transformation was completely shut down at 12 mol % of **149**.



Scheme 38: Impact of *N*-phenyl-2-aminopyridine on amination reaction of **170** with **171**.

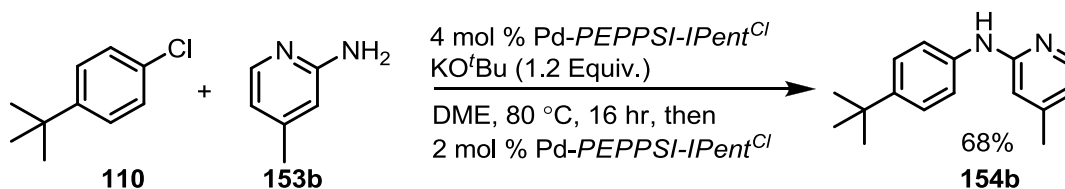
In order to confirm the importance of the relationship between the amino group and the nitrogen atom in the pyridine ring for poisoning the palladium catalyst, we performed the following control experiments (Table 13). We chose compounds **173** and **174**, where the amino group is not in close proximity to the nitrogen atom and we coupled it with the same aryl chloride (4-*tert*-butyl chlorobenzene) and with mild base (Cs₂CO₃). The reaction improved drastically from no conversion with 2-aminopyridine to full conversion with 3-aminopyridine (Table 13). This clearly demonstrates that chelating through both nitrogens is critical for the poisoning role.

Table 13: Impact of moving the primary amine from C2 to C3 on the pyridine nucleophile in the coupling of **106**.



Entry	Base (Equiv.)	Amine	Yield
1	Cs ₂ CO ₃ (3)		 88%
2	Na-BHT (1.5)		 87%
3	KO ^t Bu (1.2)		 92%
4	Cs ₂ CO ₃ (3)		 88%
5	Na-BHT (1.5)		 91%
6	KO ^t Bu (1.2)		 92%

The last control experiment that was conducted to confirm the poisoning effect of the catalyst by the product formed is shown in Scheme 39. 4-Methyl-2-aminopyridine was coupled with the same aryl chloride **106**, using the optimized conditions of 4 mol % of Pd-PEPPSI IPent^{Cl}, 1.2 Equiv. KO^tBu, DME, at 80 °C. After 16 hr, an additional 2 mol % of the catalyst was added to the reaction mixture. After 8 hours, the reaction was quenched, and the desired product was isolated in 68% yield. This increase in the yield from the original protocol (Table 8, entry 3, 45 % to 68 %) indicates that the product formed during the course of the reaction has a poisoning effect and thus decreases the catalytic activity.

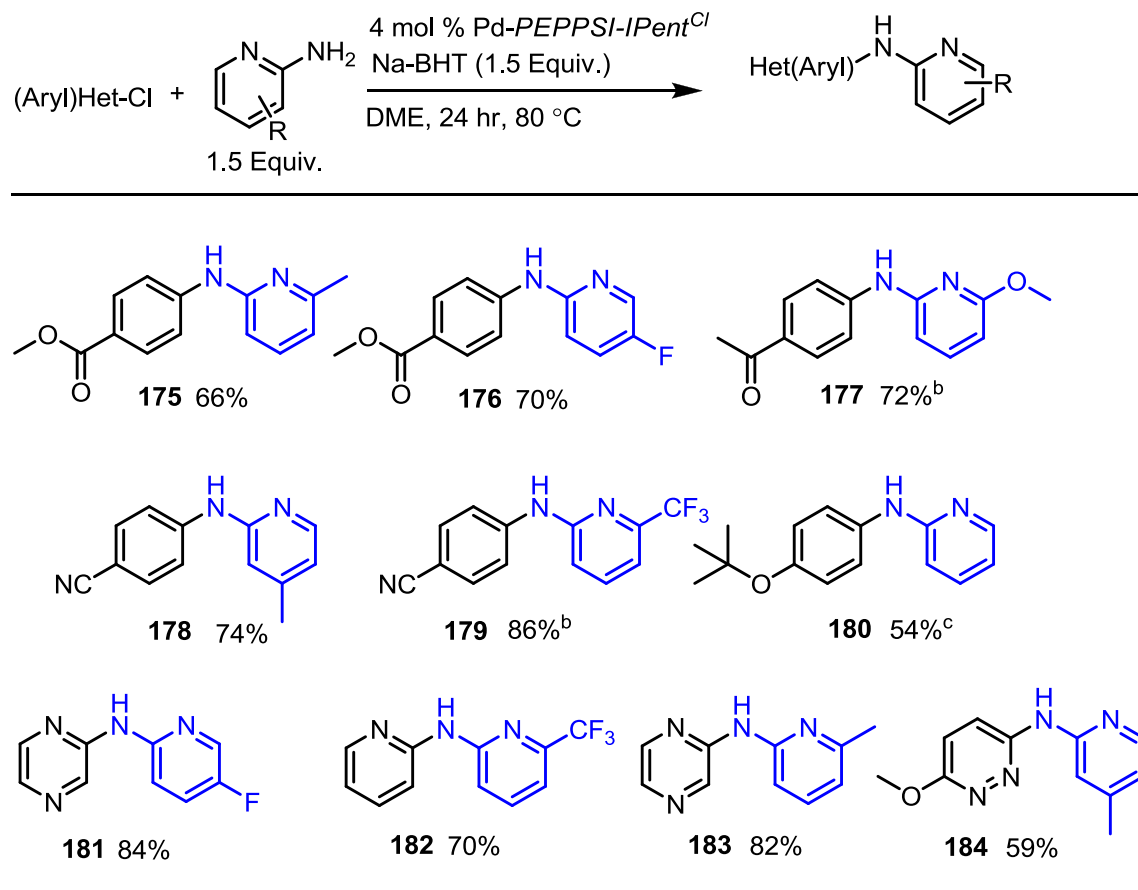


Scheme 39: Variation of the catalyst loading on coupling **106** with **150b**.

3.6 Substrate Scope:

Armed with these results, we set out to expand the substrate scope using the mildest reaction conditions possible. With Na-BHT as a base, the coupling of 2-aminopyridines with aryl and heteroaryl chlorides proceeded smoothly while tolerating base-sensitive functional groups (esters, ketones, and nitriles) (Table 14). In some cases, with the more electron-deficient aryl (heteroaryl) chlorides, the reaction delivered the target compound in excellent yield using carbonate base (e.g., **177** and **179**). The only example where the use of harsher base (KO^tBu) was necessary was for the coupling of the more electron-rich 1-*tert*-butoxy-4-chlorobenzene with unsubstituted 2-aminopyridine to give **180** in 54% yield.

Table 14: Substrate Scope for coupling 2-aminopyridine derivatives to various aryl chlorides with the mild base using Pd-PEPPSI-IPent^{Cl}.



^aExperiments were performed in duplicate and yields are following chromatography on silica gel ^bCs₂CO₃ was used as a base ^cKO^tBu was used as a base.

3.7 Conclusion:

Pd-PEPPSI-IPent^{Cl} pre-catalyst has been shown to be an effective catalyst for coupling (hetero) aryl chlorides with a variety of 2-aminopyridines under mild conditions using Na-BHT or carbonate as a base. The steric bulk around the palladium center promotes reductive elimination within the catalytic cycle and at the same time, it prevents the formation of aminopyridine-Pd coordinated resting states that retard pre-catalyst activation and/or shut down the catalyst performance completely.

Chapter 4: Experimental Procedures

General Experimental:

All experiments were conducted under an atmosphere of dry argon in oven-dried glassware using standard Schlenk techniques. Reactions were performed in microwave vials (3–5 mL) purchased from Biotage Inc. All reagents were purchased from Sigma–Aldrich or Alfa Aesar and were used without further purification unless otherwise noted. Analytical thin-layer chromatography (TLC) analysis was performed on EMD 60 F254 pre-coated glass plates and spots were visualized with UV light (254 nm) and potassium permanganate (KMnO_4) stain. Column chromatography purifications were carried out using the flash technique on EMD silica gel 60 (230–400 mesh).⁸⁷ ^1H -NMR and ^{13}C -NMR spectra were recorded on Bruker AVANCE 400 MHz, 300 MHz, and 600 MHz spectrometers. ^1H -NMR spectra recorded in CDCl_3 were referenced to the residual CHCl_3 peak (^1H NMR $\delta = 7.28$ ppm), and ^{13}C -NMR spectra were referenced to the middle resonance of the carbon triplet of CDCl_3 ($\delta = 77.0$ ppm). All chemical shifts are reported in parts per million (ppm), measured from the center of the signal except in the case of complex multiplets, which are reported as a range. Coupling constants are expressed in Hz. Splitting patterns of the peaks are abbreviated as follows: singlet (s), doublet (d), triplet (t), quartet (q), quintet (quint), sextet (sex), doublet of doublets (dd), triplet of doublet (td), septet (sep) multiplet (m), and broad singlet (bs). High-resolution mass spectrometry (HRMS) analysis was performed by the Mass Spectrometry and Proteomics Services Unit at Queen University in Kingston, Ontario. Melting points were determined using a Fisher-Johns melting point apparatus and are uncorrected.

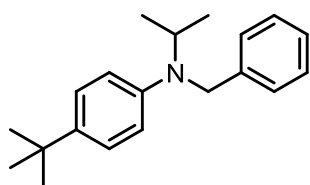
Representative Amination Procedure A:

To a conical vial (3–5 mL size) equipped with magnetic stir bar was added NaH (18 mg, 0.75 mmol, 1.5 Equiv.) and BHT (165.2 mg, 0.75 mmol, 1.5 Equiv.) after which the vial was sealed with a septum and the vial was evacuated and backfilled with Ar (3 times). The flask was then cooled to 0 °C and Et₂O (2 mL) was added. After stirring for 15 min at 0 °C, the solution was warmed up to rt and allowed to stir for an additional 15 min. Then solvent was then removed under high vacuum to yield an off-white solid. To this vial, *Pd PEPPSI-IPent^{Cl} 3-chloropyridine* (17 mg, 4 mol %) was added and the vial was evacuated and backfilled with argon (2 times). To this, 0.75 mL of DME (SureSeal, Aldrich) was added followed by the addition of aryl halide (0.5 mmol, 1.0 Equiv.) and the amine (0.75 mmol, 1.5 Equiv.) by syringe (if they are liquids). Alternatively, if the aryl halide and/or the amine were solids at room temperature, they were added to the vial with the catalyst prior to evacuation. The vial was placed in an oil bath preheated to 80 °C, and the reaction stirred at 1150–1200 rpm for 24 h. After cooling the reaction to rt, the reaction mixture was diluted with diethyl ether, and filtered through a plug of celite. The celite pad was rinsed thoroughly with diethyl ether and the organic layers were combined. The solvent was removed *in vacuo* and the residue was purified using flash chromatography on SiO₂.

Representative Amination Procedure B:

In a glovebox, a microwave vial (3–5 mL size) equipped with a magnetic stir bar was charged with Cs₂CO₃ (488 mg, 1.5 mmol, 3 Equiv.) and then the vial was sealed with a rubber septum prior to removal from the glovebox. Then, *Pd-PEPPSI-IPent^{Cl}* (17 mg, 4 mol %) was added to the vial, after which the vial was evacuated and backfilled with argon (2 times). To this, 0.75 mL of DME (SureSeal, Aldrich) was added followed by the addition of aryl halide (0.5 mmol, 1.0 Equiv.) and

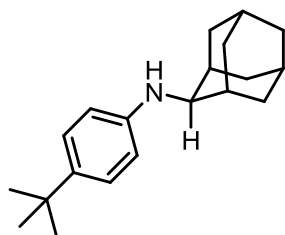
amine (0.75 mmol, 1.5 Equiv.). Alternatively, if the aryl halide and/or amine were solids at room temperature, they were added to the vial along with Pd-*PEPSI-IPent*^{Cl} prior to evacuation. The vial was placed in a preheated (80 °C) oil bath and stirred under argon at 1150–1200 rpm for 24 h. At that time, the reaction mixture was cooled to rt, diluted with diethyl ether, and filtered through a plug of celite. The celite pad was rinsed thoroughly with diethyl ether and the organic layers were combined. The solvent was removed *in vacuo* and the residue purified using flash chromatography.



***N*-Benzyl-4-(*tert*-butyl)-*N*-isopropylaniline (**108**).**

Following amination procedure A, 116 mg (83%) of **108** were obtained following flash chromatography (0% → 5% Et₂O/pentane, R_f = 0.87 in

5% Et₂O/pentane) as a white solid; m.p.: 43–45 °C; ¹H-NMR (400 MHz, CDCl₃) δ 7.40–7.37 (m, 4H), 7.9 (d, *J* = 8.4 Hz, 3H), 6.75 (d, *J* = 8.8 Hz, 2H), 4.48 (s, 2H), 4.34 (sep, *J* = 6.6 Hz, 1H), 1.36 (s, 9H), 1.29 (d, *J* = 6.6 Hz, 6H); ¹³C-NMR (100 MHz, CDCl₃) δ 147.1, 141.2, 138.8, 128.4, 126.3, 126.2, 125.9, 112.7, 48.6, 48.0, 33.7, 31.5, 19.8; HRMS (EI) [M⁺] (*m/z*) calcd. for C₂₀H₂₇N (*m/z*) 281.2144; found 281.2149.

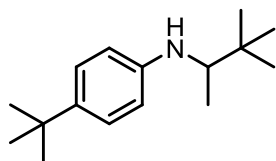


***N*-(4-(*tert*-butyl) phenyl) adamantan-2-amine (**110**).**

Following amination procedure A, 54 mg (46%) of **110** were obtained following flash chromatography (0% → 10% Et₂O/pentane, R_f = 0.33 in 10% Et₂O/pentane) as white solid. When the procedure was carried out at

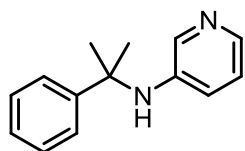
100 °C, 104 mg of **110** were obtained (78%); m.p.: 76–79 °C; ¹H-NMR (400 MHz, CDCl₃) δ 7.19 (d, *J* = 8.4 Hz, 2H), 6.77 (d, *J* = 8.4 Hz, 2H), 2.13 (bs, 3H), 1.90 (s, 6H), 1.75–1.67 (m, 6H), 1.31

(s, 9H); ^{13}C -NMR (100 MHz, CDCl_3) δ 143.2, 142.0, 125.4, 119.3, 52.1, 43.5, 36.5, 33.9, 31.5, 29.7; HRMS (EI) $[\text{M}^+]$ calcd. For $\text{C}_{20}\text{H}_{29}\text{N}$ (m/z) 283.2300; found 238.2311.



4-(*tert*-Butyl)-*N*-(3,3-dimethylbutan-2-yl) aniline (111).

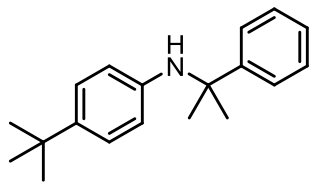
Following amination procedure A, 98 mg (84%) of **111** were obtained following flash chromatography (0% \rightarrow 5% Et_2O /pentane, $R_f = 0.77$ in 5% Et_2O /pentane) as a light-yellow solid; m.p.: 31-33 $^\circ\text{C}$; ^1H -NMR (400 MHz, CDCl_3) δ 7.24 (d, $J = 8.2$ Hz, 2H), 6.61 ($J = 8.2$ Hz, 2H), 3.35 (bs, 1H), 3.26 (q, $J = 6.4$ Hz, 1H), 1.34 (s, 9H), 1.15 (d, $J = 6$ Hz, 3H), 1.02 (s, 9H); ^{13}C -NMR (100 MHz, CDCl_3) δ 146.0, 139.2, 126.0, 112.6, 57.3, 34.7, 33.7, 31.6, 26.5, 15.8; HRMS (EI) $[\text{M}^+]$ calcd. for $\text{C}_{16}\text{H}_{27}\text{N}$ (m/z) 233.2144; found 233.2138.



***N*-(2-Phenylpropan-2-yl) pyridin-3-amine (112).**

Following amination procedure A, 100 mg (95%) of **112** were obtained following flash chromatography (10% \rightarrow 50% EtOAc /hexanes, $R_f = 0.16$ in 50% EtOAc /hexanes) as a yellow solid; m.p.: 92-95 $^\circ\text{C}$; ^1H -NMR (400 MHz, CDCl_3) δ 7.89-7.86 (m, 2H), 7.49 (d, $J = 7.6$ Hz, 2H), 7.35 (t, $J = 7.6$ Hz, 2H), 7.28-7.24 (m, 1H), 6.86 (dd, $J = 8.4$, 4.4 Hz, 1H), 6.48 (d, $J = 8.0$, 2.4 Hz, 1H), 4.20 (bs, 1H), 1.67 (s, 6H); ^{13}C -NMR (100 MHz, CDCl_3) δ 146.4, 142.1, 138.3, 138.1, 128.7, 126.6, 125.4, 123.0, 120.6, 55.8, 30.4; HRMS (EI) $[\text{M}^+]$ m/z calcd. for $\text{C}_{14}\text{H}_{16}\text{N}_2$ (m/z) 212.1313; found 212.1317.

4-(*tert*-Butyl)-*N*-(2-phenylpropan-2-yl) aniline (113**).**

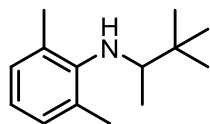


Following amination procedure A, 130 mg (97%) of **113** were obtained following flash chromatography (0 → 5% Et₂O/pentane, R_f = 0.48 in

5% Et₂O/pentane) as a yellow solid; m.p.: 66-68 °C (no literature m.p. reported); ¹H-NMR (400 MHz, CDCl₃) δ 7.60 (d, *J* = 7.4 Hz, 2H), 7.39 (dd, *J* = 8.0, 7.2 Hz, 2H), 7.30-7.28 (m, 1H), 7.09 (d, *J* = 8.6 Hz, 2H), 6.34 (d, *J* = 7.6 Hz, 2H), 3.98 (bs, 1H), 1.69 (s, 6 H), 1.28 (s, 9H); ¹³C-NMR (100 MHz, CDCl₃) δ 147.7, 143.6, 139.7, 128.4, 126.2, 125.6, 125.4, 115.0, 55.7, 33.7, 31.5, 30.7.

The spectral data are consistent with those reported in the literature.⁸⁸

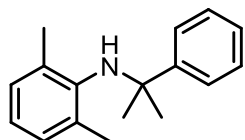
***N*-(3,3-Dimethylbutan-2-yl)-2,6-dimethylaniline (**114**).**



Following amination procedure A, 76 mg (74%) of **114** were obtained

following flash chromatography (0 → 5% Et₂O/pentane, R_f = 0.85 in 5% Et₂O/pentane) as a yellow oil; ¹H-NMR (400 MHz, CDCl₃) δ 7.01 (d, *J* = 7.2 Hz, 2H), 6.83-6.77 (m, 1H), 3.19 (q, *J* = 6.4 Hz, 1H), 2.97 (bs, 1H), 2.31 (s, 6H), 1.10 (s, 9H), 0.92 (d, *J* = 6.4 Hz, 3H); ¹³C-NMR (75 MHz, CDCl₃) δ 145.3, 129.0, 128.8, 120.8, 59.8, 34.8, 26.5, 19.3, 15.3; HRMS (EI) [M⁺] calcd. for C₁₄H₂₃N (m/z) 205.1830; found 205.1836.

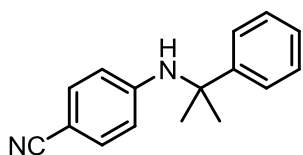
2,6-Dimethyl-*N*-(2-phenylpropan-2-yl) aniline (115**).**



Following amination procedure A, 89 mg (70%) of **115** were obtained

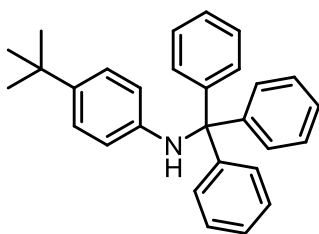
following flash chromatography (0 → 5% Et₂O/pentane, R_f = 0.61 in 5% Et₂O/pentane) as a white solid; m.p.: 43-45 °C; ¹H-NMR (300 MHz, CDCl₃) δ 7.70-7.67 (m, 2H), 7.42-7.37 (m, 2H), 7.32-7.28 (m, 1H), 7.02 (d, *J* = 7.2 Hz, 2H), 6.93- 6.88 (m, 1H), 3.35 (bs, 1H), 2.09 (s, 6H), 1.58 (s,

6H); ^{13}C -NMR (75 MHz, CDCl_3) δ 150.6, 144.2, 133.3, 128.5, 127.8, 126.1, 125.5, 122.6, 57.9, 30.8, 20.3; HRMS (EI) $[\text{M}^+]$ calcd. for $\text{C}_{17}\text{H}_{21}\text{N}$ (m/z) 239.1674; found 239.1679.



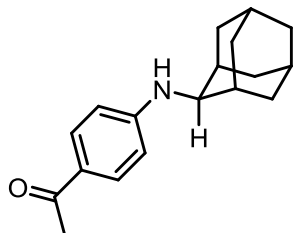
4-(2-Phenylpropan-2-ylamino) benzonitrile (116).

Following amination procedure A, 90 mg (69%) of **116** were obtained following flash chromatography (0% \rightarrow 40% Et_2O /pentane, R_f = 0.44 in 40% Et_2O /pentane) as a light brown oil; ^1H -NMR (400 MHz, CDCl_3) δ 7.45 (d, J = 7.6 Hz, 2H), 7.37 (dd, J = 8.0, 7.2 Hz, 2H), 7.30-7.25 (m, 3H), 6.32 (d, J = 8.4 Hz, 2H), 4.70 (bs, 1H), 1.70 (s, 6H); ^{13}C -NMR (100 MHz, CDCl_3) δ 149.3, 145.7, 133.1, 128.8, 126.8, 125.2, 120.4, 114.5, 98.4, 56.1, 30.4; HRMS (EI) $[\text{M}^+\text{H}^+]$ calcd. for $\text{C}_{16}\text{H}_{16}\text{N}_2$ (m/z) 237.1386; found 237.1386.



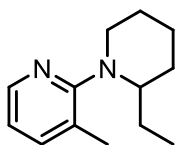
4-tert-Butyl-N-tritylaniline (117).

Following amination procedure A, 88 mg (46%) of **117** were obtained following flash chromatography (0% \rightarrow 5% Et_2O /pentane, R_f = 0.57 in 5% Et_2O /pentane) as beige solid; When the procedure was carried out at 100 $^\circ\text{C}$, 115 mg of **117** were obtained (60%); m.p.: 69-71 $^\circ\text{C}$ (literature m.p.: 152-153 $^\circ\text{C}$);⁸⁹ our additional characterization data were not available when the literature m.p. was reported which suggests that it is an error; ^1H -NMR (400 MHz, CDCl_3) δ 7.24 (d, J = 8 Hz, 6H), 7.31 (t, J = 7.2 Hz, 6H), 7.25 (m, 3H), 6.96 (d, J = 8.6 Hz, 2H), 6.33 (d, J = 8.6 Hz, 2H), 4.95 (bs, 1H), 1.23 (s, 9H); ^{13}C -NMR (75 MHz, CDCl_3) δ 145.6, 143.6, 139.7, 129.2, 127.8, 126.6, 124.9, 115.6, 71.3, 33.7, 31.4; HRMS (EI) $[\text{M}^+\text{H}^+]$ calcd. for $\text{C}_{29}\text{H}_{29}\text{N}$ (m/z) 391.2300; found 391.2309.



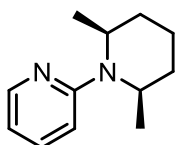
1-(4-Adamantan-1-ylamino)phenyl)ethanone (118).

Following amination procedure A, 106 mg (79%) of **118** were isolated following flash chromatography (10% → 40% Et₂O/pentane, R_f = 0.3 in 40% Et₂O/pentane) as a yellow solid; m.p.: 91-94 °C; ¹H-NMR (400 MHz, CDCl₃) δ 7.78 (d, *J* = 8.4 Hz, 2H), 6.69 (d, *J* = 8.4 Hz, 2H), 4.12 (bs, 1H), 2.50 (s, 3H), 2.16 (bs, 3H), 2.00 (bs, 6H), 1.77-1.70 (m, 6H); ¹³C-NMR (100 MHz, CDCl₃) δ 196.2, 150.1, 130.4, 126.0, 114.0, 52.0, 42.6, 36.3, 29.5, 25.9; HRMS (EI) [M⁺] calcd. for C₁₈H₂₃NO (m/z) 269.1780; found 269.1776.



2-(2-Ethylpiperidin-1-yl)-3-methylpyridine (119).

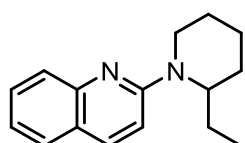
Following amination procedure A, 87 mg (84%) of **119** were obtained following flash chromatography (0% → 40% Et₂O/pentane, R_f = 0.84 in 40% Et₂O/pentane) as a yellow oil; ¹H-NMR (400 MHz, CDCl₃) δ 8.21 (d, *J* = 4.4 Hz, 1H), 7.41 (d, *J* = 7.2 Hz, 1H), 6.85 (dd, *J* = 7.4, 5.0 Hz, 1H), 3.36-3.31 (m, 1H), 3.12-3.06 (m, 1H), 2.97-2.91 (m, 1H), 2.28 (s, 3H), 1.88-1.63 (m, 4H), 1.56-1.36 (m, 4H), 0.71 (t, *J* = 7.4 Hz, 3H); ¹³C-NMR (75 MHz, CDCl₃) δ 162.8, 145.4, 139.0, 127.0, 117.9, 58.0, 48.9, 28.9, 26.3, 23.4, 21.9, 18.0, 10.3; HRMS (EI) [M⁺] calcd. for C₁₃H₂₀N₂ (m/z) 204.1626; found 204.1633.



2-(2,6-Dimethylpiperidin-1-yl)pyridine (120).

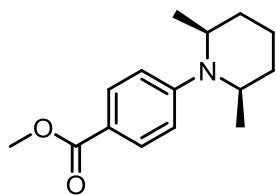
Following amination procedure A, 56 mg (70%) of **120** were obtained following flash chromatography (0% → 15% Et₂O/pentane, R_f = 0.52 in 15% Et₂O/pentane) as a yellow oil;

^1H -NMR (300 MHz, CDCl_3) δ 8.23-8.21 (m, 1H), 7.45-7.43 (m, 1H), 6.58 (d, $J = 9.0$ Hz, 1H), 6.54-6.52 (m, 1H), 4.53 (m, 2H), 1.77-1.58 (m, 6H), 2.00 (d, $J = 6.9$ Hz, 6H); ^{13}C -NMR (100 MHz, CDCl_3) δ 158.0, 148.1, 137.1, 111.5, 106.9, 45.5, 30.9, 19.0, 14.7; HRMS (EI) $[\text{M}^+\text{H}^+]$ calcd. for $\text{C}_{12}\text{H}_{18}\text{N}_2$ (m/z) 191.15428; found 191.15396.



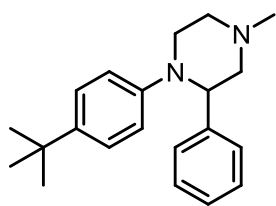
2-(2-Ethylpiperidin-1-yl)-4-methylquinoline (121).

Following amination procedure A, 104 mg (80%) of **121** were obtained following flash chromatography (0% \rightarrow 5% Et_2O /pentane, $R_f = 0.27$ in 5% Et_2O /pentane) as a yellow oil; ^1H -NMR (300 MHz, CDCl_3) δ 7.75 (d, $J = 8.4$ Hz, 1H), 7.68 (d, $J = 8.0$ Hz, 1H), 7.53-7.50 (m, 1H), 7.21 (t, $J = 7.6$ Hz, 1H), 6.85 (s, 1H), 4.63-4.54 (m, 2H), 3.01 (td, $J = 14.4, 2.4$ Hz, 1H), 2.60 (s, 3H), 1.81-1.67 (m, 8H), 0.93 (t, $J = 7.6$ Hz, 3H); ^{13}C -NMR (100 MHz, CDCl_3) δ 157.4, 148.2, 144.4, 129.0, 126.8, 123.3, 122.9, 121.3, 110.0, 53.0, 39.2, 27.6, 25.7, 22.0, 19.3, 19.3, 11.3; HRMS (EI) $[\text{M}^+]$ calcd. for $\text{C}_{17}\text{H}_{22}\text{N}_2$ (m/z) 254.1783; found 254.1779.



Methyl 4-(2, 6-cis-dimethylpiperidin-1-yl) benzoate (122).

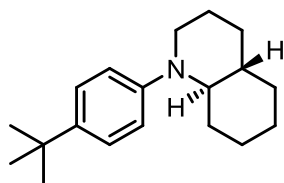
Following amination procedure A, 81 mg (66%) of **122** were obtained as inseparable isomers (1:0.07) following flash chromatography (0% \rightarrow 10% Et_2O /pentane, $R_f = 0.34$ in 10% Et_2O /pentane) as a white solid; m.p.: 75-78 $^\circ\text{C}$. Included here are the spectra of the major isomer only. ^1H -NMR (600 MHz, CDCl_3) δ 7.23 (d, $J = 6.4$ Hz, 2H), 6.87 (d, $J = 6.0$ Hz, 2H), 3.98 (bs, 2H), 3.87 (s, 3H), 1.91-1.53 (m, 6H), 1.13 (d, $J = 7.2$ Hz, 6H), ^{13}C -NMR (150 MHz, CDCl_3) δ 167.3, 152.4, 131.2, 118.5, 114.2, 51.5, 48.5, 31.5, 19.0, 15.8; HRMS (EI) $[\text{M}^+]$ calcd. for $\text{C}_{15}\text{H}_{21}\text{NO}_2$ (m/z) 247.1572; found 247.1579.



1-(4-(*tert*-Butyl)phenyl)-4-methyl-2-phenylpiperazine (123).

Following amination procedure A, 137 mg (89%) of **123** were obtained following flash chromatography (30% → 70% EtOAc/hexanes, R_f = 0.31

in 70% EtOAc/hexanes) as an orange oil; $^1\text{H-NMR}$ (400 MHz, CDCl_3) δ 7.36 (d, J = 7.2 Hz, 2H), 7.24 (dd, J = 8.0, 7.2 Hz, 2H), 7.19-7.14 (m, 3H), 6.93-6.89 (m, 2H), 4.41 (dd, J = 8.4, 3.2 Hz, 1H), 3.51 (dt, J = 12.4, 3.2 Hz, 1H), 3.20 (td, J = 11, 2.8 Hz, 1H), 2.92-2.88 (m, 1H), 2.81-2.79 (m, 1H), 2.58 (td, J = 10.4, 2.8 Hz, 1H), 2.41 (dd, J = 11.6, 8.4 Hz, 1H), 2.36 (s, 3H), 1.26 (s, 9H); $^{13}\text{C-NMR}$ (100 MHz, CDCl_3) δ 148.6, 144.0, 141.7, 128.1, 127.6, 126.6, 125.4, 120.9, 63.5, 61.6, 55.6, 53.8, 46.0, 33.9, 31.3; HRMS (EI) $[\text{M}^+]$ calcd. For $\text{C}_{21}\text{H}_{28}\text{N}_2$ (m/z) 308.2252; found 308.2248.

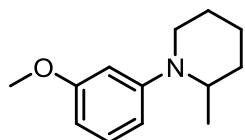


1-(4-(*tert*-butyl)phenyl)decahydroquinoline (124).

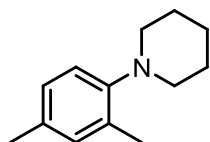
Following amination procedure A, 119 mg (88%) of **124** were obtained following flash chromatography (0% → 15% Et_2O /pentane, R_f = 0.55 in

15% Et_2O /pentane) as an orange oil; $^1\text{H-NMR}$ (400 MHz, CDCl_3) δ 7.33-7.30 (m, 2H), 7.10-7.07 (m, 2H), 3.10-3.11 (m, 1H), 2.73 (td, J = 12.0, 2.8 Hz, 1H), 2.33 (td, J = 10.0, 2.8 Hz, 1H), 1.87-1.76 (m, 1H), 1.73-1.65 (m, 6H), 1.49-1.36 (m, 1H), 1.33 (s, 9H), 1.28-1.10 (m, 4H), 1.05-0.96 (m, 1H); $^{13}\text{C-NMR}$ (100 MHz, CDCl_3) δ 149.9, 147.0, 125.4, 125.0, 65.8, 58.0, 42.5, 34.3, 33.1, 32.4, 31.6, 31.5, 26.5, 26.2, 25.5; HRMS (EI) $[\text{M}^+]$ calcd. For $\text{C}_{19}\text{H}_{29}\text{N}$ (m/z) 271.2300; found 271.2308.

2-Methoxy-6-(2-methylpiperidin-1-yl) pyridine (125).

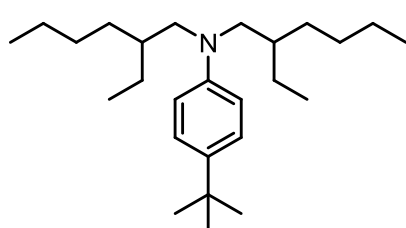


Following amination procedure A, 91 mg (88%) of **125** were obtained following flash chromatography (0% → 5% Et₂O/pentane, R_f = 0.6 in 5% Et₂O/pentane) as a light-orange oil; ¹H-NMR (400 MHz, CDCl₃) δ 7.38 (dd, *J* = 8.0, 7.8 Hz, 1H), 6.14 (d, *J* = 8.0 Hz, 1H), 6.01 (d, *J* = 8.0 Hz, 1H), 4.67 (qt, *J* = 6.8, 6.4 Hz, 1H), 4.11 (m, 1H), 3.88 (s, 3H), 2.91 (td, *J* = 12.6, 2.8 Hz, 1H), 1.82-1.46 (m 6H), 1.15 (d, *J* = 6.8 Hz, 3H); ¹³C-NMR (100 MHz, CDCl₃) δ 163.0, 158.0, 139.9, 98.0, 96.4, 52.8, 46.6, 39.4, 30.5, 25.7, 19.0, 13.6; HRMS (EI) [M⁺] calcd. for C₁₂H₁₈N₂O (m/z) 206.1419; found 206.1415.



1-(2,4-dimethylphenyl)piperidine (126).

Following amination procedure B, 87 mg (93%) of **126** were obtained by flash chromatography (0% → 2% Et₂O/pentane, R_f = 0.33 in pentane) as a yellow oil; ¹H-NMR (400 MHz, CDCl₃) δ 7.01 (s, 1H), 7.04 (d, *J* = 8 Hz, 1H), 6.99 (d, *J* = 8 Hz, 1H), 2.88 (t, *J* = 5.2 Hz, 4H), 2.35 (s, 6H), 1.81-1.75 (m, 4H), 1.66-1.62 (m, 2H); ¹³C-NMR (100 MHz, CDCl₃) δ 150.5, 132.6, 131.9, 131.6, 126.8, 118.8, 53.5, 26.7, 24.4, 20.7, 17.6. The spectral data are consistent with those reported in the literature.⁹⁰

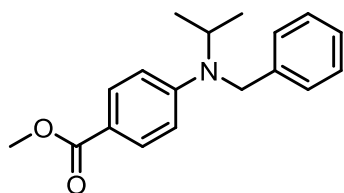


4-(*tert*-butyl)-*N,N*-bis(2-ethylhexyl)aniline (127).

Following amination procedure A, 123 mg (66%) of **127** were obtained following flash chromatography (heptane, R_f = 0.6) as a colorless oil; ¹H-NMR (300 MHz, CDCl₃) δ 7.24 (d, *J* = 8.7 Hz, 2H), 6.64 (d, *J* = 8.7 Hz, 2H),

3.28-3.09 (m, 4H), 1.81 (bs, 2H), 1.34-1.31 (m, 25H), 0.93-0.89 (m, 12H); ^{13}C -NMR (100 MHz, CDCl_3) δ (146.3, 146.3)^a, 137.5, 125.7, 112.3, 56.6, (36.8, 36.8),^a 33.6, 31.6, 30.7, 30.3, 28.8, 28.7, 23.9, 23.3, 14.1, 10.7, 10.6; HRMS (EI) $[\text{M}^+]$ calcd. for $\text{C}_{26}\text{H}_{47}\text{N}$ (m/z) 373.3709; found 373.3701.

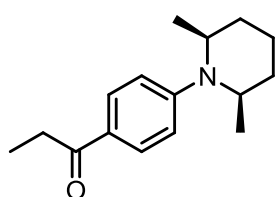
^aPeaks coalescence upon obtaining ^{13}C -NMR spectrum at 55 °C.



Methyl 4-(benzyl (isopropyl) amino) benzoate (128).

Following amination procedure A, 56 mg (40%) of **128** were obtained following flash chromatography (0% → 15% Et_2O /pentane, R_f = 0.35

in 15% Et_2O /pentane) as an orange solid; m.p.: 74-77 °C; ^1H -NMR (400 MHz, CDCl_3) δ 7.86 (d, J = 9.0 Hz, 2H), 7.33 (dd, J = 7.6, 7.2 Hz, 2H), 7.28-7.24 (m, 3H), 6.68 (d, J = 9.0 Hz, 2H), 4.52 (s, 2H), 4.38 (sep, J = 6.4 Hz, 1H), 3.85 (s, 3H), 1.26 (d, J = 6.4 Hz, 6H); ^{13}C -NMR (100 MHz, CDCl_3) δ 167.3, 152.5, 139.3, 131.3, 128.6, 126.7, 126.0, 117.3, 111.6, 51.5, 48.3, 47.9, 20.0; HRMS (EI) $[\text{M}^+]$ calcd. for $\text{C}_{18}\text{H}_{21}\text{NO}_2$ (m/z) 283.1572; found 283.1581.

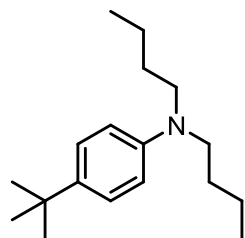


4-(1-Propanyl)-2,6-cis-dimethylpiperidin-1-yl)benzene(129).

Following amination procedure A, 73 mg (60%) of **129** were obtained as inseparable isomers (1:0.07) following flash chromatography (0% →

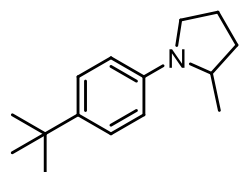
10% Et_2O /pentane, R_f = 0.20 in 10% Et_2O /pentane) as a white solid; m.p.: 72-76 °C. Included here are the spectra of the major isomer only. ^1H -NMR (600 MHz, CDCl_3) δ 7.91 (d, J = 9.0 Hz, 2H), 6.86 (d, J = 9.0 Hz, 2H), 4.06 (bs, 2H), 2.94 (q, J = 7.6 Hz, 2H), 1.89-1.55 (m, 7H), 1.23 (t, J = 7.6 Hz, 3H), 1.16 (d, J = 7.2 Hz, 6H); ^{13}C -NMR (150 MHz, CDCl_3) δ 199.1, 152.2, 130.1,

126.0, 113.5, 48.1, 31.4, 31.0, 18.9, 15.4, 8.8; HRMS (EI) $[M^+]$ calcd. for $C_{16}H_{23}NO$ (m/z) 245.1780; found 245.1786.



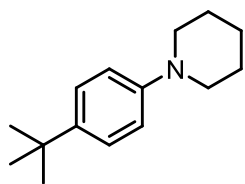
4-(*tert*-Butyl)-*N,N*-dibutylaniline (130).

Following amination procedure A, 120 mg (92%) of **130** were obtained following flash chromatography (0% → 5% Et₂O/pentane, R_f = 0.26 in pentane) as a yellow oil; ¹H-NMR (400 MHz, CDCl₃) δ 7.29 (d, J = 8.8 Hz, 2 H), 6.66 (d, J = 8.8 Hz, 2 H), 3.29 (t, J = 7.6 Hz, 4 H), 1.60 (quint, J = 7.6 Hz, 4 H), 1.41 (sex, J = 7.6 Hz, 4 H), 1.34 (s, 9 H), 1.00 (t, J = 7.6 Hz, 6 H); ¹³C-NMR (100 MHz, CDCl₃) δ 137.6, 125.9, 111.3, 50.8, 46.0, 33.6, 31.6, 29.5, 20.4, 14.0. The spectral data are consistent with those reported in the literature.⁹¹



1-(4-*tert*-Butylphenyl)-2-methylpyrrolidine (140).

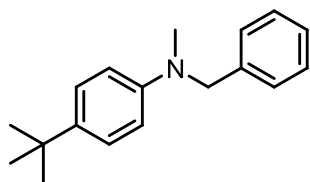
Following amination procedure B, 102 mg (94%) of **140** were obtained following flash chromatography (0% → 10% EtOAc/hexane, R_f = 0.63 in 10% EtOAc/hexane) as a light-yellow oil; ¹H-NMR (400 MHz, CDCl₃) δ 7.29 (d, J = 8.8 Hz, 2H), 6.58 (d, J = 8.8 Hz, 2H), 3.89-3.85 (m, 1H), 3.48-3.53 (m, 1H), 3.20-3.14 (m, 1H), 2.12-1.95 (m, 3H), 1.73-1.69 (m, 1H), 1.32 (s, 9H), 1.20 (d, J = 6.0 Hz, 3 H); ¹³C-NMR (100 MHz, CDCl₃) δ 145.1, 137.7, 125.9, 111.3, 53.7, 48.8, 33.7, 33.2, 31.6, 23.4, 19.7; HRMS (EI) $[M^+]$ calcd. for $C_{15}H_{23}N$ (m/z) 217.1830; found 217.1821.



1-(4-*tert*-Butylphenyl) piperidine (141).

Following amination procedure B, 103 mg (95%) of **141** were obtained following flash chromatography (0% → 10% EtOAc/hexane, R_f = 0.47 in

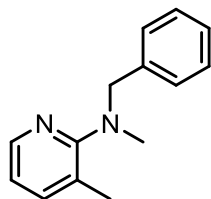
10% EtOAc/hexane) as a white solid; m.p.: 35-38 °C (lit. m.p.: 36-37 °C); $^1\text{H-NMR}$ (400 MHz, CDCl_3) δ 7.33 (d, J = 8.6 Hz, 2H), 6.94 (d, J = 8.6 Hz, 2H), 3.17 (t, J = 6.0 Hz, 4H), 1.79-1.73 (m, 4H), 1.64-1.58 (m, 2H), 1.35 (s, 9H); $^{13}\text{C-NMR}$ (100 MHz, CDCl_3) δ 149.9, 141.8, 125.7, 116.1, 50.8, 33.8, 31.4, 25.9, 24.2. The spectral data are consistent with those reported in the literature.⁹²



***N*-Benzyl-4-(*tert*-butyl)-*N*-methyl aniline (142).**

Following amination procedure B, 105 mg (83%) of **142** were obtained following flash chromatography (0% → 5% Et_2O /pentane, R_f = 0.76 in

5% Et_2O /pentane) as a white solid; m.p.: 48-50 °C (lit. m.p.: 48-49 °C); $^1\text{H-NMR}$ (400 MHz, CDCl_3) δ 7.39-7.35 (m, 2H), 7.33-7.28 (m, 5H), 6.78 (d, J = 8.8 Hz, 2H), 4.55 (s, 2H), 3.04 (s, 3H); $^{13}\text{C-NMR}$ (100 MHz, CDCl_3) δ 147.7, 139.4, 139.2, 128.5, 126.8, 126.8, 125.9, 112.1, 57.0, 38.5, 33.7, 31.5. The spectral data are consistent with those reported in the literature.⁴⁷

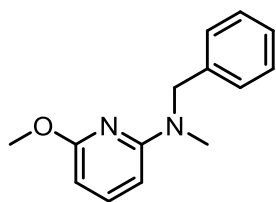


***N*-Benzyl-*N*-3-dimethylpyridin-2-amine (143).**

Following amination procedure B, 71 mg (67%) of **143** were obtained following flash chromatography (20% EtOAc/pentane, R_f = 0.68) as a light-yellow oil;

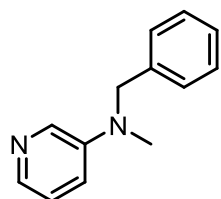
$^1\text{H-NMR}$ (400 MHz, CDCl_3) δ 8.20 (d, J = 4.6 Hz, 1H), 7.44-7.42 (m, 3H), 7.37 (dd, J = 7.6, 7.2 Hz, 2H), 7.29 (dd, J = 7.6, 6.8 Hz, 1H), 6.86 (dd, J = 7.0, 4.6 Hz, 1H), 4.37 (s, 2H), 2.79 (s, 3H),

2.36 (s, 3H); ^{13}C -NMR (100 MHz, CDCl_3) δ 162.5, 145.1, 139.4, 139.2, 128.3, 127.8, 126.8, 124.4, 117.3, 57.7, 38.9, 18.9. The spectral data are consistent with those reported in the literature.⁹³



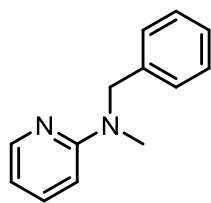
***N*-Benzyl-6-methoxy-*N*-methylpyridin-2-amine (144).**

Following amination procedure B, 111 mg (98%) of **144** were obtained following flash chromatography (10% Et_2O /pentane, $R_f = 0.74$) as a light-yellow oil; ^1H -NMR (400 MHz, CDCl_3) δ 7.43 (t, $J = 8.0$ Hz, 1H), 7.38-7.34 (m, 2H), 7.31-7.28 (m, 3H), 6.09 (d, $J = 8.0$ Hz, 2H), 4.86 (s, 2H), 3.90 (s, 3H), 3.07 (s, 3H); ^{13}C -NMR (75 MHz, CDCl_3) δ 163.0, 157.7, 140.0, 139.2, 128.4, 127.2, 126.8, 96.7, 96.4, 53.0, 52.9, 36.0. This compound has been reported in the literature but not fully characterized.⁹⁴



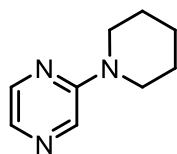
***N*-Benzyl-*N*-methylpyridin-3-amine (145).**

Following amination procedure A, 87 mg (88%) of **145** were obtained following flash chromatography (30% EtOAc /pentane $R_f = 0.3$) as a yellow oil; ^1H -NMR (400 MHz, CDCl_3) δ 8.19 (d, $J = 2.8$ Hz, 1H), 7.98 (d, $J = 4.8$ Hz, 1H), 7.35-7.31 (m, 2H), 7.27 (d, $J = 7.6$ Hz, 1H), 7.22 (d, $J = 7.6$ Hz, 2H), 7.11-7.08 (m, 1H), 6.99 (dd, $J = 8.4, 2.8$ Hz, 1H), 4.56 (s, 2H), 3.07 (s, 3H); ^{13}C -NMR (100 MHz, CDCl_3) δ 145.2, 138.0, 137.9, 134.9, 128.7, 127.1, 126.6, 123.4, 118.5, 56.1, 38.3. The spectral data are consistent with those reported in the literature.⁹⁵



***N*-Benzyl-*N*-methylpyridin-2-amine (**146**).**

Following amination procedure A, 83 mg (84%) of **146** were obtained following flash chromatography (10% Et₂O/pentane, R_f = 0.39 in 10% Et₂O/pentane) as a yellow oil; ¹H-NMR (400 MHz, CDCl₃) δ 8.25 (d, *J* = 4.4 Hz, 1H), 7.49-7.45 (m, 1H), 7.37-7.33 (m, 2H), 7.28 (d, *J* = 7.6 Hz, 3H), 6.62-6.54 (m, 1H), 6.55 (d, *J* = 8.8 Hz, 1H), 4.85 (s, 2H), 3.11 (s, 3H); ¹³C-NMR (100 MHz, CDCl₃) δ 158.8, 147.9, 138.6, 137.2, 126.9, 126.8, 111.7, 105.6, 53.1, 36.0. The spectral data are consistent with those reported in the literature.⁹⁶



2-(piperidin-1-yl)pyrazine (147**).**

Following amination procedure B, 87 mg (91%) of **147** were obtained following flash chromatography (0% → 55% Et₂O/pentane, R_f = 0.17 in 40% Et₂O/pentane) as a beige solid; m.p.: 38-39 °C (lit. m.p: 36-37 °C); ¹H-NMR (400 MHz, CDCl₃) δ 8.13 (bs, 1H), 8.03 (bs, 1H), 7.76 (d, *J* = 2.8 Hz, 1H), 3.58 (m, 4H), 1.66 (bs, 6H); ¹³C-NMR (100 MHz, CDCl₃) δ 155.1, 141.6, 131.9, 131.1, 45.5, 25.3, 24.5. The spectral data are consistent with those reported in the literature.⁹⁷

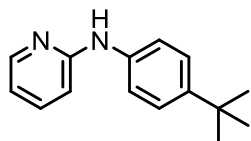
General Amination procedures for chapter 3:

Amination procedure A: In a glovebox, a microwave vial (3–5 mL size) equipped with a magnetic stir bar was charged with Cs_2CO_3 (488 mg, 1.5 mmol, 3 Equiv.) and then the vial was sealed with a rubber septum prior to removal from the glovebox. Then, $\text{Pd-PEPPSI-IPent}^{\text{Cl}}$ (17 mg, 4 mol %) was added to the vial, after which the vial was evacuated and backfilled with argon (2 times). To this, 0.75 mL of DME (SureSeal, Aldrich) was added followed by the aryl halide (0.5 mmol, 1.0 Equiv.) and 2-aminopyridine derivative (0.75 mmol, 1.5 Equiv.). Alternatively, if the aryl halide or 2-aminopyridine derivative were solids at room temperature, they were added to the vial along with $\text{Pd-PEPPSI-IPent}^{\text{Cl}}$ prior to evacuation. The vial was placed in a preheated (80 °C) oil bath and stirred under argon at 1150–1200 rpm for 24 hr. At that time the reaction mixture was cooled to rt, diluted with diethyl ether, and filtered through a plug of celite. The celite pad was rinsed thoroughly with diethyl ether and the organic layers were combined. The solvent was removed *in vacuo* and the residue purified using flash chromatography.

Amination procedure B: In a glovebox, a microwave vial (3–5 mL size) equipped with a magnetic stir bar was charged with 95% NaH (18 mg, 0.75 mmol, 1.5 Equiv.) and then the vial was sealed with a rubber septum prior to removal from the glovebox. Then, BHT (165.2 mg, 0.75 mmol, 1.5 Equiv.) were added after which the septum was replaced, and the vial evacuated and backfilled with Ar (3 times). The flask was then cooled to 0 °C and Et_2O (2 mL) was added. After stirring for 15 min at 0 °C, the solution was warmed up to rt and allowed to stir for an additional 15 min. The solvent was then removed under high vacuum to yield an off-white solid. To this vial $\text{Pd PEPPSI-IPent}^{\text{Cl}}$ (17 mg, 4 mol %) was added and the vial evacuated and backfilled with argon (2 times). Then 0.75 mL of DME (SureSeal, Aldrich) was added followed by the aryl halide (0.5 mmol, 1.0

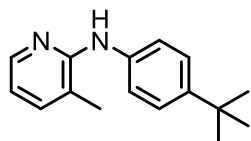
Equiv) and 2-aminopyridine derivative (0.75 mmol, 1.5 Equiv.). Alternatively, if the aryl halide or 2-aminopyridine derivative were solids at room temperature, they were added to the vial with Pd-*PEPPSI-IPent*^{Cl} prior to evacuation. The vial was placed in a preheated 80 °C oil bath and stirred under argon at 1150–1200 rpm for 24 hr. Then, the reaction mixture was cooled to rt, diluted with diethyl ether, and filtered through a plug of celite. The celite pad was rinsed thoroughly with diethyl ether and the organic layers were combined. The solvent was removed *in vacuo* and the residue purified using flash chromatography.

Amination procedure C: In a glovebox, a microwave vial (3–5 mL size) equipped with a magnetic stir bar was charged with KO^tBu (67 mg, 0.6 mmol, 1.2 Equiv.) and then the vial was sealed with a rubber septum prior to removal from the glovebox. Then, Pd *PEPPSI-IPent*^{Cl} (17 mg, 4 mol %) were added to the vial, after which it was evacuated and backfilled with argon (2 times). Then the aryl halide (0.5 mmol, 1.0 Equiv.) and 2-aminopyridine derivative (0.75 mmol, 1.5 Equiv.) were added by syringe. Alternatively, if the aryl halide or 2-aminopyridine were solids at room temperature, they were added to the vial with Pd-*PEPPSI-IPent*^{Cl} prior to evacuation. The vial was placed in a preheated (80 °C) oil bath and stirred under argon at 1150–1200 rpm for 24 hr. At that time, the reaction mixture was cooled to rt, diluted with diethyl ether, filtered through a plug of celite. The celite pad was rinsed thoroughly with diethyl ether and the organic layers were combined. The solvent was removed *in vacuo* and the residue purified using flash chromatography.



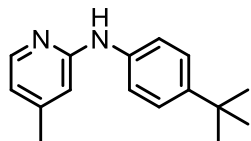
***N*-[4-(*tert*-Butyl) phenyl]pyridin-2-amine (**149**).**

Following amination procedure C, compound **149** (64 mg, 56%) was obtained following flash chromatography (5% → 20% Et₂O/pentane, *R_f* = 0.55) as an off-white solid; m.p.: 140–142 °C (no literature m.p. reported); ¹H-NMR (400 MHz, CDCl₃) δ 8.22 (d, *J* = 4.4 Hz, 1H), 7.51–7.47 (m, 1H), 7.39 (d, *J* = 8.6 Hz, 2H), 7.28 (d, *J* = 8.6 Hz, 2H), 7.06 (bs, 1H), 6.90 (d, *J* = 8.8 Hz, 1H), 6.74–6.71 (m, 1H), 1.36 ppm (s, 9H); ¹³C-NMR (100 MHz, CDCl₃) δ 156.4, 148.4, 145.9, 137.7, 137.6, 126.1, 120.6, 114.6, 107.8, 34.3, 31.4. The spectral data are consistent with those reported in the literature.⁹⁸



***N*-(4-*tert*-Butylphenyl)-3-methylpyridin-2-amine (**151a**).**

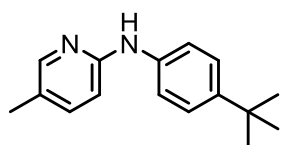
Following amination procedure C, 34 mg (28%) of **151a** were obtained following flash chromatography (2.5 → 15% Et₂O/ pentane, *R_f* = 0.28 in 15% Et₂O/pentane) as a beige solid; m.p.: 53–55 °C; ¹H-NMR (400 MHz, CDCl₃) δ 8.13 (d, *J* = 4.4 Hz, 1H), 7.49 (d, *J* = 8.6 Hz, 2H), 7.37 (d, *J* = 8.6 Hz, 3H), 6.70 (dd, *J* = 6.8, 5.2 Hz, 1H), 6.09 (br s, 1H), 2.25 (s, 3H), 1.34 ppm (s, 9H); ¹³C-NMR (100 MHz, CDCl₃) δ 154.1, 145.4, 144.9, 138.0, 137.7, 125.7, 119.6, 117.7, 114.9, 34.2, 31.4, 17.3; HRMS (EI) [*M*⁺] calcd for C₁₆H₂₀N₂ (*m/z*) 240.1626; found 240.1622.



***N*-(4-*tert*-Butylphenyl)-4-methylpyridin-2-amine (**151b**).**

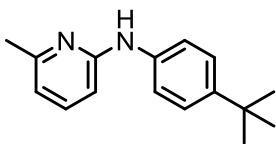
Following amination procedures A, B and C, 24 mg (18 %), 52 mg (43 %), and 54 mg (45%) of the **151b** were obtained, respectively. The product was isolated by flash chromatography (20% EtOAc/hexanes, *R_f* = 0.32) as a light-orange solid; m.p.: 117–119 °C (no

literature m.p. reported); ^1H -NMR (400 MHz, CDCl_3) δ 8.09 (d, $J = 5.2$ Hz, 1H), 7.39 (d, $J = 8.6$ Hz, 2H), 7.28 (d, $J = 8.6$ Hz, 2H), 7.24 (bs, 1H), 6.75 (bs, 1H), 6.57 (d, $J = 5.2$ Hz, 1H), 2.27 (s, 3H), 1.37 ppm (s, 9H); ^{13}C -NMR (100 MHz, CDCl_3) δ 156.7, 148.7, 147.9, 145.6, 137.9, 126.0, 120.6, 116.0, 107.9, 34.2, 31.4, 21.2; HRMS (EI) $[\text{M}^+]$ calcd for $\text{C}_{16}\text{H}_{20}\text{N}_2$ (m/z) 240.1626; found 240.1629.



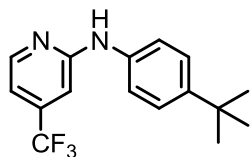
***N*-(4-*tert*-Butylphenyl)-5-methylpyridin-2-amine (151c).**

Following amination procedures B and C, 71 mg (59%) and 81 mg (67%) of **151c** were obtained, respectively. The product was isolated by flash chromatography (20% EtOAc/hexanes, $R_f = 0.5$) as an off-white solid; m.p.: 94–97 °C; ^1H -NMR (400 MHz, CDCl_3) δ 8.04 (d, $J = 1.2$ Hz, 1H), 7.36 (m, 2H), 7.33 (dd, $J = 8.4, 2.0$ Hz, 1H), 7.23 (d, $J = 8.8$ Hz, 2H), 6.84 (d, $J = 8.4$ Hz, 1H), 6.66 (bs, 1H), 2.24 (s, 3H), 1.35 ppm (s, 9H); ^{13}C -NMR (100 MHz, CDCl_3) δ 154.3, 148.0, 145.3, 138.5, 138.3, 126.0, 123.6, 119.9, 107.7, 34.2, 31.4, 17.5; HRMS (EI) $[\text{M}^+]$ calcd for $\text{C}_{16}\text{H}_{20}\text{N}_2$ (m/z) 240.1626; found 240.1615.



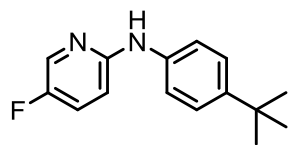
***N*-(4-*tert*-Butylphenyl)-6-methylpyridin-2-amine (151d).**

Following amination procedures A, B and C, 40 mg (33 %), 65 mg (54 %), and 90 mg (75%) of **151d** were obtained, respectively. The product was isolated by flash chromatography (20% EtOAc/hexanes, $R_f = 0.5$) as a white solid; m.p.: 86–88 °C; ^1H -NMR (400 MHz, CDCl_3) δ 7.41–7.36 (m, 3H), 7.25 (d, $J = 8.4$ Hz, 2H), 6.73 (d, $J = 8.4$ Hz, 1H), 6.62 (bs, 1H), 6.60 (d, $J = 7.2$ Hz, 1H), 2.50 (s, 3H), 1.36 ppm (s, 9H); ^{13}C -NMR (100 MHz, CDCl_3) δ 157.3, 155.8, 145.8, 138.0, 137.9, 126.1, 120.5, 114.1, 104.3, 34.3, 31.4, 24.3; HRMS (EI) $[\text{M}^+]$ calcd for $\text{C}_{16}\text{H}_{20}\text{N}_2$ (m/z) 240.1626; found 240.1616.



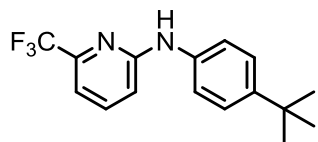
***N*-(4-*tert*-Butylphenyl)-4-(trifluoromethyl)pyridin-2-amine (**157**).**

Following amination procedure C, 62 mg (42%) of **157** were obtained following flash chromatography (2.5 → 15% EtOAc/hexanes, R_f = 0.50 in 15% EtOAc/hexanes) as a beige solid; m.p.: 119–121 °C; $^1\text{H-NMR}$ (400 MHz, CDCl_3) δ 8.33 (d, J = 5.2 Hz, 1H), 7.42 (d, J = 8.0 Hz, 2H), 7.27 (d, J = 8.0 Hz, 2H), 7.01 (bs, 1H), 6.84 (m, 2H), 1.36 (s, 9H); $^{19}\text{F-NMR}$ (376 MHz, CDCl_3) δ -66.18; $^{13}\text{C-NMR}$ (150 MHz, CDCl_3) δ 157.2, 149.7, 147.3, 140.0 (q, $^2J_{\text{CF}}$ = 33.0 Hz), 136.6, 126.4, 123.0 (q, $^1J_{\text{CF}}$ = 271.5 Hz), 121.3, 109.7 (q, $^4J_{\text{CF}}$ = 3.0 Hz), 103.4 (q, $^4J_{\text{CF}}$ = 4.5 Hz), 34.4, 31.4; HRMS (EI) $[\text{M}^+]$ calcd for $\text{C}_{16}\text{H}_{17}\text{F}_3\text{N}_2$ (m/z) 294.1344; found 294.1349.



***N*-(4-*tert*-Butylphenyl)-5-fluoropyridin-2-amine (**158**).**

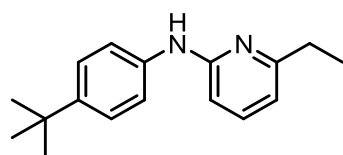
Following amination procedures B and C, 55 mg (45%) and 72 mg (59%) of **158** were obtained, respectively. The product was isolated by flash chromatography (20% EtOAc/hexanes, R_f = 0.61) as a light orange solid; m.p.: 108–110 °C; $^1\text{H-NMR}$ (400 MHz, CDCl_3) δ 8.07 (d, J = 2.8 Hz, 1H), 7.38 (d, J = 8.4 Hz, 2H), 7.27–7.23 (m, 3H), 6.85 (dd, J = 8.8, 3.6 Hz, 1H), 6.76 (br s, 1H), 1.35 ppm (s, 9H); $^{19}\text{F-NMR}$ (376 MHz, CDCl_3) δ -140.71 ppm; $^{13}\text{C-NMR}$ (100 MHz, CDCl_3) δ 154.0 (d, $^1J_{\text{CF}}$ = 243.5 Hz), 153.0, 146.0, 137.9, 135.0 (d, $^2J_{\text{CF}}$ = 24.1 Hz), 126.2, 125.2 (d, $^2J_{\text{CF}}$ = 21.1 Hz), 120.2, 108.5 (d, $^4J_{\text{CF}}$ = 4.0 Hz), 34.3, 31.4; HRMS (EI) $[\text{M}^+]$ calcd for $\text{C}_{15}\text{H}_{17}\text{FN}_2$ (m/z) 244.1376; found 244.1382.



***N*-(4-*tert*-Butylphenyl)-6-(trifluoromethyl)pyridin-2-amine (**159**).**

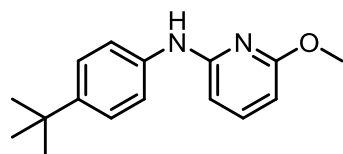
Following amination procedures A, B, and C, 44 mg (30 %), 109 mg (74 %), and 122 mg (83%) of **159** were obtained, respectively. The product was isolated by flash

chromatography (0% → 10% Et₂O/pentane, R_f = 0.23) as a dark-yellow oil; ¹H-NMR (400 MHz, CDCl₃) δ 7.60 (dd, *J* = 8.2, 7.6 Hz, 1H), 7.41 (d, *J* = 8.4 Hz, 2H), 7.30 (d, *J* = 8.4 Hz, 2H), 7.08 (d, *J* = 7.6 Hz, 1H), 6.99 (d, *J* = 8.2 Hz, 1H), 6.71 (bs, 1H), 1.36 ppm (s, 9H); ¹⁹F-NMR (376 MHz, CDCl₃) δ -68.59 ppm; ¹³C-NMR (150 MHz, CDCl₃) δ 156.5, 147.0, 146.8 (q, ²*J*_{CF} = 34.0 Hz), 138.5, 136.7, 126.3, 121.5 (q, ¹*J*_{CF} = 272.3 Hz), 121.1, 110.7 (q, ⁴*J*_{CF} = 3.0 Hz), 34.4, 31.4; HRMS (EI) [M⁺] calcd for C₁₆H₁₇F₃N₂ (m/z) 294.1344; found 294.1349.



***N*-(4-*tert*-Butylphenyl)-6-ethylpyridin-2-amine (162).**

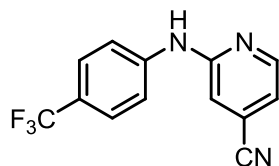
Following amination procedures A, B, and C, 32 mg (25 %), 80 mg (63 %), and 89 mg (70%) of compound **162** were obtained, respectively. The product was isolated by flash chromatography (5 → 10% EtOAc/hexanes, R_f = 0.38 in 10% EtOAc/hexanes) as a brown oil; ¹H-NMR (400 MHz, CDCl₃) δ 7.42 (dd, *J* = 8.0, 7.4 Hz, 1H), 7.37 (d, *J* = 8.2 Hz, 2H), 7.28 (d, *J* = 8.2 Hz, 2H), 6.73 (d, *J* = 8.0 Hz, 1H), 6.62 (d, *J* = 7.4 Hz, 1H), 6.52 (br s, 1H), 2.73 (q, *J* = 7.2 Hz, 2H), 1.35–1.31 ppm (m, 12H); ¹³C-NMR (100 MHz, CDCl₃) δ 162.5, 155.8, 145.6, 138.0, 137.9, 126.0, 120.2, 112.7, 104.7, 34.2, 31.4, 31.2, 13.8; HRMS (EI) [M⁺] calcd for C₁₇H₂₂N₂ (m/z) 254.1783; found 254.1779.



***N*-(4-*tert*-Butylphenyl)-6-methoxypyridin-2-amine (163).**

Following amination procedures A and B, 80 mg (63%) and 123 mg (96%) of **163** were obtained, respectively. The product was isolated by flash chromatography (5 → 20% EtOAc/hexanes, R_f = 0.66 in 20% EtOAc/hexanes) as a brown oil; ¹H-NMR (400 MHz, CDCl₃) δ 7.44–7.33 (m, 5H), 6.40 (d, *J* = 7.6 Hz, 2H), 6.22 (d, *J* = 7.6 Hz, 1H), 3.95 (s, 3H), 1.37

ppm (s, 9H); ^{13}C -NMR (100 MHz, CDCl_3) δ 163.5, 154.7, 145.3, 140.0, 137.9, 125.9, 119.9, 99.6, 99.3, 53.3, 34.2, 31.4; HRMS (EI) $[\text{M}^+]$ calcd for $\text{C}_{16}\text{H}_{20}\text{N}_2\text{O}$ (m/z) 256.1576; found 256.1570.

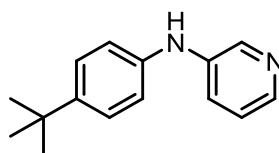


2-(4-(Trifluoromethyl)phenylamino)isonicotinonitrile (166).

Following amination procedure C, 20 mg (15 %) of **166** were obtained.

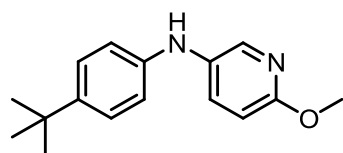
The product was isolated by flash chromatography (5% \rightarrow 20%

EtOAc/hexanes, R_f = 0.63 in 20% EtOAc/hexanes) as a beige solid m.p.: 181-183 $^\circ\text{C}$ (reported m.p.: 184-186 $^\circ\text{C}$); ^1H -NMR (400 MHz, CDCl_3) δ 8.41 (d, J = 5.2 Hz, 1H), 7.64 (d, J = 8.4 Hz, 2H), 7.55 (d, J = 8.4 Hz, 2H), 7.07 (bs, 1H), 7.03 (J = 5.2 Hz, 1H), 6.83 (bs, 1H); ^{19}F -NMR (376 MHz, CDCl_3) δ -61.97; ^{13}C -NMR (100 MHz, CDCl_3) δ 155.2, 149.8, 142.3, 126.7 (q, $^4J_{\text{CF}}$ = 3.0 Hz), 125.3 (q, $^3J_{\text{CF}}$ = 33 Hz), 124.1 (q, $^1J_{\text{CF}}$ = 270 Hz) 121.9, 119.4 (q, $^4J_{\text{CF}}$ = 3.0 Hz), 116.7, 116.6 111.3 ; HRMS (EI) $[\text{M}^+]$ calcd for $\text{C}_{13}\text{H}_8\text{F}_3\text{N}_3$ (m/z) 364.0743; found 264.0735.



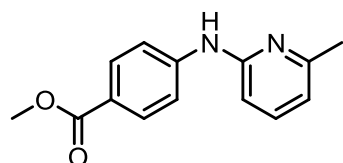
***N*-(4-*tert*-Butylphenyl)pyridin-3-amine (173a).**

Following amination procedures, A, B and C, 103 mg (92 %), 93 mg (82 %), and 104 mg (92%) of **173a** were obtained, respectively. The product was isolated by flash chromatography (60% EtOAc/hexanes R_f = 0.31 in 50% EtOAc/hexanes) as a pale-yellow solid; m.p.: 131–134 $^\circ\text{C}$ (no literature m.p. reported); ^1H -NMR (400 MHz, CDCl_3) δ 8.38 (d, J = 2.8 Hz, 1H), 8.14 (d, J = 4.8 Hz, 1H), 7.40 (d, J = 7.6 Hz, 1H), 7.35 (d, J = 8.4 Hz, 2H), 7.17–7.14 (m, 1H), 7.07 (d, J = 8.4 Hz, 2H), 6.16 (br s, 1H), 1.35 (s, 9H); ^{13}C -NMR (100 MHz, CDCl_3) δ 145.1, 141.1, 140.5, 139.4, 139.1, 126.2, 123.6, 122.5, 118.5, 34.2, 31.4 ppm. The spectral data are consistent with those reported in the literature.⁸³



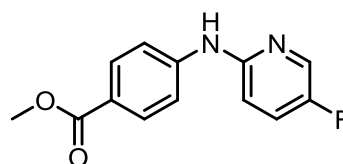
***N*-(4-*tert*-Butylphenyl)-6-methoxypyridin-3-amine (174a).**

Following amination procedures, A, B and C, 105 mg (82%), 113 mg (91%), 120 mg (94%) of **174a** were obtained respectively. The product was isolated by flash chromatography (10% EtOAc/hexanes $R_f = 0.2$ in 10% EtOAc/hexanes) as light-yellow oil; ^1H -NMR (400 MHz, CDCl_3) δ 8.00 (d, $J = 2.8$ Hz, 1H), 7.46 (dd, $J = 8.8, 2.4$ Hz, 1H), 7.3 (d, $J = 8.8$ Hz, 2H), 6.87 (d, $J = 8.8$ Hz, 1H), 6.74 (d, $J = 8.8$ Hz, 1H), 5.47 (bs, 1H), 3.95 (s, 3H), 1.33 (s, 9H); ^{13}C -NMR (100 MHz, CDCl_3) δ 160.0, 143.1, 142.1, 138.9, 133.4, 132.4, 126.2, 115.6, 110.9, 53.43, 31.6, 31.4; HRMS (EI) $[M^+]$ calcd for $\text{C}_{16}\text{H}_{20}\text{N}_2\text{O}$ (m/z) 256.0758; found 256.1604.



Methyl 4-[(6-methylpyridin-2-yl) amino]benzoate (175).

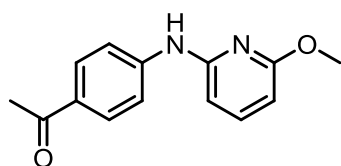
Following amination procedure B, 80 mg (66%) of **175** were obtained following flash chromatography (20% EtOAc/hexanes, $R_f = 0.28$) as a beige solid; m.p.: 144–147 °C; ^1H -NMR (400 MHz, CDCl_3) δ 7.96 (d, $J = 8.4$ Hz, 2H), 7.47 (dd, $J = 8.0, 7.6$ Hz, 1H), 7.42 (d, $J = 8.4$ Hz, 2H), 6.95 (bs, 1H), 6.78 (d, $J = 8.0$ Hz, 1H), 6.71 (d, $J = 7.6$ Hz, 1H), 3.90 (s, 3H), 2.48 (s, 3H); ^{13}C -NMR (100 MHz, CDCl_3) δ 166.9, 157.4, 153.8, 145.4, 138.1, 131.1, 122.5, 116.9, 115.7, 107.0, 51.8, 24.2; HRMS (EI) $[M^+]$ calcd for $\text{C}_{14}\text{H}_{14}\text{N}_2\text{O}_2$ (m/z) 242.1055; found 242.1051.



Methyl 4-[(5-fluoropyridin-2-yl) amino]benzoate (176).

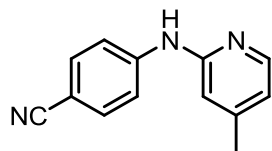
Following amination procedure B, 86 mg (70%) of **176** were obtained. Compound **176** was isolated by flash chromatography (5 → 20% EtOAc/hexanes, $R_f = 0.19$ in 20% EtOAc/hexanes) as a white solid; m.p.: 156–158 °C; ^1H -NMR (400 MHz, CDCl_3) δ

8.16 (s, 1H), 8.01–7.99 (m, 2H), 7.24–7.34 (m, 3H), 6.94–6.89 (m, 2H), 3.91 (s, 3H); ^{19}F -NMR (376 MHz, CDCl_3) δ -137.67; ^{13}C -NMR (100 MHz, CDCl_3) δ 166.8, 154.8 (d, $^1J_{\text{CF}}=247.5$ Hz), 150.8, 145.2, 135.3 (d, $^2J_{\text{CF}}=25.1$ Hz), 131.2, 125.4 (d, $^2J_{\text{CF}}=21.1$ Hz), 122.9, 116.7, 111.1 (d, $^4J_{\text{CF}}=4.0$ Hz), 51.8; HRMS (EI) $[\text{M}^+]$ calcd for $\text{C}_{13}\text{H}_{11}\text{FN}_2\text{O}_2$ (m/z) 246.0805; found 246.0810.



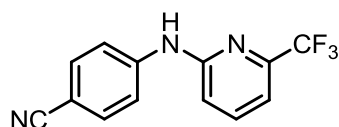
1-{4-[(6-Methoxypyridin-2-yl) amino]phenyl} ethanone (177).

Following amination procedure A, 87 mg (72%) of **177** were obtained following flash chromatography (0 \rightarrow 30% EtOAc/Hexanes, R_f = 0.41 in 30% EtOAc/Hexanes) as a yellow solid; m.p.: 143–145 $^\circ\text{C}$; ^1H -NMR (400 MHz, CDCl_3) δ 7.95 (d, J = 8.4 Hz, 2H), 7.55–7.48 (m, 3H), 6.72 (brs, 1H), 6.46 (d, J = 7.6 Hz, 1H), 6.33 (d, J = 8.0 Hz, 1H), 3.96 (s, 3H), 2.59 (s, 3H); ^{13}C -NMR (100 MHz, CDCl_3) δ 196.7, 163.5, 152.7, 145.4, 140.2, 130.2, 130.1, 117.0, 101.9, 101.7, 53.6, 26.2; HRMS (EI) $[\text{M}^+]$ calcd for $\text{C}_{14}\text{H}_{14}\text{N}_2\text{O}_2$ (m/z) 242.1055; found 242.1052.



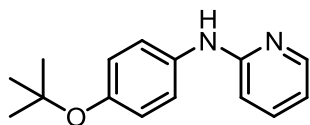
4-(4-Methylpyridin-2-ylamino)benzonitrile (178).

Following amination procedure B, 77 mg (74%) of **178** were obtained following flash chromatography (25 \rightarrow 50% Et_2O /pentane, R_f = 0.29) as a yellow solid; m.p.: 172–175 $^\circ\text{C}$; ^1H -NMR (300 MHz, CDCl_3) δ 8.17 (d, J = 5.1 Hz, 1H), 7.59–7.52 (m, 4H), 7.00 (bs, 1H), 6.75–6.73 (m, 2H), 2.34 (s, 3H); ^{13}C -NMR (150 MHz, CDCl_3) δ 154.2, 149.2, 147.9, 145.1, 133.4, 119.6, 118.4, 117.6, 111.2, 103.5, 21.1; HRMS (EI) $[\text{M}^+]$ calcd for $\text{C}_{13}\text{H}_{11}\text{N}_3$ (m/z) 209.0953; found 209.0959.



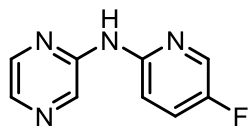
4-[6-(Trifluoromethyl)pyridin-2-ylamino]benzonitrile (179).

Following amination procedure A, 113 mg (86%) of **179** were obtained following flash chromatography (30% EtOAc/hexanes, R_f = 0.31) as a yellow solid; m.p.: 209–211 °C; $^1\text{H-NMR}$ (400 MHz, CD_3COCD_3) δ 9.25 (br s, 1H), 8.00 (d, J = 8.8 Hz, 2H), 7.91 (dd, J = 8.4, 7.8 Hz, 1H), 7.71 (d, J = 8.8 Hz, 2H), 7.34 (d, J = 7.8 Hz, 1H), 7.22 (d, J = 8.4 Hz, 1H); $^{19}\text{F-NMR}$ (376 MHz, CDCl_3) δ -68.57; $^{13}\text{C-NMR}$ (150 MHz, CD_3OD) δ 156.6, 146.8, 146.7 (q, $^2J_{\text{CF}}$ = 34.5 Hz), 139.8, 134.1, 123.1 (q, $^1J_{\text{CF}}$ = 271.5 Hz), 120.5, 119.1, 116.1, 113.0 (q, $^4J_{\text{CF}}$ = 3.0 Hz), 104.2; HRMS (EI) $[\text{M}^+]$ calcd for $\text{C}_{13}\text{H}_8\text{F}_3\text{N}_3$ (m/z) 263.0670; found 263.0677.



N-(4-*tert*-Butoxyphenyl)pyridin-2-amine (180).

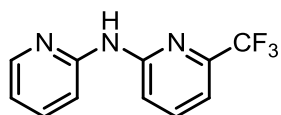
Following amination procedure C, 66 mg (54%) of compound **180** were obtained following flash chromatography (5 \rightarrow 30% EtOAc/hexanes R_f = 0.56 in 30% EtOAc/hexanes) as a brown solid; m.p.: 91–94 °C; $^1\text{H-NMR}$ (300 MHz, CDCl_3) δ 8.19 (d, J = 6.0 Hz, 1H), 7.51–7.45 (m, 1H), 7.26–7.21 (m, 2H), 7.00–6.97 (m, 2H), 6.79 (d, J = 8.4 Hz, 1H), 6.73–6.69 (m, 1H), 6.60 (brs, 1H), 1.36 (s, 9H); $^{13}\text{C-NMR}$ (100 MHz, CDCl_3) δ 156.6, 150.9, 148.3, 137.6, 135.9, 125.1, 121.7, 114.5, 107.7, 78.4, 28.7; HRMS (EI) $[\text{M}^+]$ calcd for $\text{C}_{15}\text{H}_{18}\text{N}_2\text{O}$ (m/z) 242.1419; found 242.1415.



N-(5-Fluoropyridin-2-yl)pyrazin-2-amine (181).

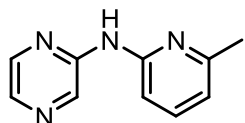
Following amination procedure B, 80 mg (84%) of **181** were obtained following flash chromatography (7 \rightarrow 30% EtOAc/hexanes, R_f = 0.24 in 30% EtOAc/hexanes) as an off-white solid; m.p.: 164–165 °C; $^1\text{H-NMR}$ (300 MHz, CDCl_3) δ 8.73 (s, 1H), 8.18 (s, 2H),

8.12 (d, $J = 2.4$ Hz, 1H), 7.92 (bs, 1H), 7.85–7.81 (m, 1H), 7.45 (m, 1H); ^{19}F -NMR (376 MHz, CDCl_3) δ 136.03; ^{13}C -NMR (100 MHz, CDCl_3) δ 155.4 (d, $^1J_{\text{CF}} = 248.5$ Hz), 150.3, 149.1, 141.4, 136.3, 135.2 (d, $^2J_{\text{CF}} = 26.1$ Hz), 134.9, 125.3 (d, $^2J_{\text{CF}} = 20.1$ Hz), 112.5 (d, $^4J_{\text{CF}} = 4.0$ Hz); HRMS (EI) $[\text{M}^+]$ calcd for $\text{C}_9\text{H}_7\text{FN}_4$ (m/z) 190.0655; found 190.0651.



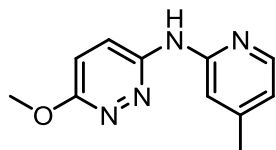
***N*-(Pyridin-2-yl)-6-(trifluoromethyl)pyridin-2-amine (182).**

Following amination procedure B, 83 mg (70%) of **182** were obtained following flash chromatography (30% EtOAc/hexanes, $R_f = 0.48$) as a white solid; m.p.: 91–93 °C; ^1H -NMR (400 MHz, CDCl_3) δ 8.23 (m, 2H), 7.76–7.64 (m, 4H), 7.21 (d, $J = 7.2$ Hz, 1H), 6.94 (dd, $J = 7.2, 6.0$ Hz, 1H); ^{19}F -NMR (376 MHz, CDCl_3) δ -68.43; ^{13}C -NMR (100 MHz, CDCl_3) δ 154.0, 153.5, 147.5, 146 (q, $^2J_{\text{CF}} = 34.2$ Hz), 138.6, 138.2, 121.5 (q, $^1J_{\text{CF}} = 274.7$ Hz), 117.2, 114.6, 112.3, 112.2 ppm; HRMS (EI) $[\text{M}^+]$ calcd for $\text{C}_{11}\text{H}_8\text{F}_3\text{N}_3$ (m/z) 239.0670; found 239.0677.



***N*-(6-Methylpyridin-2-yl)pyrazin-2-amine (183).**

Following amination procedure B, 76 mg (82%) of **183** were obtained following flash chromatography (0 → 30% EtOAc/hexanes) as a white solid; m.p.: 99–102 °C; ^1H -NMR (400 MHz, CDCl_3) δ 8.96 (s, 1H), 8.18 (s, 1H), 8.10 (d, $J = 2.4$ Hz, 1H), 7.92 (bs, 1H), 7.54 (dd, $J = 8.0, 7.6$ Hz, 1H), 7.41 (d, $J = 8.4$ Hz, 1H), 6.79 (d, $J = 7.6$ Hz, 1H), 2.49 (s, 3H); ^{13}C -NMR (100 MHz, CDCl_3) δ 157.1, 152.2, 150.6, 141.5, 138.3, 136.2, 135.3, 116.7, 108.5, 24.2; HRMS (EI) $[\text{M}^+]$ calcd for $\text{C}_9\text{H}_{10}\text{N}_4$ (m/z) 186.0905; found 186.0900.



6-Methoxy-*N*-(4-methylpyridin-2-yl)pyridazin-3-amine (184**).**

Following amination procedure B, 64 mg (59%) of **184** were obtained following flash chromatography (30 → 50% EtOAc/hexanes, $R_f = 0.15$) as a beige solid; m.p.: 191–193 °C; $^1\text{H-NMR}$ (400 MHz, CDCl_3) δ 10.08 (s, 1H), 8.37 (d, $J = 8.8$ Hz, 1H), 8.11 (s, 1H), 7.59 (s, 1H), 6.97 (d, $J = 8.8$ Hz, 1H), 6.69 (bs, 1H), 4.12 (s, 3H), 2.34 (s, 3H); $^{13}\text{C-NMR}$ (100 MHz, CDCl_3) δ 160.9, 154.5, 154.3, 148.9, 146.7, 123.0, 119.3, 117.8, 112.9, 54.3, 21.2; HRMS (EI) $[\text{M}^+]$ calcd for $\text{C}_{11}\text{H}_{12}\text{N}_4\text{O}$ (m/z) 216.1011; found 216.1088.

Part II: Generation of benzyne in flow reactors followed by subsequent Diels-Alder reactions

Chapter 5: Chemical Reactions in Flow

5.1 Introduction:

The synthesis of new compounds using traditional methods is a time consuming and labor-intensive process. In many cases, this is due to poor reaction reproducibility especially upon scale-up of the reaction, and the considerable manual effort required for monitoring, optimizing and isolating the product at each stage of the synthesis process.⁹⁹

With the increasing demand in the pharmaceutical industry to synthesize new biologically active compounds in less time and at lower cost, the need for new technologies to speed up the progress of organic synthesis is widely desirable. Continuous flow emerges as a fast, well-established and accepted technology that has the potential to address these demands and has attracted interest, both in academia and in industry.¹⁰⁰

Continuous flow chemistry has developed over the past few decades from early demonstrations of simple chemical transformation in micro-reactors¹⁰¹ to more complex, multistep synthesis.¹⁰² This evolution in synthetic methods and equipment has been motivated by several advantages of this relatively new technology over traditional batch-style chemistry that is usually performed in flasks or vessels.

In the following sections the basics principles of flow chemistry will be introduced briefly and compared against batch reactor technology, and the major benefits of flow technology will be highlighted.

5.1.1 Reaction time in Batch Versus Flow-Reactors:

Generally speaking, reactions are normally started by mixing two or more reactants at appropriate conditions (i.e. temperature, pressure, concentration, catalyst etc...) and terminated when maximum conversion of the desired product is reached.

In flow processes, the reagents are infused separately via syringe pumps, where they meet at a conjunction (T-mixer), mix, react and flow down the reactor at a controlled temperature for a specific time, which is known as a “residence time”. The residence time is controlled by two factors: a) the reactor volume and b) the flow rate. At the end of the reactor, the reagents are quenched in the collection vessel (Figure 1).

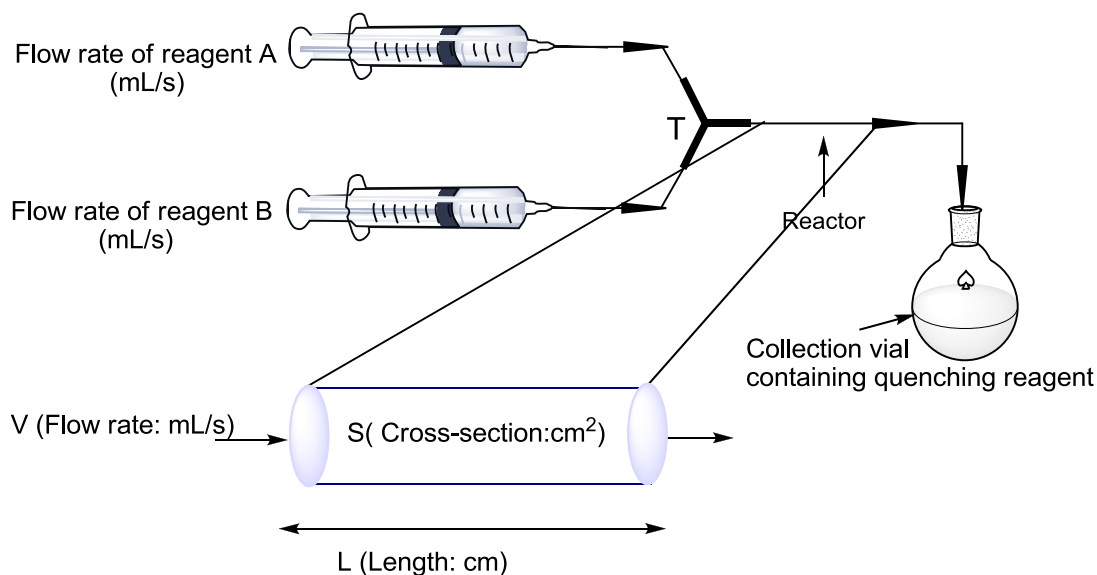


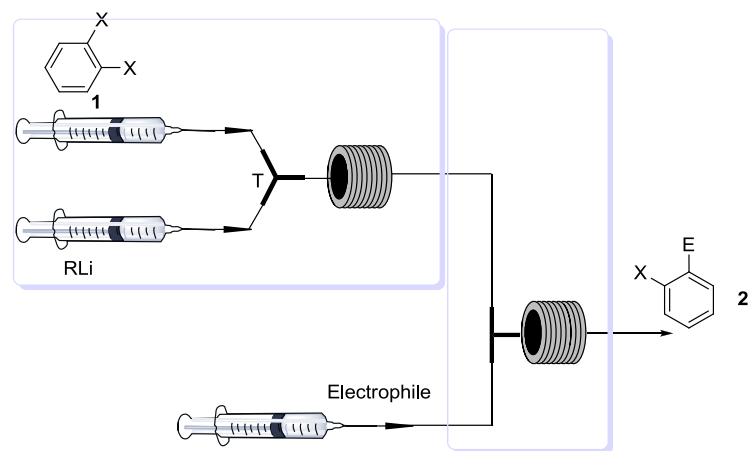
Figure 1: Chemical Reactions in Flow Setting

$$\text{Residence time}(s) = \frac{S \times L}{V(A) + V(B)}$$

V_A = Flow rate of reagent A.

V_B = Flow rate of reagent B

In contrast, in batch routine, the reaction time is determined by how long the starting materials are mixed together in one flask at a given temperature and pressure until the reaction has progressed to a suitable level of conversion to completion. One of the major challenges that is encountered by chemists is conducting extremely fast reactions as they are difficult to control in conventional-style flasks. For example, if a reaction is completed after 0.6 sec and side-product formation takes place to a significant extent after 1s; the reaction time must be adjusted within this time frame (i.e. 0.6-1 sec). This kind of adjustment is nearly impossible to achieve using the traditional batch chemistry. Therefore, the only way to control such reactions in the batch is to slow down the rate of these reactions.¹⁰³ The most common way used to decrease the reactions rate is to lower the reaction temperature and/or by higher dilution method (i. e. decrease the concentration of the reactants). Fortunately, by using a flow platform, extremely fast reactions can be carried out without the need to decrease the temperature or the reactants' concentration. The precise manipulation of the residence time can minimize side-product formation and therefore increase the yield of the target compound. This is clearly demonstrated in Yoshida's work with lithiation of *o*-dibromobenzene. It is well-known that lithium-halogen exchange of *o*-dibromobenzene generates *o*-bromophenyllithium which undergoes rapid elimination to form benzyne even at -78 °C. Conducting this reaction in a microtube at -78 °C with a residence time of 0.8 sec enabled the formation of *o*-bromophenyllithium which was subsequently trapped with an electrophile before benzyne formation takes place (Scheme 1).¹⁰⁴ It is noteworthy that for the same reaction to be conducted in a conventional flask, the temperature must be lowered to -100 °C.



Scheme 1: Quenching of *o*-bromophenyllithium with different electrophiles.

As the reaction progresses, the concentration of the reactants decays exponentially with time in batch setting while the concentration of product increases.¹⁰⁵ However, in a microfluidic device, the concentration of reactants decreases with distance and the concentration of product increases and reaches a maximum at the outlet of the reactor (assuming that the reaction is conducted under optimized conditions) (Figure 2).

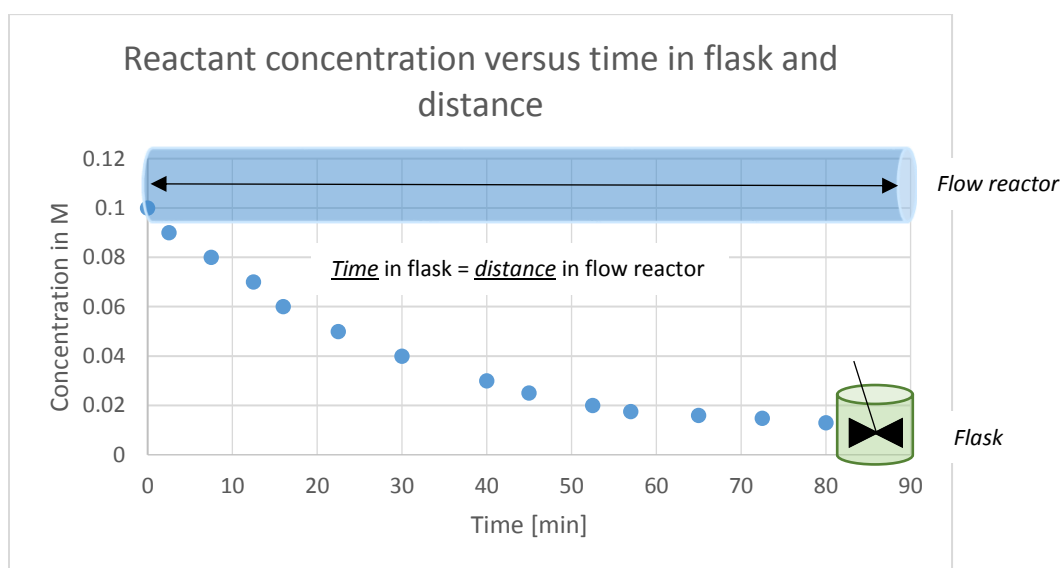


Figure 2: Reactant concentration versus time (flask reactor) or distance (flow reactor) for simple first-order reaction under well-mixed homogeneous conditions.

It is important to indicate that the concentration of a reactant and product do not change with the progress of operating time under a steady state at a specific position within the flow reactor. This means that there is no possibility of backward or forward mixing. The best way to envision this is to consider the flow reactor as an infinite series of continuous flask reactors that are separated from each other (Figure 3).

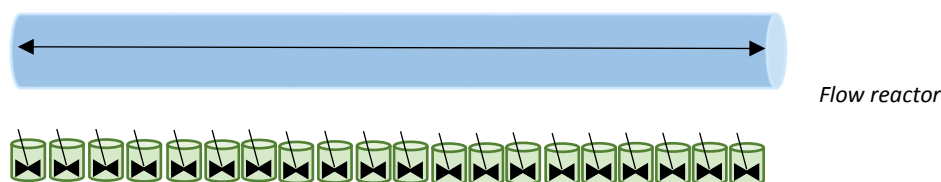


Figure 3: Flow reactor as infinite small separated flask reactors.

This is extremely beneficial for scenarios where the product can react with the starting material present in the reaction mixture. In the flask reactor, this is inevitable since the product is mixed with the starting material, thus the yield for the target compound decreases. In contrast, the ability to control both elements of time and space in the flow system, and the rapid mass-to-heat transfer in microfluidic devices lead to unique reaction outcomes that are not reproducible in the batch reactors.¹⁰⁶ The newly formed product in the flow reactor is isolated by physically removing it from the reaction stream; this will minimize side-product formation and increase the yield of the reaction.¹⁰⁷

5.1.2 Mixing in batch versus flow-reactors:

Mixing - which describes how two solutions or phases come together and become intertwined - has a profound effect on the selectivity and conversion of a reaction. To achieve high yield and selectivity of the desired product in an organic reaction, a high degree of mixing and homogeneity is extremely desirable.¹⁰⁸

Batch and flow reactions exhibit different mixing mechanisms and the Reynolds number “Re” is used to predict flow dynamics in fluids. The Reynolds number is a dimensionless mass transfer coefficient that is dependent on the flow rate, and the viscosity of the fluid. Ranges of Re values divide mixing into three regimes: turbulent, laminar, and transitional (Figure 4).

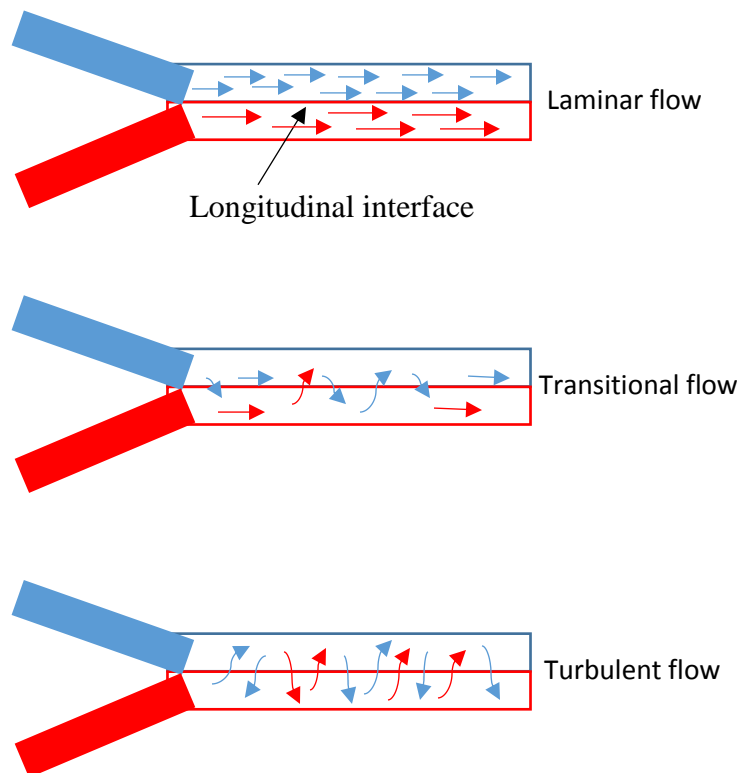


Figure 4: Types of flow

A high Re number corresponds to turbulent flow, whereas low Re values describe laminar flow which corresponds to a poor mixing ($Re < 2040$). In a batch-size reactor, mixing is transitional or laminar.¹⁰⁹ Transitional mixing results in segregation inside the vessel, with a laminar regime dominates at the outlying parts and a turbulent regime near the stirring bar. The movement of the molecules between these regions relies on diffusion.¹¹⁰ The time needed for molecular diffusion

(t_d) is directly proportional to the square of diffusion path length L and inversely proportional to the diffusion coefficient D (Equation 1). Therefore, micro-reactors have much smaller diffusion times and achieve mixing faster than in large conventional flasks. However, mixing is more complicated than simple diffusion and requires the analysis of what is known as a Damköhler number.¹¹¹

The Damköhler number (Da) is defined by the ratio of the reaction's rate to that of mass transfer by diffusion. For reactions where Da is less than 1, homogenous mixing is achieved before the reaction occurs. On the other hand, for reactions where Da is greater than 1, the reaction takes place before achieving homogeneity in the reaction medium resulting in concentration gradient within the system. This has a profound effect on competitive, consecutive side reactions, where $A+B \rightarrow C$ and $B + C \rightarrow S$ (side-product). In this case, if $Da > 1$, A and B will react before achieving homogeneity and form C in close proximity to B resulting in higher quantities of S (Figure 5).

Table 2: Diffusion time is calculated for D (diffusion coefficient) = $1 \times 10^{-5} \text{ cm}^2/\text{s}$

Diffusion time t_d (s)	Size of reactor
0.0005	1 μm
0.005	10 μm
5	100 μm
500	1 mm

$$t(d) = \frac{L^2}{D} \quad \text{Eq 1}$$

$$D = \frac{kT}{6\pi\eta r}$$

k is the Boltzman constant ($1.38 \times 10^{-23} \text{ JK}^{-1}$), T (K) is the absolute temperature, η ($\text{Kg m}^{-1} \text{ s}^{-1}$) the absolute (solute) viscosity, and r is the hydrodynamic radius (nm).

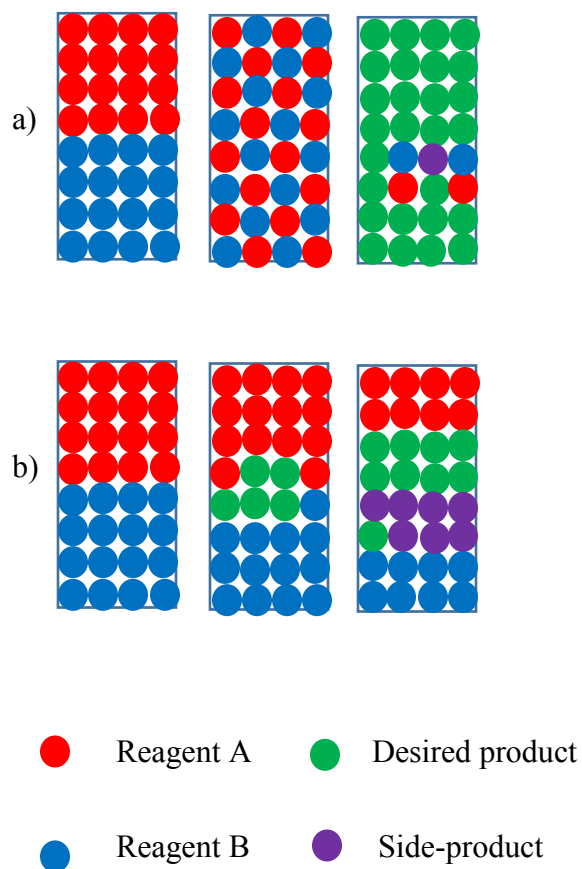


Figure 5: Da and side-product formation in reaction mixtures. a) $Da < 1$ achieve homogeneity, b) $Da > 1$ more side-product formation

For extremely fast reactions where Da is high, conducting the reaction in flow is extremely beneficial. In these cases, specialized mixers must be used to achieve a high degree of homogeneity. These mixers range from simple T or Y-shaped connection units to a more sophisticated mixer using obstacles within the microstructures to achieve more efficient mixing. The types of chemistries that benefit from enhanced mixing under flow conditions are referred to as “flash chemistry”.

5.1.3 Heat Transfer in Batch versus Flow-Reactors:

In the course of a chemical reaction, heat is transferred between the interior and the exterior of a reactor via the reactor surface. Therefore, the surface-to-volume ratio is an essential factor for heat transfer. Microfluidic devices have a surface-to-volume ratios that are several orders of magnitude larger than those of conventional flasks.¹¹² For example, a tubular reactor with an internal diameter of 1 mm has a surface-to-volume ratio 50 times greater than that of a standard 250 mL round bottom flask.¹¹³ Consequently, heat transfer occurs more rapidly in flow microreactors than in conventional flasks enabling fast cooling/heating, which results in a more homogenous temperature profile throughout the reaction mixture (Figure 6).

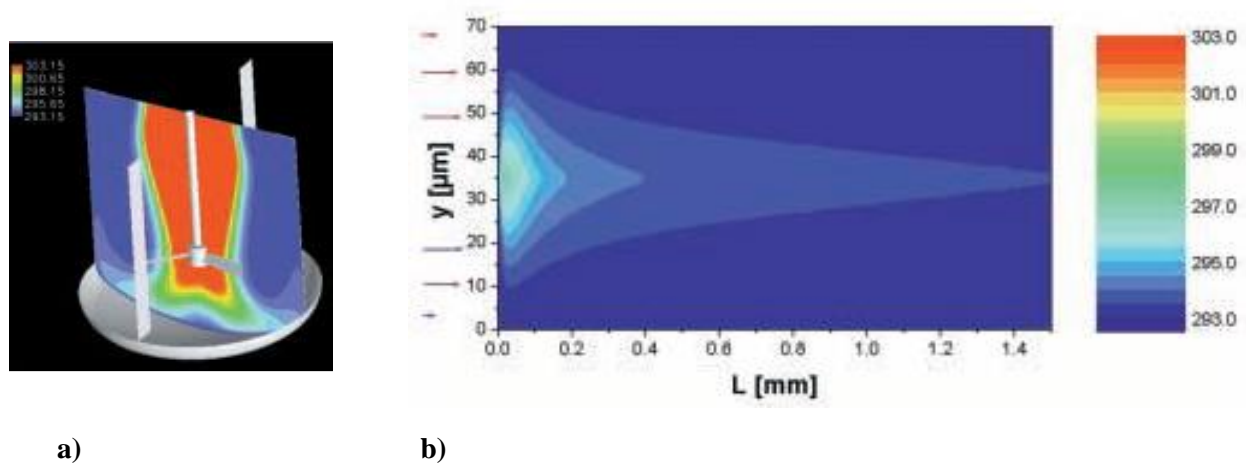


Figure 6: Temperature profiles in a batch (a) and a flow reactor (b) simulated for an exothermic model reaction between HCl and NaOH, y is the channel thickness and L is the channel length.¹¹⁴

This is beneficial for highly exothermic reactions, the effective heat-exchanging properties of the continuous flow reactor aids in maintaining a uniform temperature throughout the reaction medium and reduces side-product formation (Figure 7).¹¹⁵ Even highly unstable intermediates¹¹⁶ or explosive reactants can be handled.¹¹⁷

As an example, nitration reactions of aromatic compounds are highly exothermic where hot spots are more likely to be generated in the reaction medium, causing side-product formation. The rapid heat transfer in the flow system reduces hot spot formation and results in a better product quality compared to the batch setting (Table 2).¹¹⁸ The reaction presented below produce two products (2-nitrophenol and 4-nitrophenol) but also, other by-products such as hydroquinone, dinitro compounds, and polymeric products. The results of performing this reaction in batch versus flow are shown in table 2.

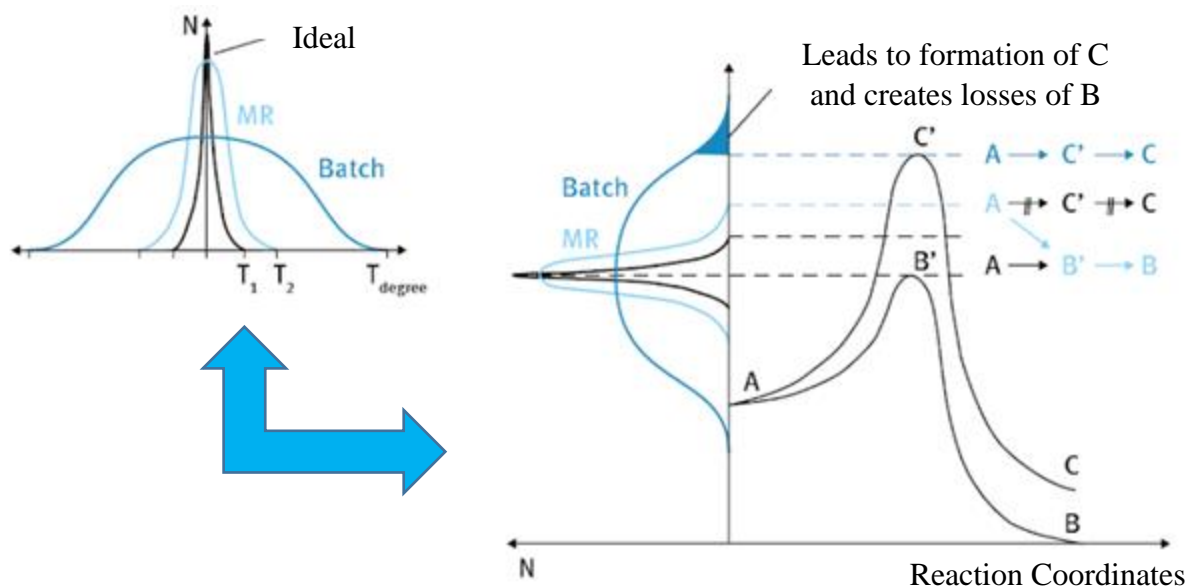
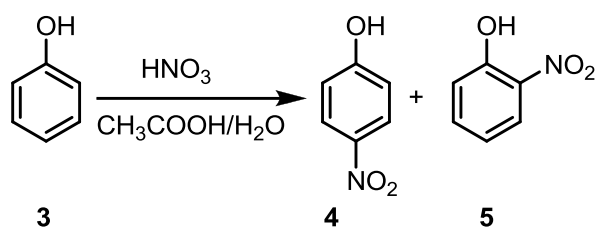


Figure 7: Temperature distribution profile in batch and in microreactor (MR).¹¹¹

Table 2: Nitration of phenol in batch and flow conditions.

	T (°C)	HNO ₃ (Equiv.)	Yield	Ratio 4-/2-nitrophenol	By-Products
<i>Batch</i>	2	2.0	30%	1.2	65%
	20	2.0	21%	0.6	77%
<i>Flow</i>	5	1.7	74%	0.9	10%
	20	1.4	77%	1.0	17%

5.1.4 In-line analysis in flow reactors:

Optimizing reaction conditions is a common practice in organic synthesis. Traditionally, this is done by collecting and analyzing samples from reaction mixtures conducted under different reaction conditions from which an optimum set of conditions or reagent choice will emerge. As a result, optimizing a reaction requires a commitment of time and consumption of large quantities of valuable materials.¹¹⁹

Flow chemistry not only allows chemists to perform reactions in a small-scale thus, requiring smaller amount of the starting materials, but because the process moves, it also enables chemists to divert flow reaction to monitoring devices such as UV/VIS, IR, NMR, mass spectrometer, and LC/MS.¹²⁰

Recently, our group had reported a second generation MACOS (Microwave Assisted Continuous Flow Organic Synthesis) system that can run reactions under high temperature and pressure. The system was shown to provide consistent performance and it can seamlessly deliver a sample to the analytical unit that is coupled with the MACOS system without any impact of the steady state of the process (Figure 8).¹²¹

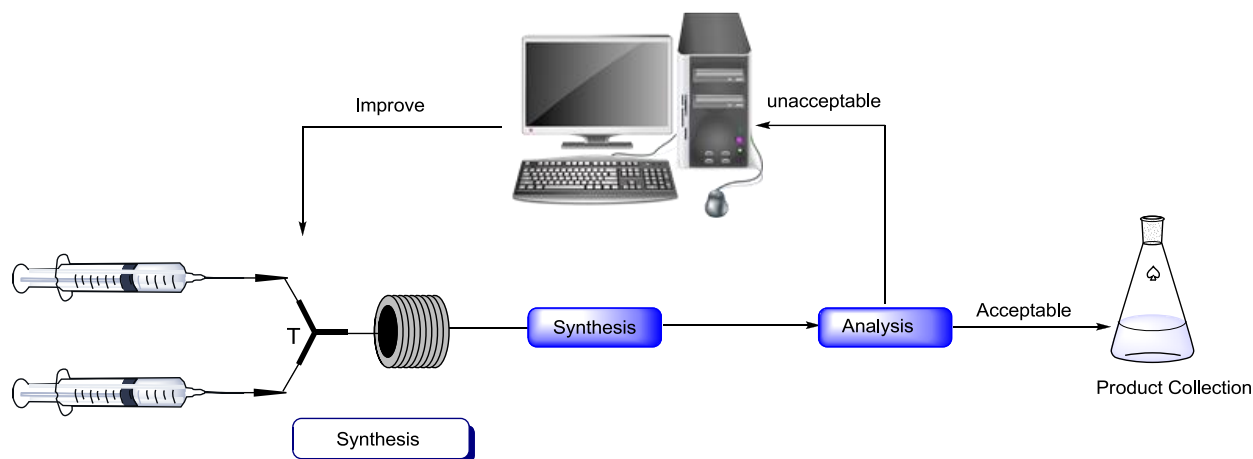
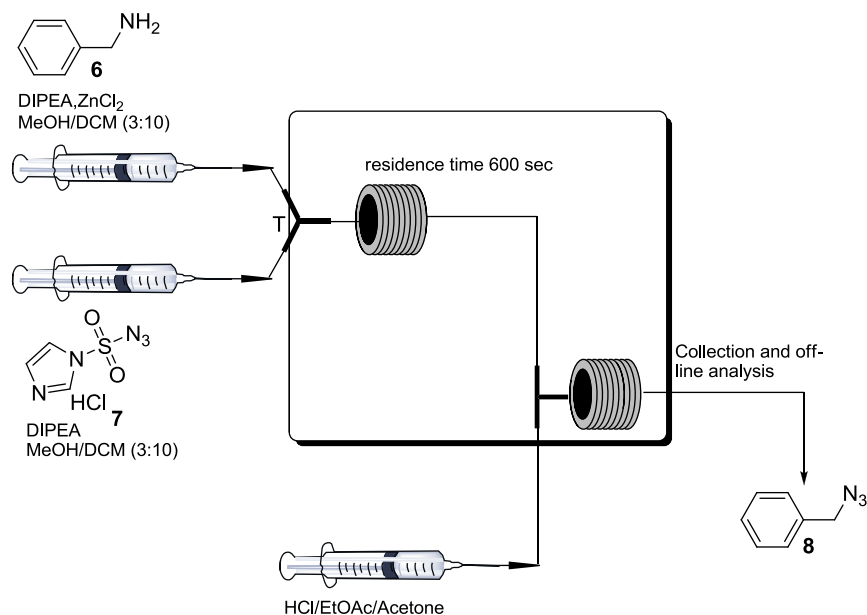


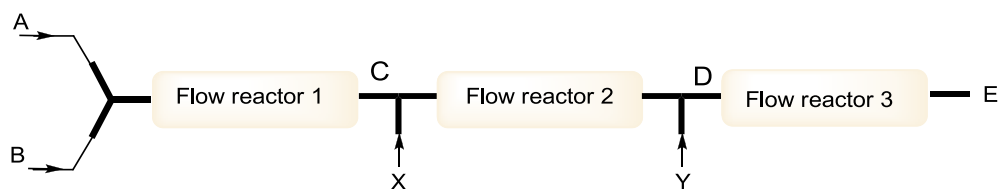
Figure 8: Second generation MACOS system with in-line analysis.

Additionally, flow chemistry offers a convenient means of preparing larger quantities of compounds by simply running optimized conditions for a longer period, or in parallel. This concept is termed “scaling-out” thus, avoiding the challenge of “scaling up” using batch reactions. This has been clearly demonstrated by a report by Rutjes, van Hest, and coworkers, where they developed a protocol to produce one gram of benzyl azide per hour in a single flow reactor at room temperature (Scheme 2).¹²²



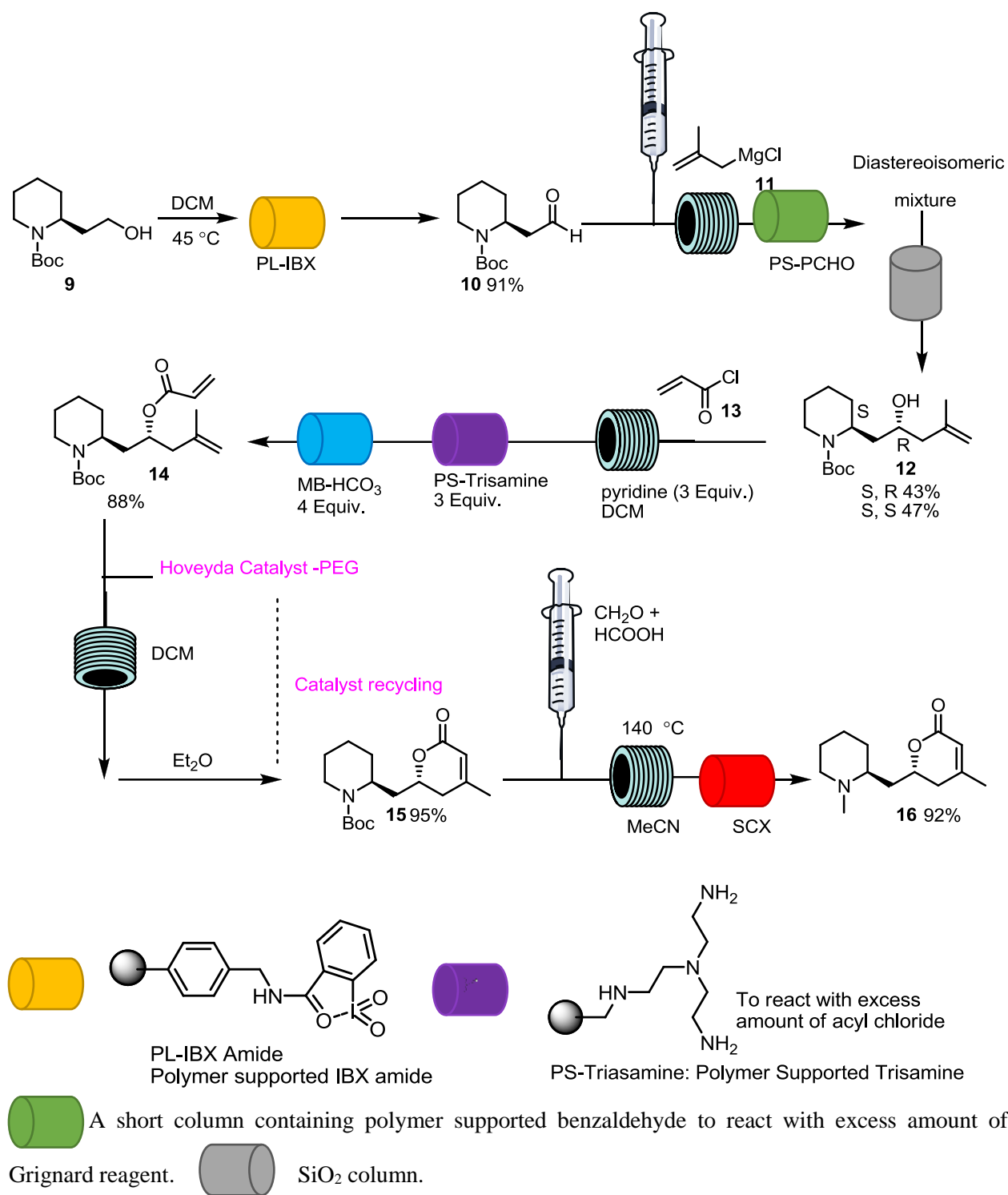
Scheme 2: Scale-up the synthesis of benzyl azide in flow reactors.

Moreover, multistep synthesis can be conducted using sequential micro-reactors where the product of the first micro-reactor flows directly to the next. The work-up steps are already installed in the flow setting.



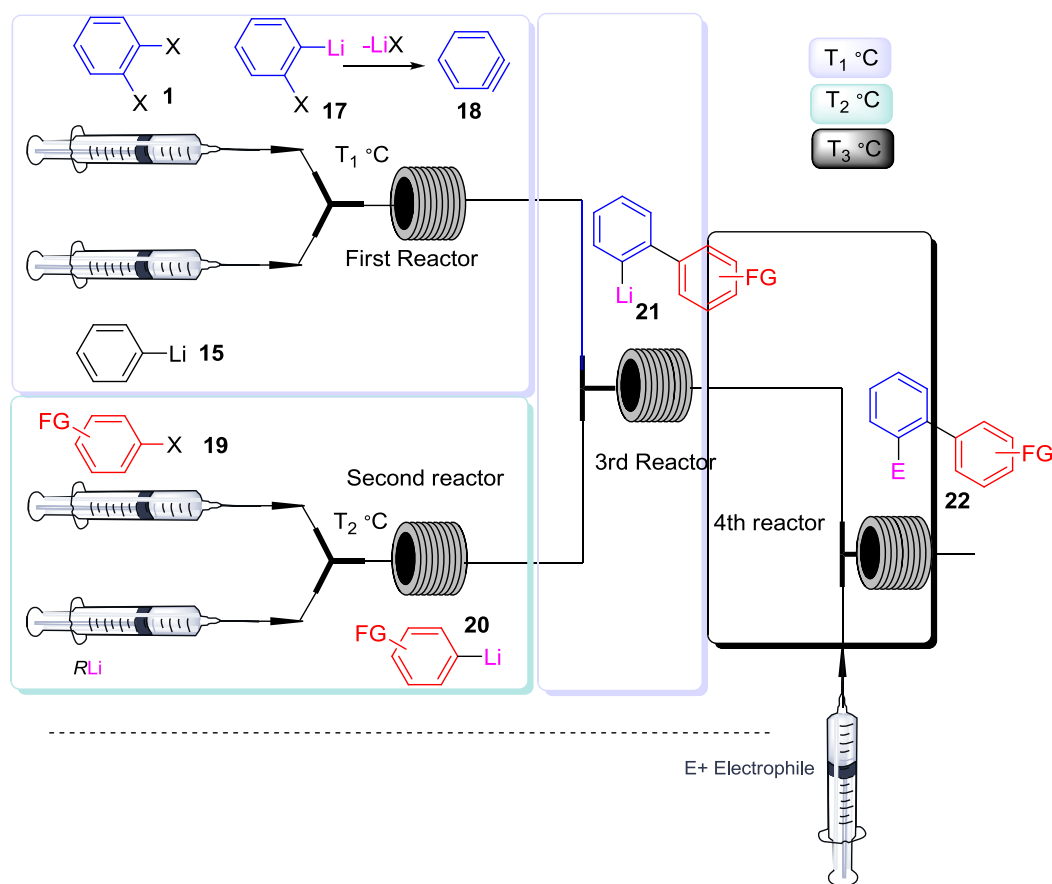
Scheme 3: Multistep synthesis in the flow.

This is well exemplified in the total synthesis of (+)-dumetorine. The process entailed five separate steps with 29% overall yield. The main advantages in performing this synthesis in flow were the precise control over the reaction conditions, the reduction in the reaction time, and minimize handling of intermediates (Scheme 4).¹²³



Scheme 4: Multistep synthesis of (+)-dumetorine in the flow.

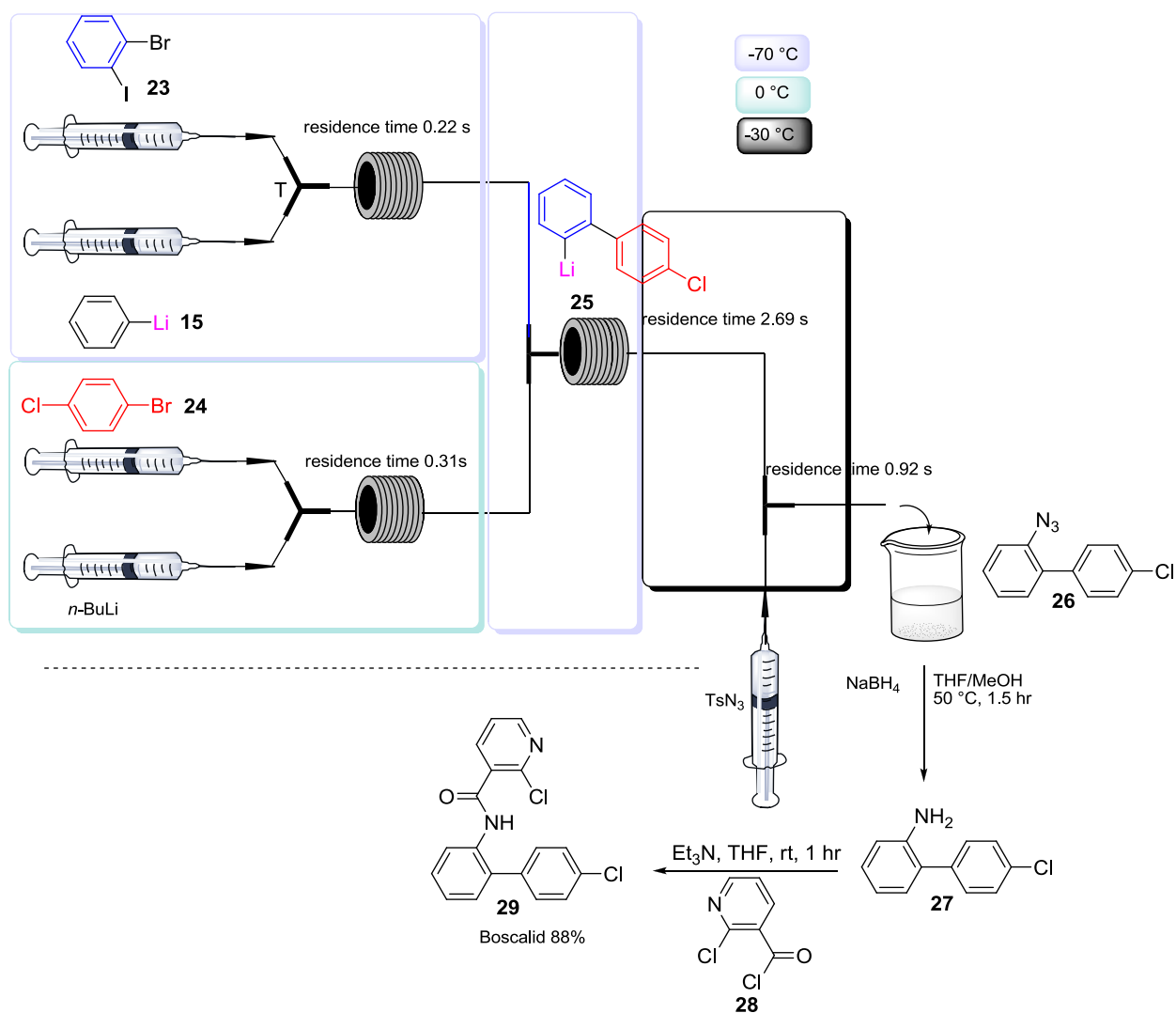
Based on all of the advantages listed above, flow reactors are ideal candidates to work with high-energy, reactive intermediates in a very controlled fashion. Chemists are now able to generate highly reactive intermediates and react them in subsequent steps before they decompose. This has been nicely demonstrated by Yoshida and coworkers where they developed a flow microreactor for three-component coupling based on flash chemistry, where carbolithiation of benzyne (generated *in situ*) with functionalized aryllithium took place, followed by reactions with electrophiles. (Scheme 5).¹²⁴



Scheme 5: Three-component coupling reaction of benzyne.

The utility of this method was demonstrated in the synthesis of boscalid (Scheme 6), an important fungicide, which belongs to the class of succinate dehydrogenase inhibitors.¹²⁵ The set up

consists of four different reactors. In the first one benzyne was generated by treating *o*-bromiodobenzene with phenyllithium. At the same time, another lithium-halogen exchange reaction takes place in the second reactor between 4-bromochlorobenzene and *n*-BuLi to deliver 4-chlorophenyllithium which reacts with the benzyne generated from the first reactor to deliver **25**. In the last reactor, **25** was subsequently quenched with TsN₃ to give 4'-chloro-2-azidobiphenyl in 60% yield. Reduction with NaBH₄ followed by the acylation reaction with **28** furnished boscalid in 88% yield. (53% from 1-bromo-2-iodobenzene).



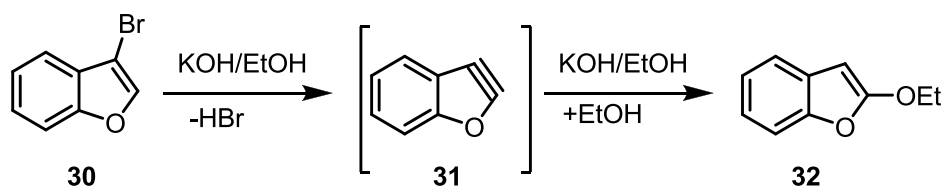
Scheme 6: Synthesis of boscalid in the flow.

Benzyne is a unique and highly reactive intermediate. Owing to its low-lying unoccupied molecular orbital (LUMO) and the high strain in its structure, benzyne is extremely reactive even at low temperature and, therefore, it must be generated *in situ*. The next section will briefly discuss the history of benzyne and its application in total synthesis.

5.2 Benzyne:

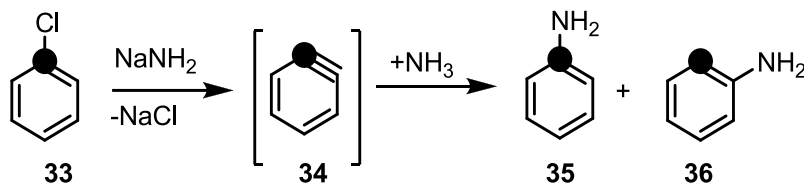
5.2.1 History and Background:

The first indication for the existence of aryne was reported by Stoermer and Kahlert in 1902.¹²⁶ The isolation of 2-ethoxybenzofuran upon treating 3-bromobenzofuran with base suggested the formation of *o*-didehydrobenzofuran (**31**) as an intermediate (Scheme 7).



Scheme 7: The first indication of the existence of aryne.

After several decades, definitive evidence for the formation of these reactive species was reported by Roberts¹⁰, Huisgen,¹²⁷ and Wittig.¹²⁸ In 1953, Roberts found a compelling evidence for benzyne formation in the reaction of ¹⁴C-labeled chlorobenzene with sodium amide (Scheme 8). The reaction produced 1:1 ratio of compounds **35** and **36**, confirming the intermediacy of a symmetrical reactive compound i.e., **34**.

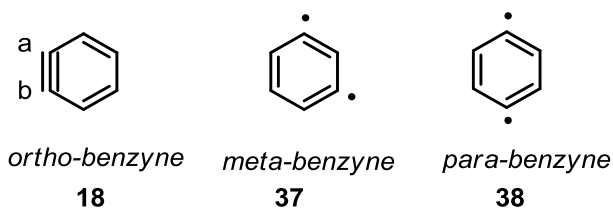


Scheme 8: ¹⁴C-Labeled chlorobenzene with sodium amide.

In 1956, Wittig and Pohmer reported the first Diels-Alder reaction of benzyne with furan, where the former reacts as a dienophile with the electron-rich diene (furan).¹²⁹ The discovery of benzyne led to a rapid development in organic synthesis, and the research in this field intensified.

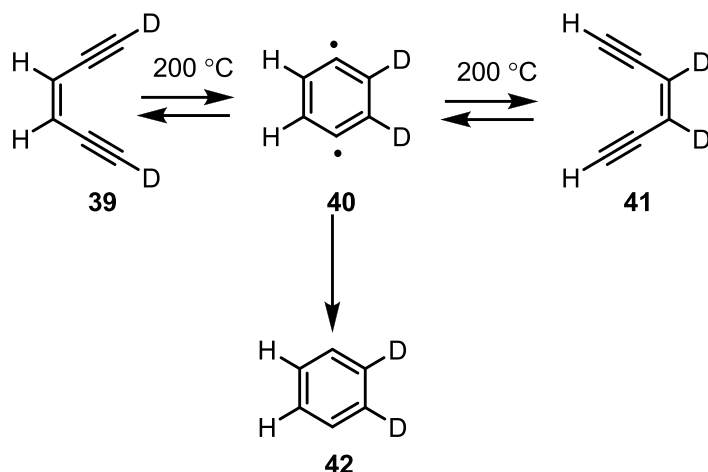
5.2.2 Benzyne isomers:

It is important to note that there are two other isomers of benzyne: *m*-benzyne and *p*-benzyne (Scheme 9).



Scheme 9: Benzyne isomers.

The theoretical and the experimental work on these two isomers is comparatively less than those done on *o*-benzyne. However, it is worth mentioning that *p*-benzyne is particularly important in the Bergman cyclization of enediyne - compounds able to cleave double-strand DNA - (Scheme 10).¹³⁰ Hydrogen abstraction by *p*-benzyne results in the formation of a phenyl radical that causes irreversible damage to the DNA strand through a second hydrogen abstraction.¹³¹

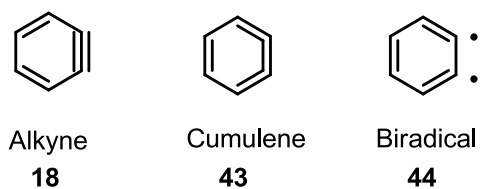


Scheme 10: *p*-Benzyne in Bergman cyclization.

Since this project deals with *o*-benzynes, the next sections will be discussing this isomer only.

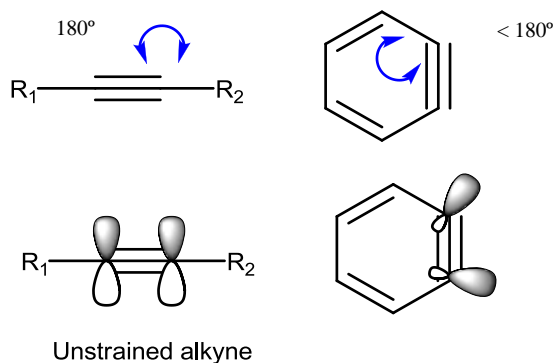
5.2.3 Structure of *o*-Benzyne:

o-Benzyne has three resonance structures (Scheme 11) where an alkyne representation is the most widely encountered, however, the diradical and the cumulene forms are significant contributors.¹³²



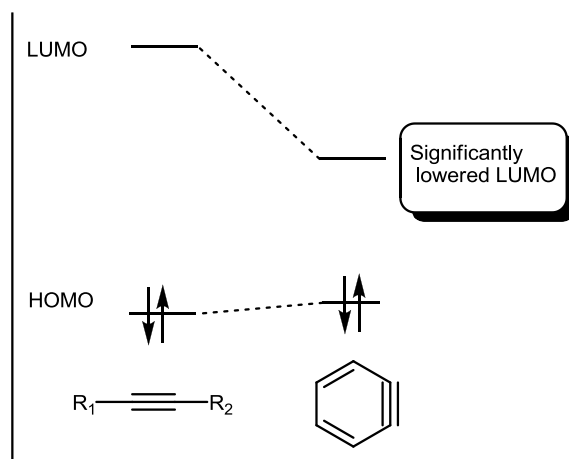
Scheme 11: Resonance structures of *o*-benzyne.

Accommodating a triple bond in a six-membered ring is geometrically constrained, therefore it is anticipated that the overlap of the in-plane *p* orbitals is reduced compared to alkynes, resulting in a weaker triple bond.



Scheme 12: Geometric strain in accommodating triple bond in six-membered rings.

In 1992, Raszishewski and co-workers assigned the vibrational frequency of a triple bond in *o*-benzyne to be 1846 cm^{-1} ¹³³ which is lower than the expected vibrational frequency of unstrained alkynes ($\sim 2200\text{ cm}^{-1}$).¹³⁴ The geometric constraints result in significant lowering of the LUMO energy for *o*-benzyne (Scheme 13). However, according to the computational studies reported by Carreira and co-workers the energy of the HOMO remains roughly unchanged.¹³⁵

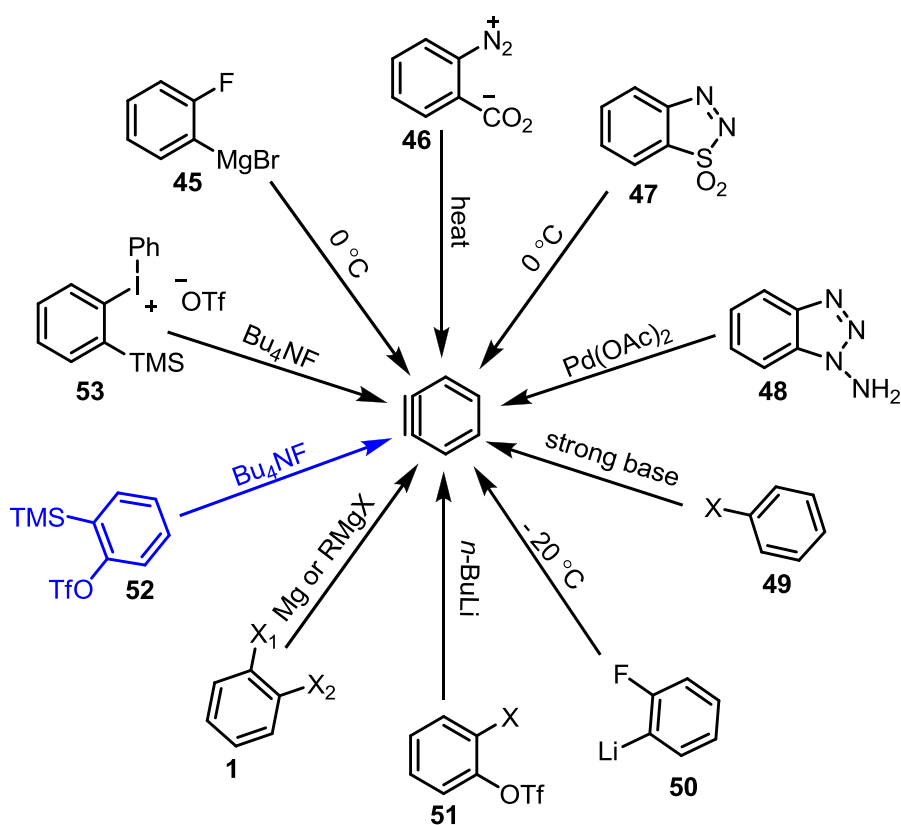


Scheme 13: Energy of LUMO in unstrained alkyne versus benzyne.

More recently, Gross *et. al.* reported an elegant method for deciphering the major resonance structure of arynes by atomic force microscopy. The results suggest that a cumulene resonance is the dominant one.¹³⁶

5.2.4 Generation of Benzyne:

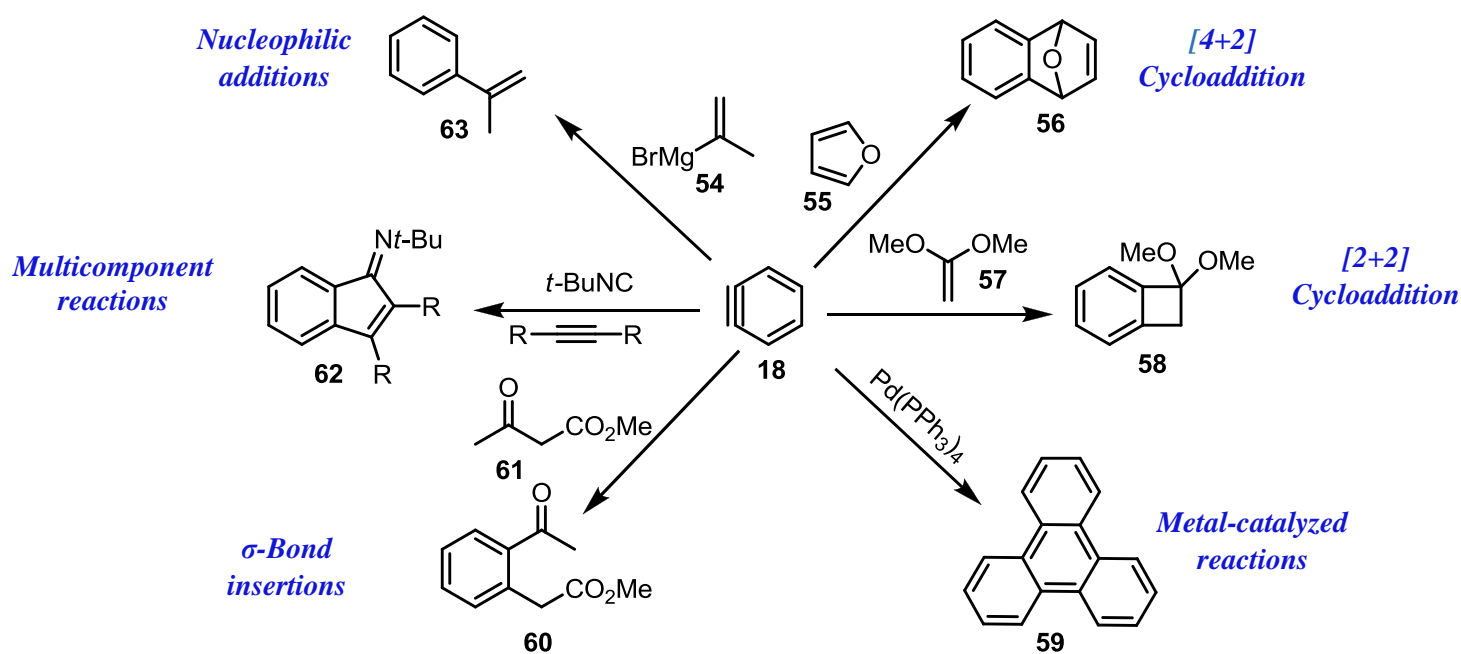
Generation of *o*-arynes requires the presence of two eliminable groups positioned *ortho* to each other. Several approaches have been developed for the generation of benzyne. Some include the use of diazonium carboxylate,¹³⁷ iodonium triflate,¹³⁸ benzotriazole,¹³⁹ halotriflate,¹⁴⁰ fluorolithium, and magnesium compounds.¹⁴¹ Perhaps the most common and versatile method to date is Kobayashi's mild fluoride-induced benzyne formation protocol (Scheme 14).¹⁴²



Scheme 14: Different methods for generating *o*-benzyne.

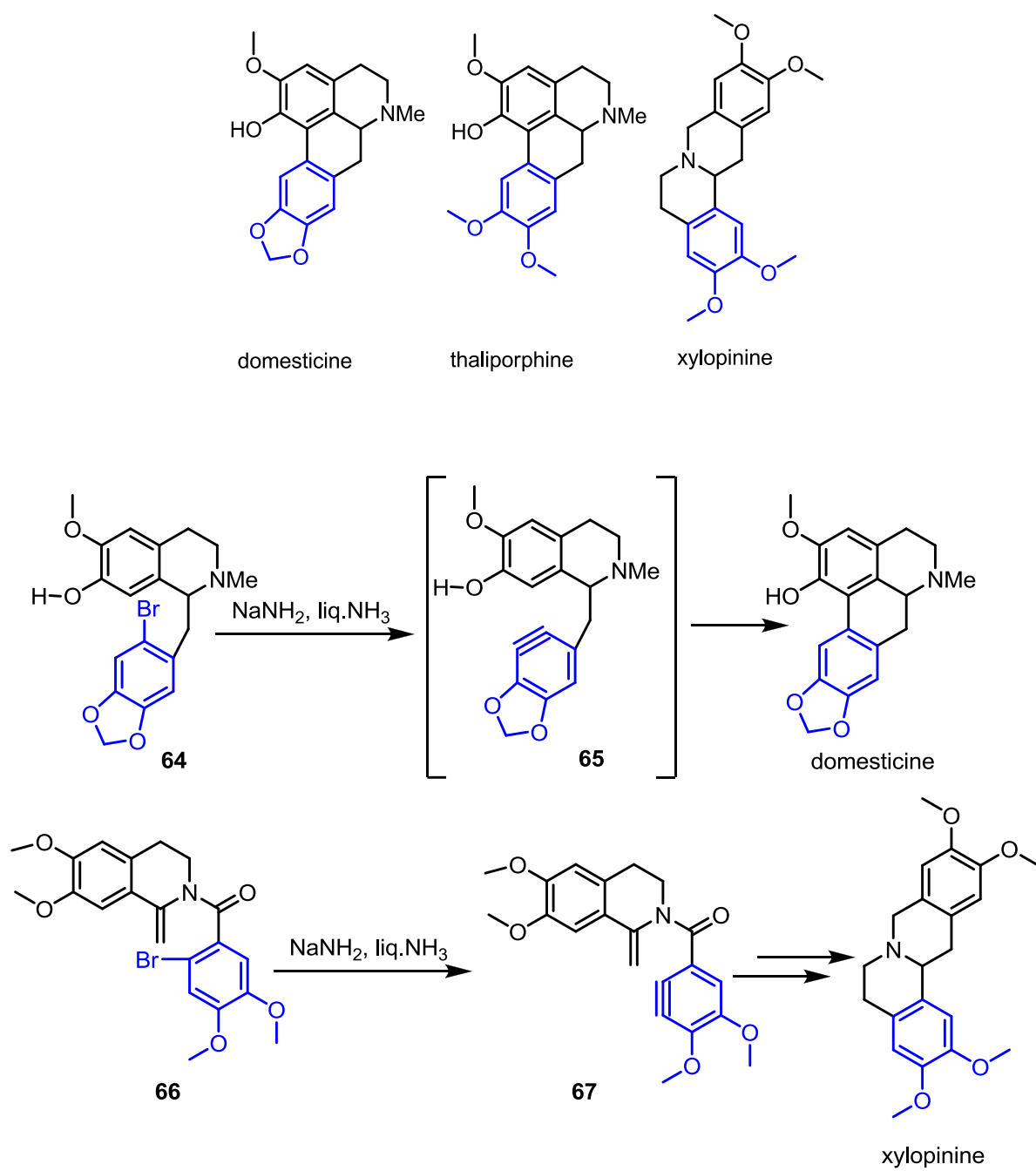
5.2.5 Reactions of Benzyne:

Benzyne derivatives have proven useful synthetically as they undergo a wide variety of transformations that enable a plethora of applications in synthesis including nucleophilic attack by neutral nucleophiles, [4 + 2] and [2 + 2] cycloadditions, sigma bond insertion, as well as metal-catalyzed reactions (Scheme 15).¹⁴³



Scheme 15: Different reactions of *o*-benzyne.

A consequence of this wide application scope is that it can be used to introduce multiple benzene rings in the core structure of the target molecules. Recent examples include the construction of polyaromatic hydrocarbons,¹⁴⁴ the use of pyridynes as building blocks,¹⁴⁵ the chemical transformation of nanotubes,¹⁴⁶ and of graphene sheet.¹⁴⁷ Additionally, they have been incorporated into the natural product synthesis of carbocycles and heterocycles, as well as promising drug candidates. The former point is exemplified in the total synthesis of domesticine,¹⁴⁸ thaliporphine,¹⁴⁹ and xylopinine (Scheme 16).¹⁵⁰



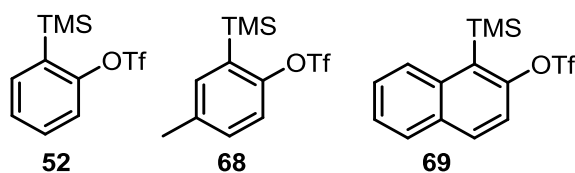
Scheme 16: Benzyne incorporation in natural products.

5.2.6 Plan of study:

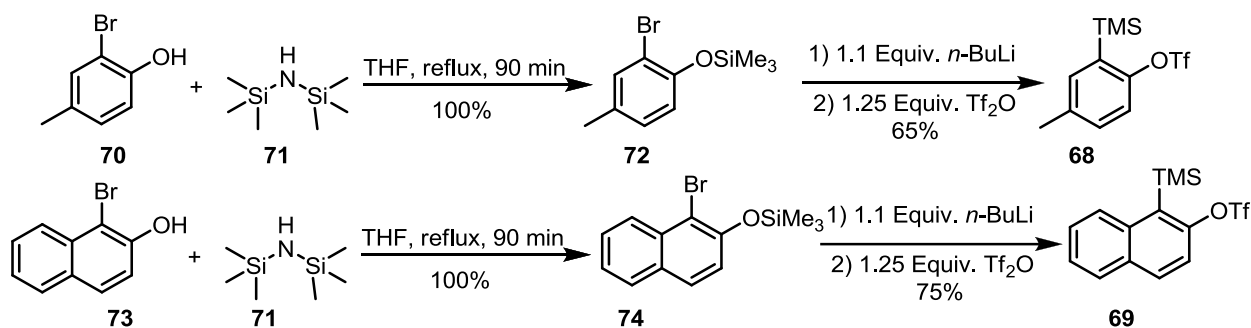
Given the rich chemistry that can be accessed using benzyne and all the advantages of flow chemistry listed above which makes it ideal to work with high-energy species, we were interested in generating various benzyne intermediates in flow at room temperature. We envisioned that the precise control of the reaction time, the efficient mixing, and the rapid mass and heat transfer in flow would enable us to trap these intermediates in [4 + 2] cycloaddition reactions at room temperature before they decompose (which is the case in conventional flask at the same temperature) with five-membered aromatic heterocycles using mild conditions to produce compounds of biomedical interest in higher yields compared to batch-setting.¹⁵¹

CHAPTER 6: Results and Discussion

Initial efforts focused on the preparation of suitable benzyne precursors for [4+2] cycloaddition reactions. Three benzyne precursors were used in this study (Scheme 17) and while compound **52** is commercially available, benzyne precursors **68** and **69** were prepared following a simple two-step protocol from their corresponding *o*- bromohydroxyarenes (Scheme 18).¹⁵²

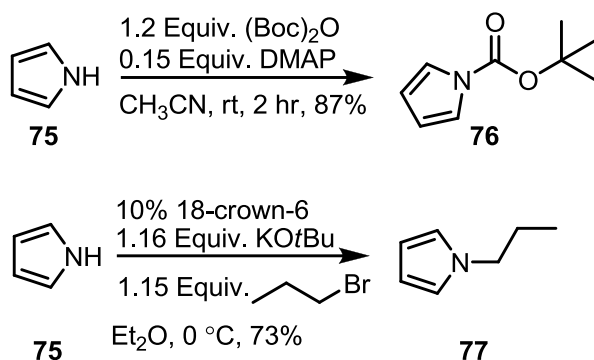


Scheme 17: Benzyne precursors used in this study.



Scheme 18: Synthesis of benzyne precursors **68** and **69**.

Some of the dienes used in this study were commercially available except for *N*-Boc pyrrole (**76**) and *N*-propyl pyrrole (**77**), which were prepared using literature procedures outlined in Scheme 19.¹⁵³



Scheme 19: synthesis of **76** and **77**.

Using flow setup illustrated in Figure 9, syringe 1 was filled with a tetrahydrofuran (THF) solution containing the benzyne precursor and diene, while the second syringe was filled with a THF solution of tetra-*n*-butylammonium fluoride (TBAF) which was used as a fluoride source. The contents of these syringes flowed into a tee (T_1) where they mixed, and the resultant solution moved into reactor R_1 before flowing into a collection vial where they are quenched in a solution of water and ether (Figure 9). The residence time in the reactor was optimized by adjusting the flow rates of syringes 1 and 2.

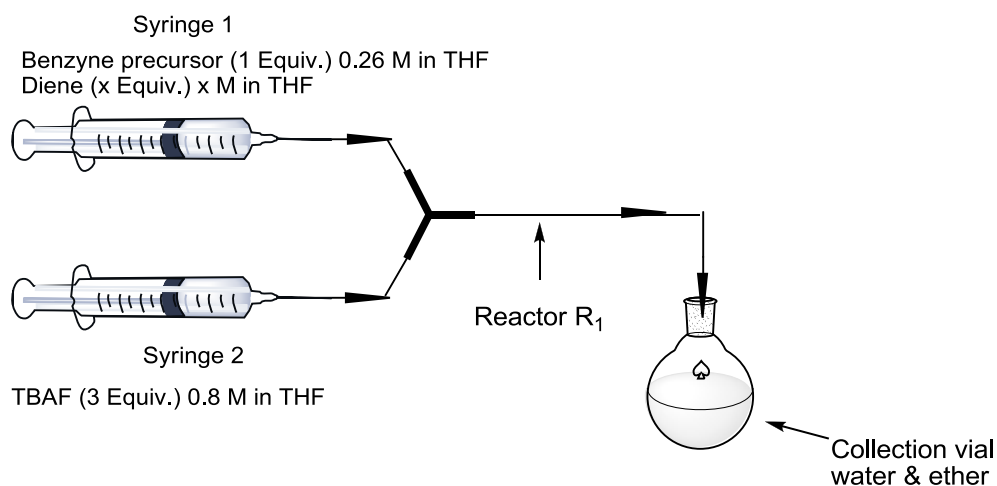
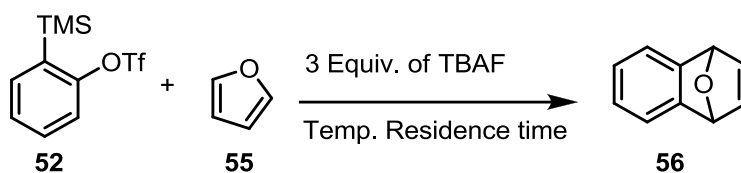


Figure 9: Flow reactor set up for-Diels-Alder reactions of benzyne intermediates.

In order to find the best optimizing conditions, we started our investigations using unsubstituted benzyne precursor **52** and furan (**55**) as the diene.

Table 3: Effect of residence time, diene equivalents and the reaction temperature on the cycloaddition of benzyne and furan.



Entry	T (°C)	Residence Time (sec)	Equiv. of 55	Con. (%) ^a (Yield of 56) ^b
1	24	6	5	43(-)
2	24	12	5	77(-)
3	24	30	5	91(-)
4	24	60	5	100 (51)
5	0	60	5	100 (53)
6	0	60	10	100 (57)
7	24	60	10	100 (60)

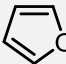
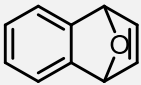
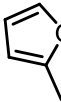
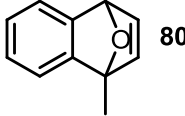
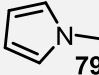
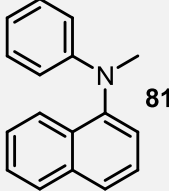
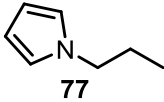
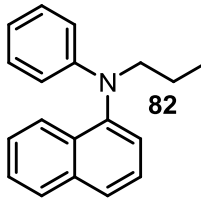
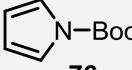
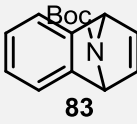
^a Percent conversion was determined by analysis of the crude ¹H-NMR spectrum. ^bYield was determined on a product that had been purified by silica gel flash chromatography.

Using a residence time of 6 sec and 5 equivalents of **55**, the reaction was first performed at room temperature resulting in 43% conversion to produce **56** (Table 3, entry 1). Increasing the residence time in R₁ from 6 seconds to 1 minute by decreasing the flow rate led to 100% conversion and the product (**56**) was isolated in 51% yield (Table 3, entry 4). In an attempt to improve the yield of product **56**, based on the assumption that the low yield is due to benzyne decompositions, the temperature was lowered to 0 °C by placing the reactor (R₁) in an ice bath. However, this change

had little impact on the reaction outcome (Table 3, entry 5). Keeping the temperature at 0 °C while doubling the equivalents of diene **55** led to a slight improvement in yield (Table 3, entry 6). Optimal results were achieved when 10 equivalents of **55** were used and the reaction was performed at room temperature (Table 3, entry 7).

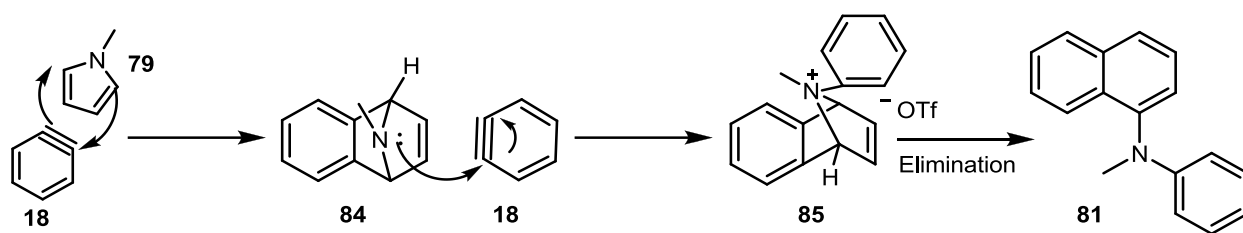
Armed with these results, we set out to explore the substrate scope of this method with different dienes using benzyne precursor **52** (Table 4)

Table 4: Reaction between benzyne precursor **52** and different dienes.^a

Entry	Diene	Product	% Isolated Yields
1	 55	 56	60
2	 78	 80	59
3	 79	 81	19
4	 77	 82	21
5	 76	 83	59

a) Reactions were performed using the flow rate step illustrated in Figure 9 and the procedure outlined in Table 3, entry 7 and the procedure outlined in Table 3, entry 7 (flow rate = 44.48 μ L/min, residence time = 1 min and the reactor volume was 77 μ L).

The expected cycloadducts were obtained in entries 1, 2 and 5 with furan, 2-methyl furan and *N*-Boc pyrrole, respectively. However, in the case of pyrroles **77** and **79** unexpected diarylamine products were obtained. In these cases, the Diels-Alder cycloadduct reacts nucleophilically with another molecule of benzyne to deliver the product observed (Scheme 20). This transformation has precedent in the literature.¹⁵⁴



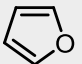
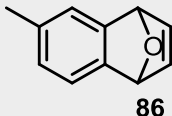
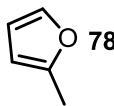
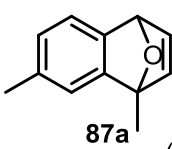
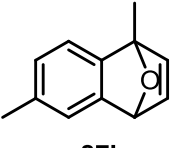
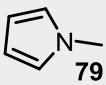
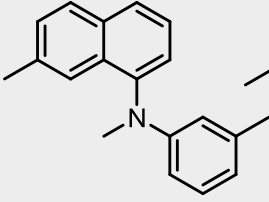
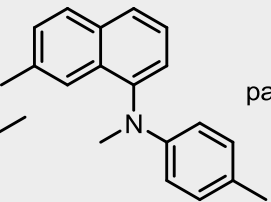
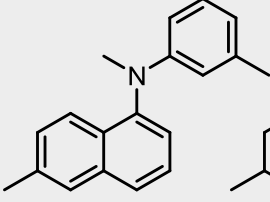
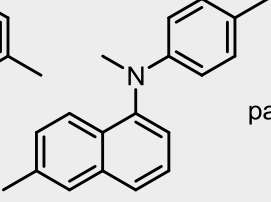
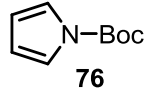
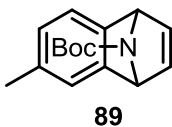
Scheme 20: Mechanism for the formation of compounds **81**.

The dienes used in this study possess varying degrees of aromaticity, which will impact their ability to undergo cycloaddition. In 2013, Horner and Karadakov illustrated that furans derivatives were found to be less aromatic than pyrroles.¹⁵⁵ Therefore, the nucleophilicity of these dienes will decrease as the degree of aromaticity increases, in other words, it will be expected that furan and furan derivatives will react more readily with benzyne than pyrroles, and the results obtained are in line with this hypothesis. Higher yields were obtained with furan and 2-methyl furan (Table 4, entry 1, and 2) compared to pyrroles (Table 4, entry 3 and 4). Also, all the attempts to cyclize benzyne precursor **52** with thiophene, which possesses the highest aromatic character in comparison to furan and pyrroles completely failed.

Benzyne precursor **68** was investigated next (Table 5). Cycloadduct **86** was obtained by the reaction of **68** with furan (**55**) in a good yield. The reaction between 2-methyl furan (**78**) proceeded with no regioselectivity giving rise to **87a** and **87b** in equal amounts (Table 5, entry 2). Upon reacting benzyne precursor **68** with *N*-methyl pyrrole, 4 isomers were obtained (2 pairs), and based

on a number of 2D NMR experiments (2D-TOCSY, COSY, and NOSEY), the ratio of the two pairs of products (i.e. pair 1: **88a-88b** and pair 2 **88c-88d**) were found to be 1.2:1, and the ratio of the *meta* to *para* within pair 1 (**88a: 88b**) is (1.3 :1) which is presumably equal to the ratio of the *meta* to the *para* isomer within pair 2.

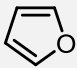
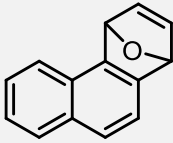
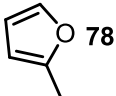
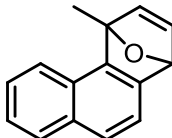
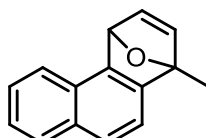
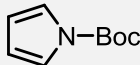
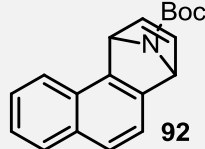
Table 5: Reaction between benzyne precursor **68** and different dienes.^a

Entry	Diene	Product	%Isolated Yields
1	 55	 86	68
2	 78	 87a (1 :1)  87b	59 ^b
3	 79	<div style="display: flex; flex-direction: column; align-items: center;"> <div style="display: flex; justify-content: space-around; width: 100%;"> <div style="text-align: center;">  88a </div> <div style="text-align: center;">  88b </div> </div> <div style="display: flex; justify-content: space-around; width: 100%;"> <div style="text-align: center;">  88c </div> <div style="text-align: center;">  88d </div> </div> <div style="margin-top: 10px;"> pair 1 pair 2 </div> </div>	28 ^b
4	 76	 89	49

^a Reactions were performed using the flow setup illustrated in Figure 9 and the procedure outlined in Table 3, entry 7 (flow rate = 44.5 $\mu\text{L}/\text{min}$, residence time = 1.2 min, and the reactor volume was 76 μL). ^b Ratio was determined by 2D ¹H-NMR spectroscopic experiments.

Very good yields were obtained when benzyne precursor **69** was employed (Table 6). Cycloaddition between furan (**55**) and the benzyne precursor **69** delivered the expected product **90** in a very good yield (Table 6, entry 1). Upon reacting **69** with **78**, two inseparable isomers were obtained in nearly equal ratio (0.82:1) (Table 6, entry 2).

Table 6: Reaction between benzyne precursor **69** and different dienes.^a

Entry	Diene	Product	% Isolated Yields
1	 55	 90	71
2	 78	 91a  91b	76 ^b
3	 76	 92	66

^a Reactions were performed using the flow setup illustrated in Figure 9 and the procedure outlined in Table 3, entry 7 (flow rate = 44.5 μ L/min, residence time = 1.72 min).

^b Ratio was determined by 2D ¹H-NMR spectroscopic experiments.

As shown in Tables 3-6, the expected cycloadducts were formed, however, the yields in some instances are lower than anticipated, which is attributed to the short half-life of benzyne intermediates formed during the course of the reaction. To examine this, a series of control experiments were conducted. In the first experiment, we used the set-up shown in Figure 10. At room temperature, a solution containing benzyne precursor **52** in THF was met at the first tee (T₁) by a TBAF solution from syringe 2, and the resultant mixture was allowed to react for 1 min.

which was the optimal residence time to produce the maximum level of cycloadduct. Then a solution of furan in THF (5 Equiv.) was introduced from syringe 3 into the flow stream at the end of R₁, and the mixture was allowed to react for 1 min in R₂ before quenching in the collection vial V₁. Analysis of the crude reaction mixture showed no sign of product formation, indicating the benzyne decomposition had taken place before the Diels-Alder reaction could occur.

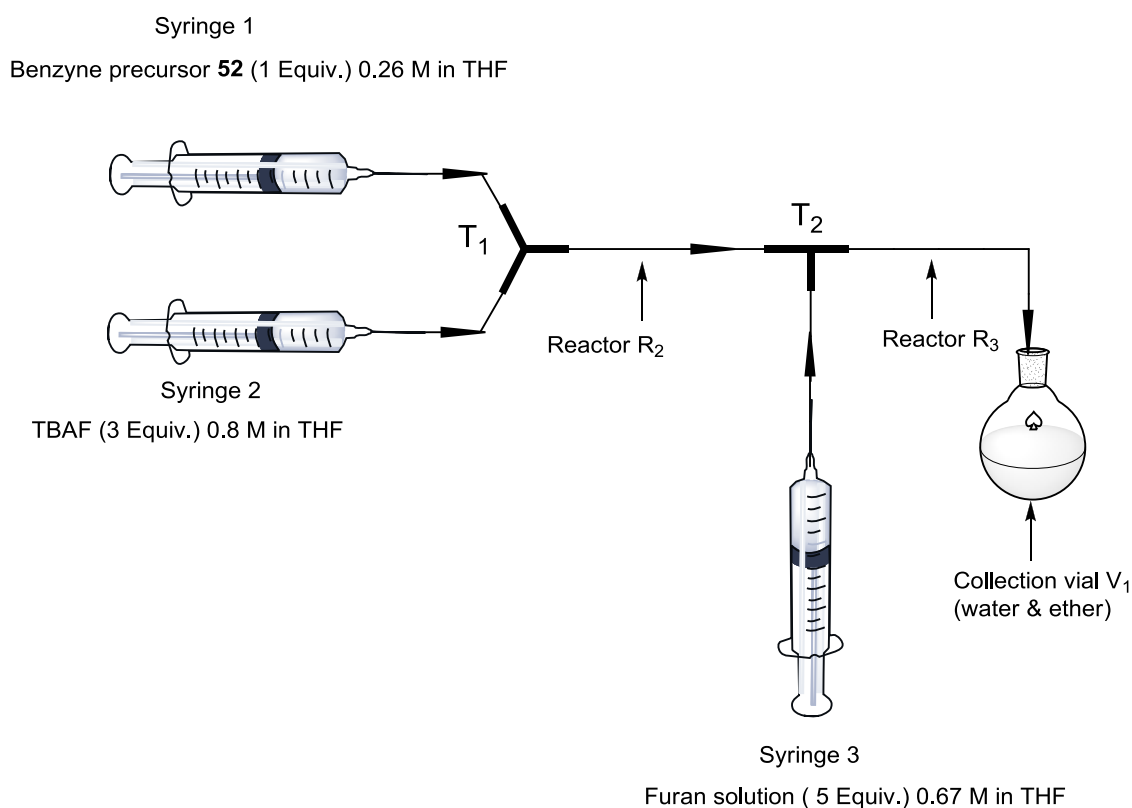
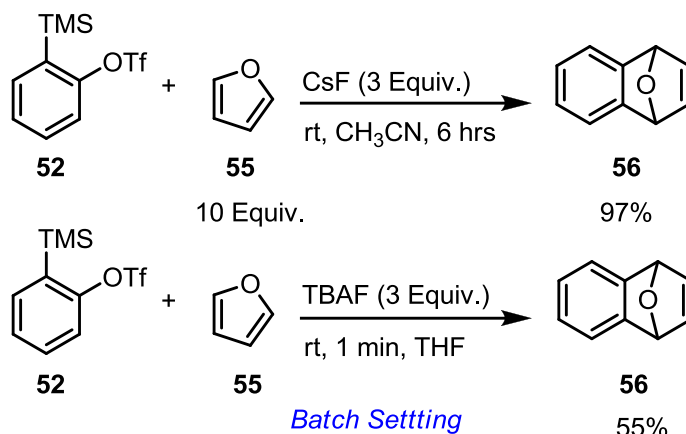


Figure 10: Reactor design used for control experiments to examine benzyne lifetime.

The second control reaction between **52** and furan (**55**) was performed in a conventional flask where cesium fluoride (CsF) was used as the fluoride source instead of TBAF (Scheme 21).



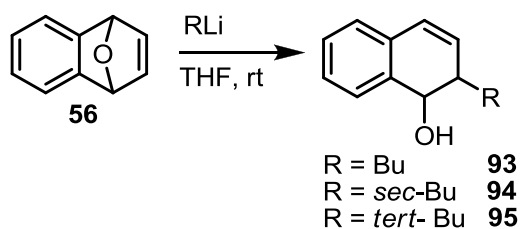
Scheme 21: Control experiments conducted in the batch setting.

The batch reaction was performed in acetonitrile as a solvent instead of THF since CsF is more soluble in the former.¹⁵⁶ The reaction proceeded nicely, providing cycloadduct **56** in 97% yield, whereas the same reaction performed using TBAF produced almost half the level of product (55% yield). The TBAF result compares very well to the results obtained when this reaction is run in flow (Table 3, entry 4, 51% yield). We attribute this to the difference in the benzyne concentration in each case (i.e. CsF versus TBAF). Due to the low solubility of CsF (0.093 +/- 0.008 mM at rt),⁹³ the concentration of the highly reactive benzyne intermediate will be relatively low, and as a result, decreases the rate of side reactions of benzyne with itself. However, in the case of TBAF, which is completely soluble in THF, the consumption of starting material to generate benzyne is much faster. The higher relative concentration of benzyne in the case of TBAF facilitates the formation of side-products, especially at the beginning of the reaction when benzyne concentration will be the highest.

Moving forward, we investigated the ring opening of oxabicyclic alkene **56** with different organolithiums using a flow system outlined in Figure 9 to produce the corresponding 1, 2-

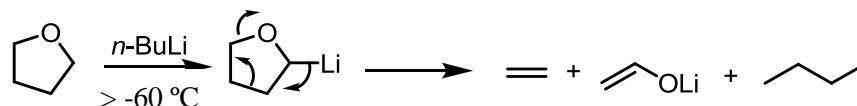
dihydronaphthols, as these are important precursors for antibiotic synthesis.¹⁴⁶ The optimized reaction conditions for ring opening steps are shown in Table 7.

Table 7: Ring Opening of **56** with different organolithiums.



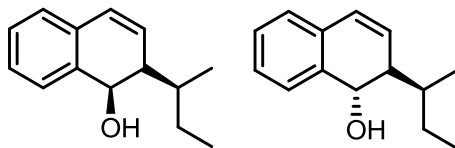
Entry	RLi (x Equiv.)	Residence time (s)	Flow rate ($\mu\text{L}/\text{min}$)	% Yield
1	<i>n</i> -BuLi (2)	3	20	40
2	<i>Sec</i> -BuLi (1.1)	4	15	72
3	<i>tert</i> -BuLi (1.4)	6	10	83

As we increase the steric bulk of the organolithiums, the yield of the reaction increases (Table 7). The low yield of **93** (Table 7, entry 1) can be explained by the side reaction of *n*-BuLi with the solvent. *Ortho* lithiation of tetrahydrofuran followed by retro 3+ 2 cycloaddition to produce ethene and acetaldehyde upon protonation (Scheme 22).¹⁵⁷



Scheme 22: side reaction between *n*-BuLi and THF.

It is noteworthy that the reaction of *n*-BuLi and *tert* BuLi led to a single product (as observed in the ¹H-NMR spectra), but the reaction of *sec*-BuLi with **56**, produced two inseparable isomers, syn and anti products (1:1 ratio based on ¹H-NMR spectroscopy).



Scheme 23: Syn and anti products formed in Table 7, entry 2.

With the optimized conditions in hand for both steps (i.e. Diels-Alder reaction and the ring opening of cycloadduct with different organolithiums), we want to create a more appealing system that enables us to access 1,2-dihydronaphthols in one reactor. Hence, we set-up the microfluidic device shown in Figure 11.

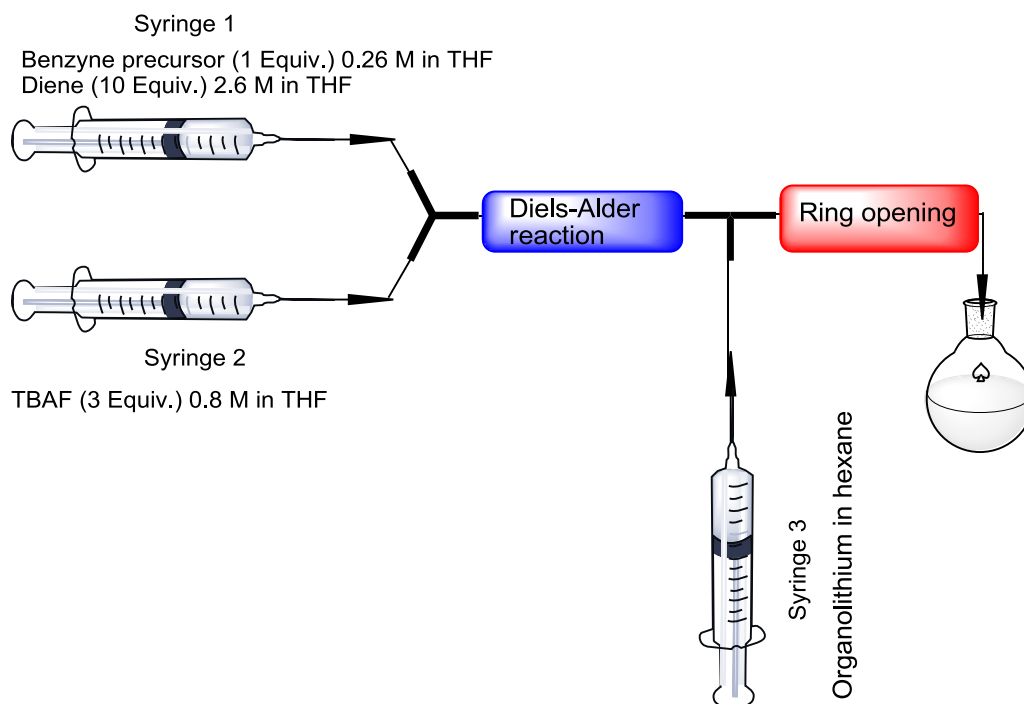


Figure 11: Design reactor used to synthesize 1, 2-dihydronaphthols from benzyne precursors.

This system consists of two reactors, the first one is for Diels-Alder reaction and the second one is for the ring opening of the oxabicyclic alkene that is expected from the first reactor. The concentration of the starting materials matches those of the optimized conditions in Figure 6. We

started our investigation with the simplest benzyne precursor **52** as dienophile, furan (**55**) as a diene, TBAF as the fluoride source and *n*-BuLi as the organolithium. The results obtained were summarized in Table 8.

Table 8: Optimization study for the synthesis of **93** directly from **52**.

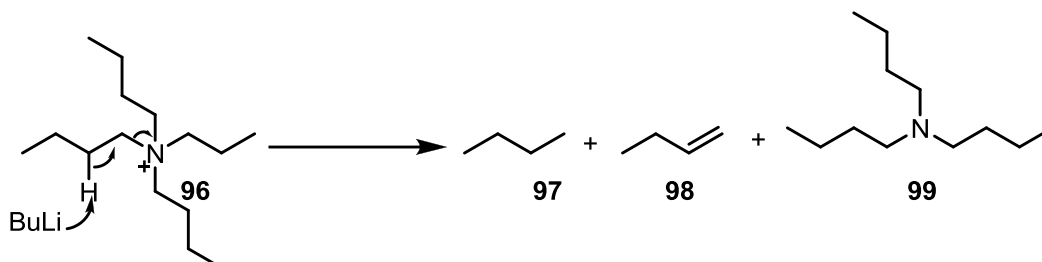
Entry	% Conversion to 56	Equiv. <i>n</i> -BuLi	% Conversion to 93 ^a
1	100	1	15
2	100	2	22
3	100	5	50
4	100	12	70
5	100	15	85
6	100	18	100

^a Percent conversion was determined by analysis of the crude ¹H-NMR spectrum.

The results obtained in Table 8 contradict the optimized conditions for the ring opening step where only 2 equivalents of the organolithium was needed to drive the reaction to completion. Upon using 1 equivalent of the *n*-BuLi, the ring opening of oxabicyclic alkene proceeded to only 22% conversion (Table 8, entry 1). Complete conversion was achieved only when 18 equivalents of *n*-BuLi was used (Table 8, entry 6). The need for the vast excess amount of organolithium can be explained either by the side reaction of the water content in the TBAF (5 wt%) with organolithium to produce butane or by a hoffman type elimination reaction to produce butane (**97**) and 1-butene (**98**) along with tributylamine (**99**) (Scheme 24). Butane and 1-butene are gases at room temperature

(boiling points of -1 °C, -6.3 °C, respectively) so we were unable to observe these by ¹H-NMR spectroscopy, however, this would explain the bubble formation observed in the second reactor.

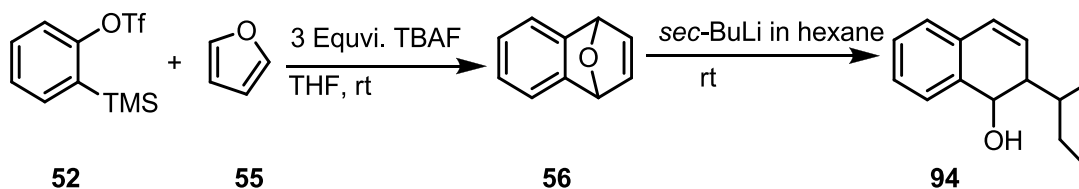
Another



Scheme 24: Hoffman elimination reaction between organolithium and TBAF.

The same trend was observed upon using 1.7 equivalents of *sec*-BuLi in the ring opening step where only 11% conversion (Table 9, entry 1), which was improved to 50 % conversion when 7.3 equivalents of *sec*-BuLi were employed (Table 9, entry 3).

Table 9: Optimization study for the synthesis of **94** directly from **52**.



Run	Equiv. <i>Sec</i> -BuLi	% Conversion to 94 ^a
1	1.7	11
2	3	22
3	7.3	50

^a Percent conversion was determined by analysis of the crude ¹H-NMR spectrum.

Unfortunately, the use of TBAF and THF is unavoidable since it is important to ensure complete solubility of all reagents in the reactor (tetramethylammonium fluoride would require a more polar solvent)¹⁵⁸. Thus, an excess amount of organolithium is needed to compensate for that lost in side reactions listed above (Scheme 22 and 24).

Conclusion:

We have developed a protocol for generating benzyne derivatives using flow chemistry. These highly reactive intermediates were trapped in Diels–Alder reactions with 5-membered heterocycle dienes to generate in most cases the expected cycloadducts. The yield of cycloadduct is highly dependent on the rate of the reaction between the highly reactive benzyne intermediate and the diene. Low yields were obtained with dienes possessing high aromatic character. Benzyne can react with itself to give by-products competitively with the desired cycloaddition. This reaction may be a good candidate for the slow introduction of one of the reactants, TBAF in this case, by adding it into the flow stream in multiple entry points along the reactor's length, thus, providing the equivalent of “dropwise addition” for flow. This would slow the rate of benzyne formation thereby possibly reducing undesired side reactions.

For the multistep synthesis of 1,2-dihydro naphthols derivatives in one reactor, successful results were obtained for the first reaction ([4+2] cycloaddition) while attempts to drive the ring opening step to completion failed unless excess amounts of the organolithiums were used. The formation of bubbles in the second reactor created undesirable back pressure and resulted in inaccurate residence time.

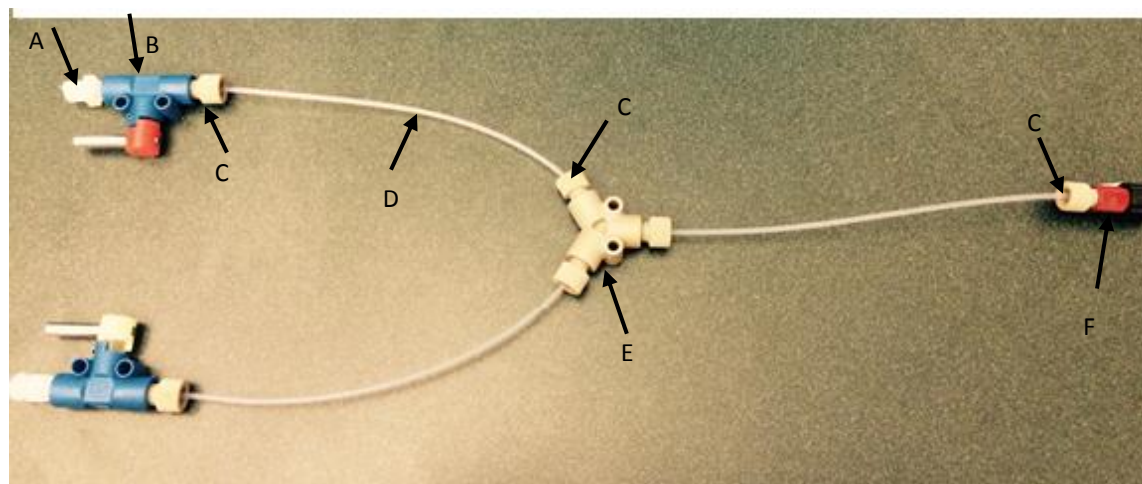
Chapter 7: Experimental Procedures

General Experimental:

All flasks and vials were flame-dried under vacuum and purged with Ar (3 times) prior to use. All reagents were purchased from Sigma-Aldrich or Alfa Aesar and were used without further purification unless otherwise noted. THF and Et₂O were distilled over sodium/benzophenone under argon atmosphere prior to use. Organolithium reagents were titrated using 1,3-diphenylacetone p – tosylhydrazone prior to use. Analytical thin layer chromatography TLC was performed on EMD 60 F254 pre-coated glass plates and spots were visualized with UV light (254 nm) and stained using either potassium permanganate (KMnO₄) or *p*-anisaldehyde. Column chromatography purifications were carried out using either the flash technique on EMD silica gel 60 (230 – 400 mesh), basic Al₂O₃, or neutral Al₂O₃. Nuclear magnetic resonance (NMR) for ¹H-NMR and ¹³C-NMR spectra were recorded on Bruker AVANCE 400 MHz and 300 MHz spectrometers. ¹H-NMR spectra recorded in CDCl₃ were referenced to the CHCl₃ peak (¹H-NMR δ = 7.28) while ¹³C-NMR spectra were referenced to the middle resonance of the carbon triplet of CDCl₃ (δ = 77.0 ppm). All chemical shifts are reported in parts per million (ppm), measured from the center of the signal except in the case of multiplets of more than one proton, which are reported as a range. Coupling constants are expressed in Hz. Splitting patterns of the peaks are abbreviated as follows: singlet (s), doublet (d), triplet (t), quartet (q), quintet (quint) sextet (sex), doublet of doublet (dd), multiplet (m), and broad singlet (bs). Resolution Mass Spectrometry (HRMS) analysis was performed by the Mass Spectrometry and Proteomics Services Unit at Queen University in Kingston, Ontario. Melting points were determined using a Fisher-Johns melting point apparatus and are uncorrected. Flow experiments were conducted in (perfluoroalkoxyalkane)

PFA tubing with 1/16" outer diameter and 0.03" ID (internal diameter). The tubings were connected to the syringes by ferm lurex, 1/4-28 male polyprop and the reagents were infused via syringe pumps (New Era, model number: NE_4000). At the point of mixing the starting materials; Peek-Y connector possessing 0.02" opening and 1.7 μ L swept volume was used. (See the figure below). All tubing, connectors, valves, and fittings were purchased from IDEX Health and Science LLC.

Figure 1 Reactor used in the flow reactions



A: Ferm lurex 1/4-28 male polyprop

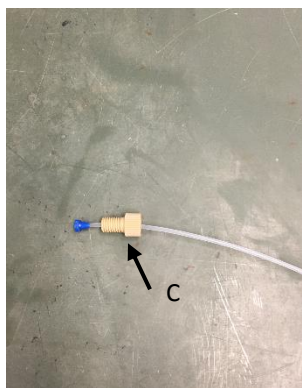
B: Valve

C: Flangeless PEEK fittings and PEEK ferrules

D: PFA tubing with 1/16" outer diameter and 0.03" internal diameter

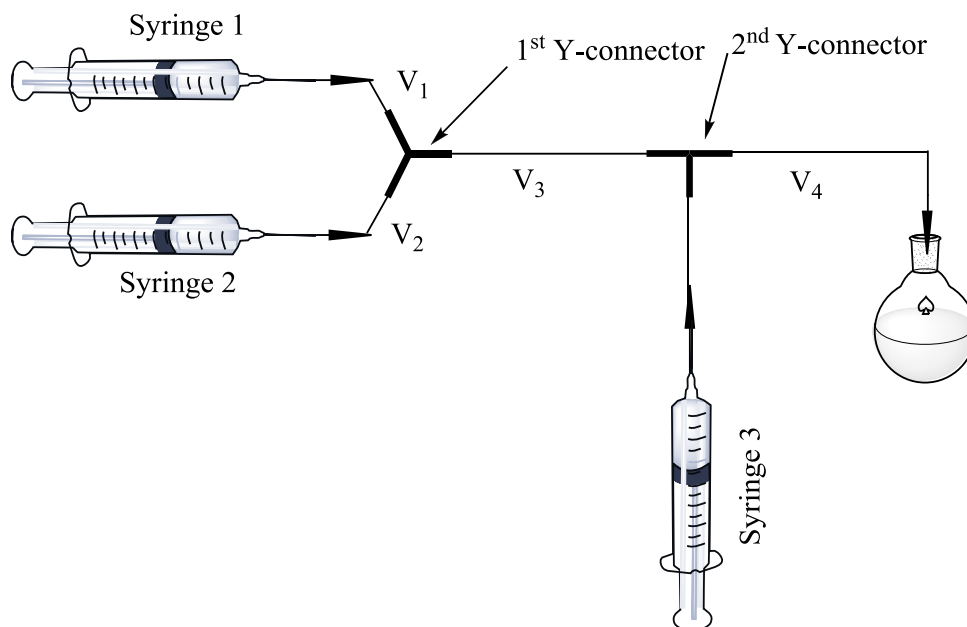
E: PEEK-Y connector

G: Female Luer adapter



General Set-up for the flowed reaction:

Two solutions were prepared in 4 mL vials equipped with magnetic stirring bars. Into the first vial were added the benzyne precursor (0.8 mmol, 1 Equiv. x mL) the diene (8mmol, 10 Equiv. x mL) and enough THF were added to reach a total volume of 3 mL. In a second vial, TBAF (2.4 mmol, 3 Equiv.) was diluted in THF to get 3 mL solution. These two solutions were then loaded into two 3 mL syringes. The two syringes were connected to the reactor and set into New Era syringe pumps. The pumps start to infuse the reagents through the reactor and a collection vial was placed at the end of the reactor. The collection vial contained a biphasic mixture of water and ether and the solution was vigorously stirred as the effluent from the reactor flowed into it to ensure were thoroughly quenched. Following the reaction, the organic layer was separated, dried over anhydrous MgSO_4 , filtered and concentrated *in vacuo*. The crude mixture was then purified by flash chromatography on silica, or alumina (basic or neutral) depending on the product formed, see details below.



V_1 = volume of the tube that connects syringe 1 to the Y connector.

V_2 = volume of the tube that connects syringe 2 to the Y connector.

$V_1 = V_2$

V_3 = volume of the reactor.

V_4 = volume of the tube that connects syringe 3 to the 2nd Y connector.

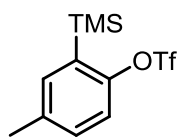
The volume of $(V_1 + V_2 + V_3) =$ the volume V_4

General Set-up for flowed reaction in Figure 11:

Three solutions were prepared in 4 mL Vials equipped with magnetic stirring bars. In the first vial, we added the benzyne precursor (0.5 mmol, 1 Equiv. x mL) the diene (8 mmol, 10 Equiv. x mL) and enough THF were added to get a total volume of 1.5 mL. In the second vial, TBAF (3 Equiv.) was added and diluted with THF to get a total volume of 1.5 mL. In the last vial, the organolithium (x Equiv. x mL) were added and diluted with hexanes to get a total volume of 3 mL. The contents of these vials were loaded into the three syringes 1, 2 and 3 respectively. The three syringes were

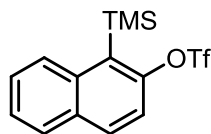
connected to the reactor and set into New Era syringe pumps, and a pressurized collection vial was placed at the end of V₄. The pumps start to infuse the contents of syringes 1 and 2 at the same flow rate ($x \mu\text{L}/\text{min}$), while the contents of syringe 3 flowed at flow rate = $2x \mu\text{L}/\text{min}$. The residence time in the first reactor was equal to 1 minute, while the residence time in the second reactor was adjusted according to Table 7.

Synthesis of Benzyne precursors:



4-Methyl-2-(trimethylsilyl) phenyl trifluoromethane sulfonate (**68**).

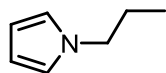
A solution of 2-bromo-4-methylphenol (1.85g, 10 mmol) and HMDS (2.06 mmol, 10 mmol, 1 Equiv.) in 40 mL of THF was heated under reflux for 90 min. At this time, the solvent was evaporated to remove the excess NH_3 and unreacted HMDS. The expected product was suitable to be used directly in the next step. The crude product was dissolved in 40 mL THF, cooled down to -80°C and $n\text{-BuLi}$ (4.6 mL, 2.35 M, 11mmol, 1.1 Equiv.) was added drop-wise. After stirring for 20 min at -80°C , a freshly distilled Et_2O (40 mL) was added followed by drop-wise addition of Tf_2O (2.1mL, 12.5 mmol, 1.2 Equiv.) and the mixture was allowed to stir for 1 hr while maintaining the temperature at -80°C . The reaction was then quenched with cold, saturated NaHCO_3 and the two phases were separated. The aqueous layer was extracted with Et_2O and the combined organic layers were dried over anhydrous MgSO_4 , filtered and concentrated under reduced pressure. The crude product was then purified by column chromatography using basic alumina (pentane, $R_f = 0.46$ in pentane); $^1\text{H-NMR}$ (CDCl_3) δ 7.32 (s, 1H), 7.24 (s, 2H), 2.41 (s, 3H), 0.45 (s, 9H); $^{13}\text{C-NMR}$ (CDCl_3) δ 153.1, 137.2, 136.7, 132.2, 131.7, 119.3, 118.5 (q, $J = 320$ Hz, CF_3), 20.8, -0.8. Spectral data of **68** are in accordance with those reported in the literature.¹⁵⁹



1-(Trimethylsilyl)naphthalen-2-yl trifluoromethane sulfonate (**69**).

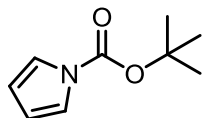
Following the same procedure used to prepare **68** with 1-bromonaphthalen-2-ol, 2.9 g (83 % yield) were obtained as colorless oil following column chromatography (basic alumina, 1 % EtOAc in hexanes, R_f = 0.6 in 10 % EtOAc/hexane); $^1\text{H-NMR}$ (CDCl_3) δ 8.26 (d, J = 8.4 Hz, 1H), 7.93 (m, 2H), 7.60 (m, 2H), 7.45 (d, J = 9.2 Hz, 1H), 0.64 (s, 9H); $^{13}\text{C-NMR}$ (CDCl_3) δ 152.5, 137.5, 132.4, 129.3, 129.0, 128.8, 126.7, 126.3, 120, 118.7 (q, J = 320 Hz, CF_3), 2.2. Spectral data of **69** are in accordance with those reported in the literature.¹⁶⁰

Synthesis of Dienes:



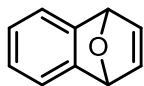
N-Propyl-pyrrole (**77**).

To a 200 mL round bottom flask were added, 18-crown-6 (0.8 g, 3 mmol, 1 % Equiv.) followed by 50 mL of diethyl ether and, potassium *tert*-butoxide (3.9 g, 35 mmol, 1.16 Equiv.). After stirring for 10 min, pyrrole (2 g, 30 mmol) was added in one shot and the mixture further stirred for 15 min. In a separate flask, 1-bromopropane (4.23 g, 35 mmol, 1.16 Equiv.) was dissolved in 20 mL of diethyl ether and the resultant solution was added dropwise to the pyrrole mixture and the mixture stirred for 3 hours. At that time, the reaction was quenched with water and the aqueous layer was washed with Et_2O . The combined organic layers were dried over anhydrous MgSO_4 , filtered and concentrated *in vacuo*. The crude mixture was purified on SiO_2 , (0 \rightarrow 15% Et_2O /pentane) to afford the desired product as a colorless oil (2.81 g, 86 % yield); $^1\text{H-NMR}$ (CDCl_3) δ 6.69 (m, 2H), 6.18 (m, 2H), 3.87 (t, J = 7.2 Hz, 2H), 1.83 (m, 2H), 0.95 (t, J = 7.5 Hz, 3H); $^{13}\text{C-NMR}$ (CDCl_3) δ 120.5, 107.7, 51.3, 24.8, 11.3. The spectra data of the product are in accordance with those reported in the literature.¹⁶¹



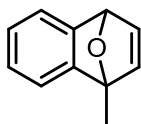
tert-Butyl 1H-pyrrole-1-carboxylate (76).

To a 100 mL round bottom flask containing pyrrole (2.0 g, 29.8 mmol) in acetonitrile (30 mL) were added di-*tert*-butyl dicarbonate ((Boc)₂O) (7.8 g, 35.7 mmol, 1.2 Equiv.) and 4-(dimethylamino) pyridine (DMAP) (0.5 g, 4.49 mmol, 0.125 Equiv.) After the mixture was stirred at rt for 2 h, the solvent was removed *in vacuo*. The resulting crude product was then purified on (basic Al₂O₃; hexanes, R_f = 0.82 in 20% EtOAc in hexanes) to afford the desired compound as a colorless oil (4.4 g, 88% yield); ¹H-NMR (CDCl₃) δ 7.27 (m, 2H), 6.24 (m, 2H), 1.63 (s, 9H). ¹³C-NMR (CDCl₃) δ 148.8, 119.8, 111.8, 83.5, 27.9. The spectra data of **76** are in accordance with those reported in the literature.¹⁵³



1, 4-dihydro-1, 4-epoxynaphthalene (56).

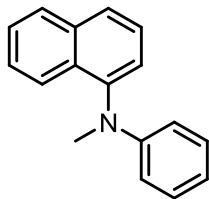
Purification was carried out on silica using 10% EtOAc/ hexanes (R_f = 0.34 in 10% EtOAc/ hexanes) to deliver the desired product as a white crystal m.p.: 46-48 °C reported m.p.: 53-54 °C (69 mg, 60%); ¹H-NMR (CDCl₃) δ 7.30-7.28 (m, 2H), 7.06 (s, 2H), 7.02-7.00 (m, 2H), 5.75 (s, 2H); ¹³C-NMR (CDCl₃) δ, 148.9, 143.0, 124.9, 120.2, 82.3. The spectra data of the product are in accordance with those reported in the literature.¹⁶²



1-Methyl -1, 4-dihydro-1, 4-epoxynaphthalene (80).

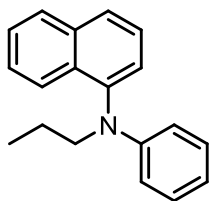
Purification was carried out on silica using 20% EtOAc/hexanes (R_f = 0.57 in 20% EtOAc/hexanes) to deliver the desired product as a light-yellow oil (74 mg, 59%); ¹H-NMR (CDCl₃) δ 7.25 (d, *J* = 6.4 Hz, 1H), 7.20 (d, *J* = 6.4 Hz, 1H), 7.07 (d, *J* = 5.2 Hz, 1H), 7.01-7.051

(m, 2 H), 6.81 (d, $J = 5.2$ Hz), 5.67 (s, 1 H), 1.97 (s, 3H); ^{13}C -NMR (CDCl_3) δ 151.2, 150.4, 145.5, 144.2, 124.8, 124.6, 119.8, 118.7, 89.3, 81.7, 15.1. The spectra data of the product are in accordance with those reported in the literature.¹⁶³



***N*-Methyl-*N*-phenylnaphthalen-1-amine (81).**

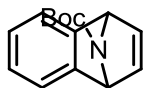
N-methyl pyrrole was distilled prior to conducting the reaction. Purification of the crude product was carried out on silica using a gradient (100% hexanes \rightarrow 10% EtOAc/ hexanes, $R_f = 0.64$ in 10%EtOAc/ hexanes) to produce the desired product as a light-yellow oil (18 mg, 19% yield); ^1H -NMR (CDCl_3) δ 7.94 (m, 2H), 7.83 (d, $J = 8.4$ Hz, 1H), 7.56-7.52 (m, 2H), 7.46 (m, 1H), 7.40 (d, $J = 7.2$ Hz, 1H), 7.20 (dd, $J = 7.6, 7.2$ Hz, 2H), 6.77 (t, $J = 7.2$ Hz, 1H) 6.66 (d, $J = 7.6$ Hz, 2H), 3.44 (s, 3H); ^{13}C -NMR (CDCl_3) δ 150.1, 145.4, 135.1, 131.3, 128.9, 128.4, 126.6, 126.4, 126.3, 126.2, 125.2, 123.8, 117.2, 113.5, 40.2. The spectra data of the product are in accordance with those reported in the literature.¹⁵⁴



***N*-phenyl-*N*-propylnaphthalen-1-amine (82).**

Purification was carried out on silica using a gradient (100% pentane \rightarrow 10%Et₂O/pentane $R_f = 0.38$ in pentane) to produce the desired product as a yellow oil (22 mg, 21%); ^1H -NMR (CDCl_3) δ 7.95 (d, $J = 8.0$ Hz, 1H), 7.89-7.84 (m, 2H), 7.56-7.50 (m, 2H), 7.46-7.41 (m, 2H), 7.16 (dd, $J = 8.0, 7.6$ Hz, 2H), 6.71 (t, $J = 7.2$ Hz, 1H), 6.58 (d, $J = 8.0$ Hz, 2H), 3.74 (t, $J = 8.0$ Hz, 2H), 1.80 (quint, $J = 7.6$ Hz, 2H), 0.96 (t, $J = 7.6$ Hz, 3H); ^{13}C -NMR (CDCl_3) δ 149.50, 143.5, 135.3, 131.7, 129.0, 128.5, 126.8, 126.8, 126.4, 126.3, 126.1,

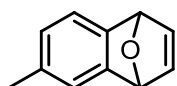
124.0, 116.6, 113.1, 54.4, 21.0, 11.4; HRMS (ESI) [M^+] calcd. for $C_{19}H_{19}N$ (m/z) 261.1517; found 261.1511.



***tert*-Butyl-1,4-dihydro-1,4-epiminonaphthalene-9-carboxylate (83).**

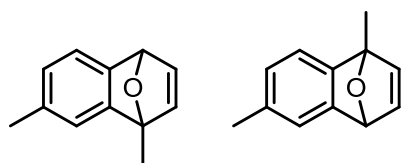
Purification using basic alumina (10% Et_2O /pentane, R_f = 0.29, in 10% Et_2O /pentane) provided the desired product as a white solid (105 mg, 59%) m.p.: 64-66 °C, reported m.p.: 70-72 °C; 1H -NMR ($CDCl_3$) δ 7.28 (bs, 2H), 6.99-9.97 (m, 4H), 5.52 (bs, 2H), 1.41 (s, 9H); ^{13}C -NMR ($CDCl_3$) δ 155.0, 148.2, (143.4, 142.3)*, 124.8, (120.9, 102.4)* 80.4, (66.7, 66.0)*, 28.0; ^{13}C -NMR ($CDCl_3$) at 55 °C δ 155.0, 148.4, 142.0 (bs), 124.8, 120.6 (bs), 80.4, 66.50 (bs), 28.1. The spectra data of the product are in accordance with those reported in the literature.¹⁶²

* Peaks coalesce upon increasing the temperature.



6-Methyl-1,4-dihydro-1,4-epoxynaphthalene (86).

Purification was carried out on silica neutralized with Et_3N using a gradient 10% \rightarrow 20% Et_2O /pentane, R_f = 0.33 in 10% Et_2O /pentane to deliver the desired product as a colorless oil (85 mg, 68%); 1H -NMR ($CDCl_3$) δ 7.17 (d, J = 7.2 Hz, 1H), 7.14 (s, 1H), 7.10 (m, 2H), 6.81 (d, J = 6.8 Hz, 1H), 5.72 (d, J = 5.2 Hz, 2H), 2.34 (s, 3H); ^{13}C -NMR ($CDCl_3$) δ 149.4, 146.0, 143.3, 142.8, 134.7, 125.0, 121.6, 120.0, 82.3, 82.2, 21.30. The spectra data of the product are in accordance with those reported in the literature.¹⁶³

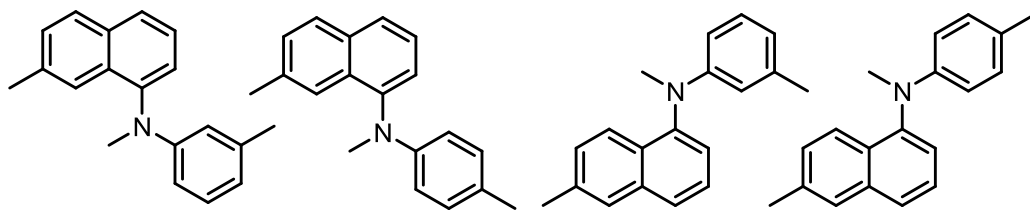


1,7-Dimethyl-1, 4-dihydro-1, 4-epoxynaphthalene (87 a) &

1,6- dimethyl-1, 4-dihydro-1, 4-epoxynaphthalene (87 b):

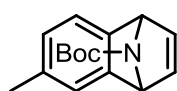
Purification was carried out on silica using (10% Et₂O/pentane,

$R_f = 0.38$ in 10% Et₂O/pentane) to deliver the desired cycloadducts as inseparable isomers (ratio of **87a** to **87b** is 1:1) as yellow oil (80 mg, 59%); ¹H-NMR (CDCl₃) δ 7.11 (d, $J = 7.2$ Hz, 1H), 7.07 (s, 1H), 7.05-7.03 (m, 4H), 6.82-6.76 (m, 4H), 5.62-5.60 (m, 2H), 2.33 (s, 3H), 2.32 (s, 3H), 1.93 (s, 6H); ¹³C-NMR (CDCl₃) δ 151.6, 150.9, 148.4, 147.6, 145.7, 145.3, 144.50, 144.0, 134.7, 134.4, 124.8, 124.6, 121.2, 120.2, 119.6, 118.4, 89.3, 89.2, 81.7, 81.6, 21.3, 21.2, 15.2, 15.2. The spectra data of the two products are in accordance with those reported in the literature.¹⁶²



***N*,7-Dimethyl-*N*-(*m*-tolyl)naphthalen-1-amine (88 a), *N*,7-dimethyl-*N*-(*p*-tolyl)naphthalen-1-amine (88 b) *N*,6-dimethyl-*N*-(*m*-tolyl)naphthalen-1-amine (88 c), *N*,6-dimethyl-*N*-(*p*-tolyl)naphthalen-1-amine (88 d).** Purification was carried out on silica using toluene ($R_f = 0.9$ in toluene) to deliver the desired product as inseparable isomers (30 mg, 28% yield); The spectral data reported are for the four isomers **88a**, **88b**, **88c** and **88d**. The ratio of pair 1 (i.e. **88a** and **88b**) to that of pair 2 (i.e. **88c** and **88d**) is (1.2: 1) and the ratio of **88a** to **88b** is (1.3:1), and the ratio of **88c** to **88d** is presumably the same (i.e. 1.3:1); ¹H-NMR (CDCl₃) δ 7.85-7.81 (m), 7.80-7.76 (m), 7.73-7.71 (m), 7.48-7.40 (m), 7.38-7.29 (m), 7.10-6.98 (m), 6.59-6.55 (m), 6.49-6.43 (m), 3.38 (s), 3.37 (s), 3.37 (s), 2.53 (s), 2.48 (s), 2.27 (s); ¹³C-NMR (CDCl₃) δ 150.2, 150.2, 148.2, 148.1,

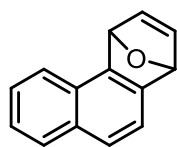
145.7, 145.4, 145.3, 145.0, 138.6, 136.1, 136.1, 135.9, 135.8, 135.4, 134.9, 133.4, 133.3, 131.7, 131.7, 129.6, 129.5, 129.4, 128.7, 128.7, 128.6, 128.6, 128.5, 128.5, 128.3, 127.4, 126.5, 126.4, 126.3, 126.3, 126.1, 125.9, 125.6, 125.5, 125.0, 124.3, 123.8, 123.8, 122.6, 122.5, 118.1, 118.0, 114.1, 114.0, 113.9, 113.7, 110.8, 110.7, 40.4, 40.2, 40.2, 40.1, 29.7, 22.0, 21.8, 21.6, 20.3; HRMS (ESI) $[M]^+$ calcd. for $C_{19}H_{19}N$ (m/z) 261.1517; found 261.1522.



***tert*-Butyl- 6 - methyl -1,4-dihydro-1,4-epiminonaphthalene-9-carboxylate (89).**

Purification was carried out on basic alumina using (10% → 20% Et_2O /pentane, R_f = 0.31 in 10% Et_2O /pentane) to deliver the desired product as a colorless oil (100 mg, 49% yield); 1H -NMR ($CDCl_3$) δ 7.14 (m, 2H), 6.98 (bs, 2H), 6.78 (d, J = 9.2 Hz, 1H), 5.84 (bs, 2H), 2.31 (s, 3H), 1.42 (s, 9H); ^{13}C -NMR ($CDCl_3$) δ 155.1, 148.5, 145.2, (143.8, 143.2, 142.6, 142.2)*, 134.6, 124.9, (122.4, 121.9)* (120.7, 120.3)*, 80.5, (66.6, 66.1)*, 28.2, 21.3. While the 1H -NMR spectrum showed good agreement with the literature, a number of signals are reported here in the ^{13}C -NMR spectrum are not reported in the literature report, although some of their reported peaks do appear to be coincident with those listed above.¹⁶²

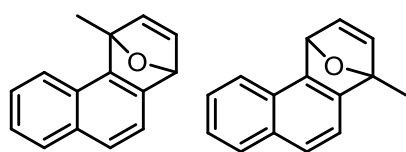
*Peaks coalesce upon increasing the temperature.



1,4-Dihydro-1,4-epoxyphenanthrene (90).

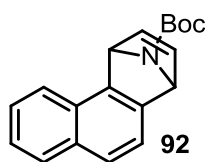
Purification was carried out on basic alumina (1% $EtOAc$ /hexanes, R_f = 0.16 in 5% $EtOAc$ /hexanes.) to deliver the desired product as a white crystals (107 mg, 71%) m.p.: 83-85 °C, reported m.p.: 86 °C; 1H -NMR ($CDCl_3$) δ 7.85 (m, 2H), 7.61 (d, J = 8.0 Hz, 1H), 7.56 (d, J =

8.0 Hz, 1H), 7.49 (dd, $J = 7.6, 7.2$ Hz, 1H), 7.40 (dd, $J = 7.6, 7.2$ Hz, 1H), 7.23 (bs, 2H), 6.29 (bs, 1H), 5.96 (bs, 1H); ^{13}C -NMR (CDCl_3) δ 148.3, 147.8, 144.9, 143.4, 131.7, 128.7, 127.6, 126.2, 125.3, 125.1, 122.6, 119.3, 83.4, 81.2. The spectra data of the product are in accordance with those reported in the literature.¹⁶⁴



4-Methyl-1,4-dihydro-1,4-epoxyphenanthrene (91a) & 1-methyl-1,4-dihydro-1,4-epoxyphenanthrene (91b).

Purification was carried out on basic alumina (5% EtOAc/ hexanes, $R_f = 0.56$ in 20% EtOAc/hexanes) to deliver the desired product as inseparable isomers, (ratio of **91a** to **91b** is (0.82:1)) as a pale yellow oil (130 mg, 76%); ^1H -NMR (CDCl_3) δ 8.09 (d, $J = 8.4$ Hz, 1H), 7.90-7.87 (m, 2H), 7.84 (d, $J = 8.4$ Hz, 1H), 7.64-7.61 (m, 2H), 7.54-7.48 (m), 7.43-7.38 (m, 2H), 7.25 (d, $J = 5.2$ Hz, 1H), 7.22 (m, 1H), 7.05 (d, $J = 5.6$ Hz, 1H), 6.99 (d, $J = 5.2$ Hz, 1H), 6.22 (s, 1H), 5.84 (s, 1H), 2.38 (s, 3H), 2.10 (s, 3H); ^{13}C -NMR (CDCl_3) δ 150.6, 150.1, 149.1, 148.1, 147.3, 146.8, 145.9, 144.7, 132.3, 131.5, 129.2, 128.7, 128.0, 127.3, 126.1, 126.0, 125.8, 125.3, 125.0, 124.5, 122.6, 122.3, 118.9, 117.9, 91.5, 90.5, 82.2, 80.5, 18.7, 15.4; HRMS (ESI) $[\text{M}^+]$ calcd. for $\text{C}_{15}\text{H}_{12}\text{O}$ (m/z) 208.0888; found 208.0881.

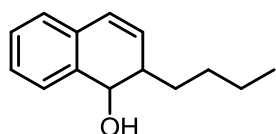


tert-Butyl-1,4-dihydro-1,4-epiminophenanthrene-11-carboxylate (92).

Purification was carried out on basic alumina using 5% EtOAc/ hexanes ($R_f = 0.58$ in 20% EtOAc/hexanes) to deliver the desired product as white crystals (154 mg, 66%); m.p.: 120-122 °C; ^1H -NMR (CDCl_3) δ 7.92 (d, $J = 8.4$ Hz, 1H), 7.85 (d, $J = 8.4$ Hz, 1H), 7.58 (bs, 2H), 7.50 (t, $J = 7.6$ Hz, 1H), 7.41 (t, $J = 7.2$ Hz, 1H), 7.21 (bs, 1H), 7.15 (bs, 1H), (6.14, 6.06)* (bs, 1H), (5.76, 5.73)* (bs, 1H), (1.43, 1.40)* (s, 9H); ^{13}C -NMR (CDCl_3) δ 155.0, (147.5, 147.3)*, 146.7,

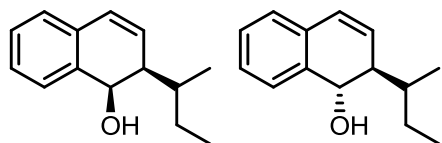
145.2, (144.1, 144.0)*, 142.6, 131.5, 128.6, (127.9, 127.8)*, 126.2, 125.0, (122.8, 122.5)*, 120.1, 119.5, 80.60, (67.9, 67.3)*, 28.1; HRMS (ESI) $[M^+]$ calcd. for $C_{19}H_{19}N$ (m/z) 293.1416; found 293.1425.

*Peaks coalesce upon increasing the temperature.



2-propyl-1, 2-dihydronaphthalen-1-ol (93).

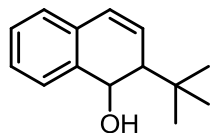
Purification was carried out on silica using 10% EtOAc/hexanes, R_f = 0.35 in 10% EtOAc/hexanes to deliver the desired compound (34 mg, 40%) as a white solid; m.p.: 61-63 °C (Lit. m.p.: 66-67 °C); 1H -NMR ($CDCl_3$) δ 7.36 (d, J = 7.2 Hz, 1 H), 7.33-7.24 (m, 2H), 7.15 (d, J = 7.2 Hz, 1H), 6.56 (m, 1H), 5.86 (m, 1H), 4.62 (bs, 1H), 2.51-2.47 (m, 1H), 1.88-1.79 (m, 1H), 1.59-1.39 (m, 4H), 0.97 (t, J = 7.6 Hz, 3H); ^{13}C -NMR ($CDCl_3$) δ 136.6, 132.6, 131.2, 128.4, 127.5, 126.6, 126.4, 70.2, 40.3, 29.3, 29.0, 28.7, 22.8, 14.1. The spectral data are consistent with those reported in the literature.¹⁶⁵



2-sec-Butyl-1, 2-dihydronaphthalen-1-ol (94).

Purification was carried out on silica using 10% Et₂O in hexanes (R_f = 0.45 in 10% Et₂O in hexanes) to deliver the desired product as inseparable isomers as colorless oil (70 mg, 72%); 1H -NMR ($CDCl_3$) δ 7.26-7.24 (m, 6 H), 7.16 (t, J = 6.6 Hz, 2H), 6.63 (dd, J = 9.6, 2.8 Hz, 2H), 6.01-5.97 (m, 2H), 2.36-2.33 (m, 1H), 2.27-2.24 (m, 1H), 1.94-1.66 (m, 6H), 1.47-1.30 (m, 2H), 1.20 (d, J = 6.4 Hz, 3H), 1.06 (d, J = 6.4 Hz, 3H), 1.02-0.97 (m, 6H); ^{13}C -NMR ($CDCl_3$) δ 137.1, 136.9, 132.6, 129.6, 129.3, 128.7, 128.5, 127.9, 127.6, 127.3, 127.1,

126.4, 126.4, 69.7, 69.4, 45.1, 45.0, 33.4, 33.3, 26.9, 26.5, 16.9, 16.5, 11.1, 11.0. The spectral data of one product (syn) are consistent with those reported in the literature.¹⁶⁶



2-*tert*-butyl-1, 2-dihydronaphthalen-1-ol (95).

Purification was carried out on silica using 10% Et₂O in hexanes (R_f = 0.6 in 10% Et₂O in hexanes) to deliver the desired product as a colorless oil (84 mg, 83%); ¹H-NMR (CDCl₃) δ 7.34-7.24 (m, 3H), 7.22-7.16 (m, 1H), 6.76 (dd, J = 9.9, 3 Hz, 1H), 6.08 (m, 1H), 4.79 (bs, 1H), 2.25 (m, 1H), 1.48 (m, 1H), 1.21 (s, 9H); ¹³C-NMR (CDCl₃) δ 137.2, 132.3, 128.9, 128.6, 127.7, 127.6, 127.4, 126.4, 70.2, 50.3, 32.3, 28.6. The spectral data are consistent with those reported in the literature.¹⁶⁷

Chapter 8: References

-
- ¹ Hoerr, R.; Noveldner, M.; *CNS Drug Rev.* **2002**, 8, 143-158.
- ² Federsel, H.J.; Hedberg, M.; Qvarnström, F. R.; Sjögren, M. P.T.; Tian, W. *Acc. Chem. Res.* **2007**, 40, 1377-1384.
- ³ Singh, M.; Schott, J. T.; Leon, M. A.; Granata, R. T.; Dhah, H. K.; Welles, J. A.; Boyce, M. A.; Oseni-Olalemi, H. S.; Mordaunt, C. E.; Vargas, A. J.; Patel, N. V.; Maitra, S. *Bioorg. Med. Chem. Lett.* **2012**, 22, 6252-6255.
- ⁴ Liu, Y.; Wang, C.; Bai, Y.; Han, N.; Jiao, J.; Qi, X. *Org. Process. Res. Dev.* **2008**, 12, 490-495.
- ⁵ Chu-Moyer, M. Y.; Ballinger, W. E.; Beebe, D. A.; Berger, R.; Coutcher, J. B.; Day, W. W.; Li, J.; Mylari, B. L.; Oates, P.J.; Weekly, R. M.; *J. Med. Chem.* **2002**, 45, 511-528.
- ⁶ <https://cen.acs.org/content/dam/cen/supplements/CEN-supplement092014.pdf>, page 26.
- ⁷ Sakamoto, T.; Koga, Y.; Hikota, M.; Matsuki, K.; Murakami, M.; Kikkawa, K.; Fujishige, K.; Kotera, J.; Omori, K.; Morimoto, H.; Yamada, K. *Bioorg. Med. Chem. Lett.* **2014**, 24, 5460-5465.
- ⁸ Bunnett, J. F.; Zahler, R. E. *Chem. Rev.* **1951**, 49, 273-412.
- ⁹ Rappoport, Z. The Chemistry of anilines part 1; **2007**, John Wiley & Sons, West Sussex. Pg 457-458.
- ¹⁰ a) Roberts, J. D.; Simmons, E. H.; Carlsmith, A. L.; Vaughan, W. C. *J. Am. Chem. Soc.* **1953**, 75, 3290-3291; b) Roberts, J. D.; Simmons, E. H.; Carlsmith, A. L. *J. Am. Chem. Soc.* **1956**, 78, 601-611.

-
- ¹¹ Hoffman, R. W. Dehydrobenzene and Cyclo alkynes, Academic press, New York, **1967**.246-255.
- ¹² Gowling, E. W.; Kettle, S. F. A.; Sharpless, G. M. *Chem. Commun.* **1968**, 21-22.
- ¹³ Millar, I. T.; Heaney, H. *Q. Rev. Chem. Soc.* **1957**, *11*, 109-120.
- ¹⁴ Wittig, G.; Bickelhaupt, F. *Chem. Ber.* **1958**, *91*, 883-894.
- ¹⁵ a) March, J. *Advanced Organic Chemistry*, Wiley, New York, **1992** b) Larock, R. C. *Comprehensive Organic Transformations: A Guide to Functional Group Preparations*, Wiley, - VCH, New York, **1999**, pg 823.
- ¹⁶ Kaneda, K.; Kuwahara, H.; Imanaka, T. *J. Mol. Catal. A. Chem.* **1994**, *88*, L267-L270
- ¹⁷ Gilman, H., McCraker, R.. *J. Am. Chem. Soc.* **1927**, *49*,1052-1061
- ¹⁸ Bartoli, G. *Acc. Chem. Res.***1984**, *17*, 109-115.
- ¹⁹ Sapountzis, I.; Knochel, P. *J. Am. Chem. Soc.* **2002**, *124*, 9390-9391.
- ²⁰ Sandtov, A. H.; Stuart, D. R. *Angew. Chem. Int. Ed.* **2016**, *55*, 15812-15815.
- ²¹ Ullmann, F.; Ber. Dtsch. Chem. Ges. **1903**, *36*, 2382-2384.
- ²² Goldberg, I. *Ber. Dtsch. Chem. Ges.* **1906**, *39*, 1691-1692.
- ²³ Lindley, J. *Tetrahedron* **1984**, *40*, 1433-1456
- ²⁴ Chan, D. M. T.; Monaco, K. L.; Wang, R.-P.; Winters, M. P.; *Tetrahedron Lett.* **1998**, *39*, 2933-2936
- ²⁵ Evans, D.A.; Katz, J. L.; West, T. R. *Tetrahedron. Lett.* **1998**, *39*, 2973-2940.
- ²⁶ Lam, P. Y. S.; Clark, C. G.; Saubern, S.; Adams, J.; Winters, M. P.; Chan, D. M. T.; Combs, A. *Tetrahedron. Lett.* **1998**, *39*, 2941- 2944.
- ²⁷ Collaman, J. P.; Zhong, M. *Org. Lett.* **2000**, *2*, 1233-1236.

-
- ²⁸ Vantourout, J. C.; Law, R. P.; Isidoro-Llobet, A.; Atkinson, S. J.; Watson, A. J. B. *J. Org. Chem.* **2016**, *81*, 3942-3950.
- ²⁹(a) King, A. E.; Brunold, T. C.; Stahl, S. S. *J. Am. Chem. Soc.* **2009**, *131*, 5044-5045; (b) King, A. E.; Ryland, B. L.; Brunold, T. C.; Stahl, S. S. *Organometallics* **2012**, *31*, 7948-7957.
- ³⁰ Vantourout, J. C.; Miras, H. N.; Isidro-Llobet, A.; Sproules, S.; Watson, A. J. B. *J. Am. Chem. Soc.* **2017**, *139*, 4769-4779.
- ³¹ Kosugi, M.; Kameyama, M.; Migita, T. *Chem. Lett.* **1983**, 927-928.
- ³² Kondratenko, N. V.; Kolomeitsev, A.; Mogilevskaya, V. O.; Varlamova, N. M.; Yagupol'kii, L. M. *Translated from: Zh. Org. Khim.* **1986**, *22*, 1721-1729.
Original Article submitted March 26, 1985.
- ³³ Wolfe, J. P.; Wagaw, S.; Buchwald, S. L. *J. Am. Chem. Soc.* **1996**, *118*, 7215-7216.
- ³⁴ Cong, M.; Fan, Y.; Raimundo, J. M.; Tang, J. Peng, L. *Org. Lett.* **2014**, *16*, 4074-4077.
- ³⁵ Marcoux, J.-F.; Wagaw, S.; Buchwald, S. L. *J. Org. Chem.* **1997**, *62*, 1568-1569.
- ³⁶ Vo, G. D.; Hatwig, J. F. *J. Am. Chem. Soc.* **2009**, *131*, 11049-11061.
- ³⁷ Vici, M. S.; Germaneau, R. F.; Navarro-Fernandez, O.; Stevens, E. D.; Nolan, S. P. *Organometallics* **2002**, *21*, 5470-5472. b) Sayah, M.; Organ, M. G. *Chem. Eur. J.* **2013**, *19*, 16196- 16199.
- ³⁸ Pompeo, M.; Farmer, J. L.; Froese, R. D. J.; Organ, M. G. *Angew. Chem. Int. Ed.* **2014**, *53*, 3223-3226.
- ³⁹ Hartwig, J. F.; Richards, S.; Barañano, D.; Paul, F. *J. Am. Chem. Soc.* **1996**, *118*, 3626-3633.
- ⁴⁰ (a) Tolman, C.A. *J. Am. Chem. Soc.* **1970**, *92*, 2953-2956; (b) Tolman, C.A. *J. Am. Chem. Soc.* **1970**, *92*, 2956-2965.

-
- ⁴¹ A. R. Chianese, X. W. Li, M. C. Janzen, J. W. Faller, R. H. Crabtree, *Organometallics*, **2003**, 22, 1663-1667.
- ⁴² White, D.; Taverner, B. C.; Leach, P. G. L.; Coville, N. J. *J. Comput. Chem.* **1993**, 14, 1042–1049.
- ⁴³ Guram, A. S.; Rennels, R. A.; Buchwald, S. L. *Angew. Chem. Int. Ed.* **1995**, 34, 1348-1350.
- ⁴⁴ Louie, J.; Hartwig, J. F. *Tetrahedron Lett.* **1995**, 36, 3609-3612.
- ⁴⁵ Driver, M. S.; Hartwig, J. F. *J. Am. Chem. Soc.* **1996**, 118, 7217-7218.
- ⁴⁶ Hamann, B. C.; Hartwig, J. F. *J. Am. Chem. Soc.* **1998**, 120, 3694-3703.
- ⁴⁷ Wolfe, J. P.; Wagaw, S.; Marcoux, J.-F.; Buchwald, S. L. *Acc. Chem. Res.* **1998**, 31, 805-818.
- ⁴⁸ Hamann, B. C.; Hartwig, J. F. *J. Am. Chem. Soc.* **1998**, 120, 7369-7370.
- ⁴⁹ Old, D. W.; Wolf, J. P.; Buchwald, S. L. *J. Am. Chem. Soc.* **1998**, 120, 9722-9723.
- ⁵⁰ Wolfe, J. P.; Tomori, H.; Saighi, J. P.; Yin, J. J.; Buchwald, S. L.; *J. Org. Chem.* **2000**, 65, 1158-1174.
- ⁵¹ Huang, X.; Anderson, K. W.; Zim, D.; Jiang, L.; Klapars, A.; Buchwald, S. L. *J. Am. Chem. Soc.* **2003**, 125, 6653-6655.
- ⁵² Fors, B. P.; Waston, D. A.; Biscoe, M. R.; Buchwald, S. L. *J. Am. Chem. Soc.* **2008**, 130, 13552-13554.
- ⁵³ Widenhoefer, R. A.; Buchwald, S. L. *J. Am. Chem. Soc.* **1996**, 118, 3534-3542.
- ⁵⁴ Shen, Q.; Shekhar, S.; Stambuli, J. P.; Hartwig, J. F. *Angew. Chem. Int. Ed.* **2005**, 44, 1371-1375.
- ⁵⁵ Viciu, M. S.; Kelly III, R. A.; Stevens, E. D.; Naud, F.; Studer, M.; Nolan, S. *Org. Lett.* **2003**, 5, 1479-1482.

-
- ⁵⁶ (a) Voges, M. H.; Romming, C.; Tilset, M. *Organometallics* **1999**, *18*, 529-533; (b) Herrmann, W. A.; Kocher, C. *Angew. Chem. Int. Ed.* **1997**, *36*, 2163-2187.
- ⁵⁷ Pauling, L. *J. Chem. Soc. Chem. Commun.* **1980**, 688-689.
- ⁵⁸ Ugai, T. Tanaka, R.; Dokawa, T. *J. Pharm. Soc. Jpn.* **1943**, *63*, 269-300.
- ⁵⁹ Breslow, R. *J. Am. Chem. Soc.* **1958**, *80*, 3719-3726.
- ⁶⁰ Wanzlick, H.W. *Angew. Chem. Int. Ed.* **1962**, *1*, 75-80.
- ⁶¹ Arduengo, A. J. Harlow, R. L.; Kline, M. *J. Am. Chem. Soc.* **1991**, *113*, 361-363.
- ⁶² Herrmann, W. A., Elison, M. Fisher, J., Köcher, C.; Artus, G. R. J. *Angew. Chem. Int. Ed.* **1995**, *34*, 2371-2374.
- ⁶³ (a) Hillier, A. C., Sommer, W. J.; Yong, B. S. Peterson, J. L.; Cavallo, L.; Nolan, S. P. *Organometallics* **2003**, *22*, 4322-4326; (b) Poater, A.; Cosenza, B.; Correa, A.; Giudice, S.; Ragone, F.; Scarano, V.; Cavallo, L. *Eur. J. Inorg. Chem.* **2003**, 1759-1766.
- ⁶⁴ Chianese, A. R.; Li, X. W.; Janzen, M. C.; Faller, J. W.; Crabtree, R. H. *Organometallics*, **2003**, *22*, 1663-1667.
- ⁶⁵ Kelly III, R. A.; Clavier, H.; Giudice, S.; Scott, N. M.; Stevens, E. D.; Bordner, J.; Samardjiev, I.; Hoff, C. D.; Cavallo, L.; Nolan, S. P. *Organometallics* **2008**, *27*, 202-210.
- ⁶⁶ Leuthäßer, S.; Schwarz, D.; Plenio, H. *Chem. Eur. J.* **2007**, *13*, 7195-7203.
- ⁶⁷ Cawley, M. J.; Cloke, F. G. N.; Fitzmaurice, R. J.; Pearson, S. E.; Scott, J. S.; Caddick, S. *Org. Biomol. Chem.* **2008**, *6*, 2820-2825
- ⁶⁸ Navarro, O.; Kaur, H.; Mahjoor, P.; Nolan, S. P. *J. Org. Chem.* **2004**, *69*, 3173-3180.
- ⁶⁹ Farmer, J. F.; Hunter, H. N.; Organ, M. G. *J. Am. Chem. Soc.* **2012**, *134*, 17470-17473.

-
- ⁷⁰ (a) Pompeo, M.; Froese, R. D.; Hadei, N.; Organ, M. G. *Angew. Chem. Int. Ed.* **2012**, *51*, 11354-11357; (b) Atwater, B.; Chandrasoma, N.; Mitchell, D.; Rodriguez, M. J.; Pompeo, M.; Froese, R. D. J.; Organ, M. G. *Angew. Chem. Int. Ed.* **2015**, *54*, 9502-9506.
- ⁷¹ (a) Lombardi, C.; Day, J.; Chandrasoma, N.; Mitchell, D.; Rodriguez, M. J.; Farmer, J. L. Organ, M. G. *Organometallics*, **2017**, *36*, 251-254; (b) Lombardi, C.; Mitchell, D.; Rodriguez, M. J.; Organ, M. G. *Eur. J. Org. Chem.* **2017**, 1510-1513; (c) Sharif, S.; Rucker, R. P.; Chandrasoma, N.; Mitchell, D.; Rodriguez, M. J.; Froese, R. D.; Organ, M. G. *Angew. Chem. Int. Ed.* **2015**, *54*, 9507-9511.
- ⁷² EROS Encyclopedia of Reagents for Organic Synthesis.
- ⁷³ Ruiz-Castillo, P.; Blackmond, D. G.; Buchwald, S. L. *J. Am. Chem. Soc.* **2015**, *137*, 3085-3092.
- ⁷⁴ Hofman, S.; Berghe, T. V.; Devisscher, L.; Hassannia, B.; Lyssens, S.; Joossens, J.; Veken, P. V. D.; Vandenabeele, P.; Augustyns, K. *J. Med. Chem.* **2016**, *59*, 2041-2053.
- ⁷⁵ Park, N. H.; Vinogradova, E. V.; Surry, D. S.; Buchwald, S. L. *Angew. Chem. Int. Ed.* **2015**, *54*, 8259-8262.
- ⁷⁶ Rucker, R. P.; Whittaker, A. M.; Dang, H.; Lalic, G. *Angew. Chem. Int. Ed.* **2012**, *51*, 3953-3956.
- ⁷⁷ Kempe, R.; Arndt, P. *Inorg. Chem* **1996**, *35*, 2644-2649.
- ⁷⁸ Araki, K.; Mutai, T.; Shigemitsu, Y.; Yamada, M.; Nakajima, T.; Kuroda, S.; Shimao, I. *J. Chem. Soc., Perkin Trans. 2* **1996**, 613-617.
- ⁷⁹ (a) Chen, W.; Zhan, P.; Rai, D.; Clercq, E. D.; Pannecouque, C.; Balzarini, J.; Zhou, Z.; Liu, H.; Liu, X. *Bioorg. Med. Chem.* **2014**, *22*, 1863-1872; (b) Negoro, N.; Terao, Y.; Mikami, S.; Yukawa, T. Novel fused Cyclic Compound and Use Thereof. US 2012/0172351 A1, **2012**

-
- ⁸⁰ (a) Vorbruggen, H. *Advances in Amination of Nitrogen Heterocycles*; Academic press: San Diego, **1990**; Vol. 49. (b) Gupton, J. T.; Idoux, J. P.; Baker, G.; Colon, C.; Crews, A. D.; Jurss, C. D.; Rampi, R. C. *J. Org. Chem.* **1983**, *48*, 2933-2936
- ⁸¹ Gfesser, G. A.; Bayburt, E. K.; Cowart, M.; DiDomenico, S.; Gomtsyan, A.; Lee, C.-H.; Stewart, A. O.; Jarvis, M. F.; Kowaluk, E. A.; Bhagwat, S. S. *Eur. J. Med. Chem.* **2003**, *38*, 245-252.
- ⁸² Manna, S.; Serebrennikova, P.O.; Utepova, I.A.; Antonchick, A.P.; Chupakhin, O.N. *Org. Lett.* **2015**, 17-4588-459.
- ⁸³ Dhayalan, V.; Sämman, C.; Knochel, P. *Chem. Commun.* **2015**, *51*, 3239-3242.
- ⁸⁴ Scott, N. M.; Schareina, T.; Kempe, R. *Eur. J. Inorg. Chem.* **2004**, 3297-3304.
- ⁸⁵(a) Hu, P.; Dong, Y.; Wu, X.; Wei, Y.; *Front. Chem. Sci. Eng.* **2016**, *10*, 389-395; b) Fuhrmann, H.; Brenner, S.; Aendt, P.; Kempe, R. *Inorg. Chem.* **1996**, *35*, 6742-6745; c) Kempe, R.; Brenner, S.; Arndte, P. *Organometallics* **1996**, *15*, 1071-1074; e) Kawasaki, M.; Suzuki, Y.; Terashima, S. *Chem. Lett.* **1984**, 239-242.
- ⁸⁶ Farmer, J. L.; Pompeo, M.; Lough, A. J.; Organ, M. G. *Chem. Eur. J.* **2014**, *20*, 15790-15798.
- ⁸⁷ Still, W.C.; Khan, M.; Mirta, A. *J. Org. Chem.* **1978**, *43*, 2923-2925.
- ⁸⁸ Tseberlidis, G.; Zardi, P.; Caselli, A.; Cancogni, D.; Fusari, M.; Lay, L.; Gallo, E. *Organometallic*, **2015**, *34*, 3774-3781.
- ⁸⁹ Verkade, P. E.; Nijon, H.; Tollenaar, F. D.; Van Rij, J. H.; Van Leeuwen, M. *Recueil* **1952**, *71*, 1007-1011.
- ⁹⁰ Wolf, J. P.; Buchwald, S. L. *J. Am. Chem. Soc.* **1997**, *62*, 1264-1267.
- ⁹¹ Urgaonkar, S.; Xu, J-H, Verkade, J. G. *J. Org. Chem.* **2003**, *68*, 8416-8423.
- ⁹² Wolfe, J. P.; Buchwald, S. L. *J. Org. Chem.* **1997**, *62*, 1264-1267.

-
- ⁹³ Dastbaravardeh, N.; Kirchner, K.; Schnürch, M.; Mihovilovic, M. D. *J. Org. Chem.* **2013**, *78*, 658-672.
- ⁹⁴ Withbroe, G. J.; Singer, R. A.; Sieser, J. E. *Org. Process Res. Dev.* **2008**, *12*, 480-489.
- ⁹⁵ Hoi, K. H.; Çalimsiz, S.; Froese, R. D.; Hopkinson, A.; Organ, G. M. *Chem. Eur. J.* **2011**, *17*, 3086-3090.
- ⁹⁶ Ilie, A.; Roiban, G-D.; Reetz, M. T. *Chemistry Select* **2017**, *2*, 1392-1397.
- ⁹⁷ Gandy, M. N.; Raston, C. L.; Stubbs, K. A. *Org. Biomol. Chem.* **2014**, *12*, 4594-4597.
- ⁹⁸ Doherty, S.; Knights, J. C.; Smyth, C. H.; Harrington, R. W.; Clegg, W. *Organometallics* **2008**, *27*, 1679-1682.
- ⁹⁹ Browne, L. D.; Wright, S.; Deadman, B. J.; Dunnage, S.; Baxendale, I. R., Turner, R., M.; Ley, S.V. *Rapid Commun. Mass. Spectrom.* **2012**, *26*, 1999-2010.
- ¹⁰⁰ a) Roberge, D. M.; Kochmann, N. *Org. Process Res. Dev.*, **2008**, *12*, 905-910; b) O'Brien, M.; Taylor, N.; Polyzos, A.; Baxendale, I. R.; Ley, S. V. *Chem. Sci.* **2011**, *2*, 1250–1257; (c) Gutmann, B.; Cantillo, D.; Kappe, C. O. *Angew. Chem., Int. Ed.* **2015**, *54*, 6688–6728; (d) Wiles, C.; Watts, P. *Green Chem.* **2012**, *14*, 38–54.
- ¹⁰¹ Plutschack, M. B.; Pieber, B.; Gilmore, K.; Seeberger, P.H. *Chem. Rev.* **2017**, *117*, 11796-117893.
- ¹⁰² Webb, D.; Jamison, T. F. *Chem. Sci.* **2010**, 675-680.
- ¹⁰³ Yoshida, J. I.; *Flash Chemistry: Fast organic synthesis in Microsystems*, New York, Jhon Wiley and Sons **2008**, 69-104.
- ¹⁰⁴ Usutani, H.; Tomida, Y.; Nagaki, A.; Okamoto, H.; Nokami, T.; Yoshida, J-I *J. Am. Chem. Soc.* **2007**, *129*, 3046-3047.

-
- ¹⁰⁵ Valera, F.E.; Quaranta, M.; Moran, A.; Blacker, J.; Armstrong, A.; Cabral, J. T.; Blackmond, D. G. *Angew. Chem. Int. ed.* **2010**, *49*, 2478-2485.
- ¹⁰⁶ Yoshida, J.; Nagaki, A.; Kim, H. *Nature Comm.* **2011**, *5*, 332-337
- ¹⁰⁷ Organ, M. G.; Li, C.; Yoo, W.; Shore, G. *Chem. Eur. J.* **2010**, *16*, 126-133.
- ¹⁰⁸ Darvas, F.; Dormán, Hessel, V. *Flow Chemistry Volume 1*, ; *Deutsche Nationalbibliothek* **2014**, pg 27.
- ¹⁰⁹ Paul, E. L.; Atiemo-Obeng, V. A.; Kresta, S. M. *Handbook of Industrial Mixing: Science and Practice*; John Wiley & Sons, **2004**; pg 1385.
- ¹¹⁰ Lamberto, D. J.; Alvarez, M. M.; Muzzio, F. *J. Chem. Eng. Sci.* **1999**, *54*, 919-942.
- ¹¹¹ Shah, S. I.; Kostiuk, L. W.; Kresta, S. M. *Int. J. Chem. Eng.* **2012**, 16-33.
- ¹¹² a) Mason, B. P.; Price, K. E.; Steinbacher, J. L.; Bogdan, A. R.; McQuade, D. T. *Chem. Rev.* **2007**, *107*, 2300-2318; b) Fukuyama, T.; Rahman, T.; Sato, M.; Ryu, I. *Synlett* **2008**, 151-163.
- ¹¹³ Vapourtec Flow Chemistry Lab Teaching Manual, <http://www.vapourtec.co.uk>
- ¹¹⁴ Schwalbe, T.; Autze, V.; Wille, G. *Chimia* **2002**, *56*, 636-646.
- ¹¹⁵ a) Hartman, R. L.; McMullen, J. P.; Jensen, K. F. *Angew. Chem. Int. Ed.* **2011**, *50*, 7502-7519.
b) Kockmann, N.; Roberge, D. M. *Chem. Eng. Technol.* **2009**, *32*, 1682-1694.
- ¹¹⁶ Nalivela, K.S.; Tilley, M.; McGuire, M. A.; Organ, M. G. *Chem Eur. J.* **2014**, *20*, 6603-6607.
- ¹¹⁷ Brandt, J. C.; Wirth, T. *Beilstein J. Org. Chem.* **2009**, *5* No 30.
- ¹¹⁸ Ducry, L.; Roberge, D. M. *Angew. Chem. Int. Ed.* **2005**, *44*, 7972-7975.
- ¹¹⁹ Carlson, R. *Design and Optimization in Organic Synthesis*, Elsevier Science, Amsterdam, New York, **1992**.
- ¹²⁰ a) Schilling, M.; Nigge, W.; Rdzinski, A.; Neyer, A.; Hergenröder, R. *Lab. Chip.* **2004**, *4*, 220-224; b) Jackman, R. J.; Floyd, T. M.; Ghodssi, R.; Schmidt, M. A.; Jensen, K. F. *J.*

Micromech. Microeng. **2001**, 11, 263-269; c) Lu, H.; Schmidt, M. A.; Jensen, K. F. *Lab. Chip.*

2001, 1, 22-28.

¹²¹ Somerville, K.; Tilley, M.; Li, G.; Lawryshyn, Y.; Bender, T.; Organ, M. G. *Org. Proc. Res. Dev.* **2014**, 18, 1310–1314.

¹²² Delville, M. M. E.; Nieuwland, P. J.; Janssen, P.; Koch, K.; Hest, J. C. M.; Rutjes, F. P. J. T. *Chem. Engineering. J.* **2011**, 167, 556-559.

¹²³ Riva, E.; Rencurosi, A.; Gagliardi, S.; Passarella, D.; Martinelli, M. *Chem. Eur. J.* **2011**, 17, 6221-6226.

¹²⁴ Nagaki, A.; Ichinari, D.; Yoshida, J. *J. Am. Chem. Soc.* **2014**, 136, 12245–12248.

¹²⁵ (a) Kuck, K.-H.; Gisi, U. In *Modern Crop Protection Compounds*; Krämer, W., Schirmer, U., Eds.; Wiley-VCH: Weinheim, **2007**; Vol. 2, pg 415–432; (b) Earley, F. In *Modern Crop Protection Compounds*; Krämer, W., Schirmer, U., Eds.; Wiley-VCH: Weinheim, **2007**; Vol. 2, pg 433–538; (c) Eicken, K.; Goetz, N.; Harreus, A.; Ammermann, E.; Lorenz, G.; Rang, H. European Patent EP0545099, November 24, **1993**; (d) Engel, S.; Oberding, T. WO Patent 2006/092429, September 8, **2006**.

¹²⁶ Stoermer, R.; Kahlert, B.; *Ber. Dtsch. Chem. Ges.* **1902**, 35, 1640-1646.

¹²⁷ a) Huisgen, R.; Rist, H. *Naturwissenschaften* **1954**, 41, 358-359; b) Huisgen, R., Knorr, R. *Tetrahedron let.* **1963**, 1017-1021.

¹²⁸ Wittig, G. *Naturwissenschaften* **1942**, 30, 696-703.

¹²⁹ Wittig, G.; Pohmer, *Chem. Ber.* **1956**, 89, 1334-1351.

¹³⁰ Jones, R. R.; Bergman, R. G. *J. Am. Chem. Soc.* **1972**, 94, 660-661.

¹³¹ Chen, P. *Angew. Chem. Int. Ed.* **1996**, 35, 1478-1480.

-
- ¹³² Anslyn, E. V.; Dougherty, D. A. *Modern Physical Organic Chemistry, University Science Books*, **2006**, pg 612.
- ¹³³ Rasziszewski, J. G.; Hess, B. A. J.; Zahradnik, R. *J. Am. Chem. Soc.* **1992**, *114*, 52-57
- ¹³⁴ Wade, L. G. *Organic Chemistry*, 6th ed; Pearson Prentice Hall: New Jersey, **2006**, pg 531.
- ¹³⁵ Gampe, C. M.; Carreira, E. M. *Angew Chem. Int. Ed.* **2012**, *51*, 3766
- ¹³⁶ Pavliček, N.; Schuler, B.; Collazos, S.; Moll, N.; Pérez, D.; Guitián, E.; Meyer, G.; Peña, D.; Gross, L. *Nature. Chem.* **2015**, *7*, 623-928.
- ¹³⁷ Fridman, L.; Logullo, F.M. *J. Am. Chem. Soc.* **1963**, *85*, 1549-1550.
- ¹³⁸ Kitamura, T.; Yamane, M. *J. Chem. Soc., Chem. Commun.* **1995**, 983-984.
- ¹³⁹ Campbell, C. D.; Rees, J. *J. Chem. Soc.* **1969**, 742-747.
- ¹⁴⁰ Matsumoto, T.; Hosoya, T.; Katsuki, M.; Suzuki, K. *Tetrahedron Lett.* **1991**, *32*, 6735-6736.
- ¹⁴¹ Yoshida, H.; Shirakawa, E.; Honda, Y.; Hiyama, T. *Angew. Chem. Int. Ed.* **2002**, *41*, 3247-3249.
- ¹⁴² Himeshima, Y.; Sonoda, T.; Kobayashi, H. *Chem. Lett.* **1983**, *12*, 1211-1214.
- ¹⁴³ Tadross, P. M.; Stolz, B. M. *Chem. Rev.* **2012**, *112*, 3550-3577.
- ¹⁴⁴ a) Xiao, J.; Duong, H. M.; Liu, Y.; Shi, W.; Ji, L.; Li, G.; Li, S.; Liu, X-W, Ma, J.; Wudl, F. *Angew. Chem. Int. Ed.* **2012**, *51*, 6094-6098; b) Schuler, B.; Collazos, S.; Gross, L.; Meyer, G.; Pérez, D.; Guitián, E.; Peña, D. *Angew. Chem. Int. Ed.* **2014**, *53*, 9004-9008.
- ¹⁴⁵ Garg, N. K.; Goetz, A. E. *Nature Chem.* **2012**, *5*, 54-60.
- ¹⁴⁶ Criado, A.; Vizuete, M.; Gómez-Escalonilla, M. J.; García-Rodríguez, S.; Fierro, J. L. G.; Cobas, A.; Peña, D.; Guitián, E.; Langa, F. *Carbon*, **2013**, *63*, 140-148.
- ¹⁴⁷ Zhong, X.; Jin, J.; Li, S.; Niu, Z.; Hu, W.; Li, R.; Ma, J. *Chem. Commun.* **2010**, *46*, 7340-7342.

-
- ¹⁴⁸ Kametani, T.; Shibuya, S.; Kigasawa, K.; Hiiragi, M.; Kusama, O. *J. Chem. Soc., C* **1971**, 15, 2712–2714.
- ¹⁴⁹ Kametani, T.; Shibuya, S.; Kano, S. *J. Chem. Soc. Perkin Trans. 1* **1973**, 1212–1214.
- ¹⁵⁰ Kametani, T.; Sugai, T.; Shoji, Y.; Honda, T.; Satoh, F.; Fukumoto, K. *J. Chem. Soc., Perkin Trans. 1* **1977**, 1151–1155.
- ¹⁵¹ Kaelin, D. E.; Lopez, O. D.; Martin, S. F. *J. Am. Chem. Soc.* **2001**, 123, 6937–6938.
- ¹⁵² Lakshmi, V.; Wefelscheid, U. K.; Kazmaier, U. *Synlett*, **2011**, 3, 345–348.
- ¹⁵³ (a) Salman, H.; Abraham, Y.; Tal, S.; Meltzman, S.; Kapon, M.; Tessler, N.; Speiser, S.; Eichen, Y. *Eur. J. Org. Chem.* **2005**, 2207–2212; (b) Guida, W. C.; Mathre, D. J. *J. Org. Chem.* **1980**, 45, 3172–3176.
- ¹⁵⁴ Cant, A. A.; Bertrand, G. H. V.; Henderson, J. L.; Roberst, L.; Greaney, M. F. *Angew. Chem. Int. Ed.* **2009**, 48, 5199–5202.
- ¹⁵⁵ Horner, K. E.; Karadakov, P. B. *J. Org. Chem.* **2013**, 78, 8037–8043
- ¹⁵⁶ Wynn, D. A.; Roth, M. M.; Pollard, B. D. *Talanta*, **1984**, 31, 1036–1040.
- ¹⁵⁷ Clayden, J.; Yasin, S. *New. J. Chem.* **2002**, 26, 191–192.
- ¹⁵⁸ Schimler, S. D.; Ryan, S. J.; Bland, D. C.; Anderson, J. E.; Sanford, M. S. *J. Org. chem.* **2015**, 80, 12137–12145.
- ¹⁵⁹ Lakshmi, V.; Wefelscheid, U.K.; Kazamaier, U. *Synlett*, **2011**, 3, 345–348.
- ¹⁶⁰ Pena, D.; Perez, D.; Guitian, E.; Castedo, L.; *J. Org. Chem.* **2000**, 65, 6944–6950.
- ¹⁶¹ Guida, W. C.; Mathre, D. J. *J. Org. Chem.* **1980**, 45, 3172–3176.
- ¹⁶² Kovács, S.; Csincsi, Á.; Nagy, T.; Boros, S.; Timári, G.; Novák, Z. *Org. Letter.* **2012**, 14, 2022–2025.

-
- ¹⁶³ Kitamura, T.; Yamane, M.; Inoue, K. Y.; Todaka, M.; Fukatsu, N.; Meng, Z.; Fujiwara, Y. *J. Am. Chem. Soc.* **1999**, *121*, 11674-11679.
- ¹⁶⁴ Jung, K.; Koreeda, M.; *J. Org. Chem.* **1989**, *54*, 5667-5675.
- ¹⁶⁵ Bertozzi, F.; Pineschi, M.; Macchia, F.; Arnold, L. A.; Minnaard, A. J.; Feringa, B. L. *Org. Chem.* **2002**, *4*, 2703-2705.
- ¹⁶⁶ Shukla, P.; Sharma, A.; Pallavi, B.; Cheng, C. H. *Tetrahedron* **2015**, *71*, 2260-2266.
- ¹⁶⁷ Lautens, M.; Renaud, J-L.; Hiebert, S. *J. Am. Chem. Soc.* **2000**, *122*, 1804-1805.